UNIVERSITÀ DEGLI STUDI DELLA TUSCIA DI VITERBO

DIPARTIMENTO DI SCIENZE E TECNOLOGIE PER L'AGRICOLTURA, LE FORESTE, LA NATURA E L'ENERGIA

Dafne
Dipartimento di scienze e tecnologie per l'Agricoltura, le Foreste, la Natura e l'Energia

Corso di Dottorato di Ricerca in Biotecnologie Vegetali – XXV Ciclo

Functional characterization of the *parthenocarpic fruit* mutation in tomato (*Solanum lycopersicum* L.)

(AGR/07)

Tesi di dottorato di:

Dott. Fabrizio Ruiu

Coordinatore del corso

Prof.ssa Stefania Masci

Firma……

Tutore

Prof. Andrea Mazzucato

Firma……

11 Giugno 2013


Alla
mia
famiglia

Summary

Parthenocarpy is the production of seedless fruits in the absence of pollination and/or fertilization. This process has been extensively studied in tomato (*Solanum lycopersicum* L.) because it offers a method to overcome unfavourable environmental conditions that reduce pollen production, anther dehiscence and, as a consequence, fruit set.

Among the different sources of genetic parthenocarpy described in tomato, the *parthenocarpic fruit* (*pat*) mutation, object of the thesis, is of particular interest because of its strong expressivity, high fruit set and enhanced fruit quality.

Previous studies have thoroughly characterized the *pat* mutation from the genetic, biochemical and qualitative standpoint. More recent research described the complexity of the *pat* syndrome, which associates a strong competence for parthenocarpy with a complex floral phenotype, involving stamen (reduced length and carpelloid features) and ovule (arrested integument growth and loss of viability) development.

By a positional cloning approach, the *Pat* locus was mapped on the long arm of chromosome 3 and recently, by a candidate gene approach, nine candidates have been addressed as potentially responsible for the mutant phenotype. Among them, four genes, known to be involved in reproductive processes, were sequenced in the wild type (WT) and near-isogenic *pat* line. After sequencing, a single point mutation was found only in the tomato ortholog of *ATHB15,* also known as *CORONA* (*CNA*) or *INCURVATA4* (*ICU4*), in Arabidopsis. *ATHB15/CNA/ICU4* is a transcription factor (TF) belonging to the class III HD-Zip subfamily protein. Accordingly to this finding, in tomato, we named this gene *Solanum lycopersicum HB15* (*SlHB15*).

Starting from this background, the thesis aimed to confirm that *SlHB15* is involved in biological processes that, if deregulated, could lead to parthenocarpy and to highlight differentially expressed genes in the WT and *pat* ovary during fruit set.

Using different bioinformatic tools, the amino acid substitution found in the SlHB15 protein encoded by the *pat* allele was predicted to be not tolerated for the protein function. In addition, following an *in silico* comparative approach between *ATHB15/CNA/ICU4* in Arabidopsis and *SlHB15* in tomato, interesting highlights about its involvement in the regulation of auxin homeostasis in plant tissues and biological processes (e.g. flower development and fruit set) were found (**Chapter 2**).

So far, RNA interference and complementation experiments performed for the genetic confirmation of the mutation were not definitive, but promising observations of putatively *SlHB15*-silenced plants reinforced the hypothesis that *SlHB15* underlies the *pat* mutation. Furthermore, in order to find phenotypic similarities between *pat* and single mutants for its ortholog *ATHB15/CNA/ICU4 in* Arabidopsis, a characterization of the *cna-1* (loss-of-

function) and *icu4-1* (gain-of-function) mutants for this gene, was performed. Interestingly, pleiotropic effects showed by *pat* (e.g. deviation of the number of cotyledons and aberrant ovules) and parthenocarpy, were also observed in these mutants, indicating again that *SlHB15* could represent the locus of the *pat* mutation (**Chapter 3**).

A microarray experiment was performed in order to identify differentially expressed genes (DEGs) in the WT and *pat* ovary during fruit set. Based on their expression pattern, the DEGs were categorized into five groups of clusters representing different biological trends. One of the groups deserving more attention was named 'Controlling complex' and contained putative negative or positive regulators of fruit set (genes up- or down-regulated at pre-athesis in the WT ovary and deregulated in the *pat* mutant). Interesting genes belonging to this group encoded tomato orthologs of Arabidopsis TFs regulating the meristem differentiation and development of floral organs, such as SHOOTMERISTEMLESS (STM), BIG PETALp (BPEp), AINTEGUMENTA (ANT) and CRABS CLAW (CRC). These findings represented new insights, because so far these genes belonging respectively to the KNOX, bHLH, AP2/ERF and YABBY families of TFs had never been so directly associated to parthenocarpy. Finally, these TFs and other selected genes were studied also in other pathenocarpic systems (*pat-2*, *pat-3/pat-4*, *EMS-iaa9* and *RNAi-ARF7*) in order to increase the understanding of parthenocarpy in tomato and to find homologies between these different sources for such an agronomically important trait (**Chapter 4**).

Finally, a genetic interaction study between *pat* and *Curl* (*Cu*), a mutation responsible for the overexpression of the gene *LeT6/TKn2* (tomato ortholog of *STM* in Arabidopsis) in vegetative and floral organs, was performed. Overall, the phenotypic and molecular characterization of the *pat Cu* double mutant confirmed findings previously reported and indicated that KNOX family members, such as LeT6/TKn2, may act as negative regulators of the fruit set (**Chapter 5**).

Taken together, results obtained from this thesis increased the understanding of the genetic and molecular bases of fruit set and parthenocarpy in tomato.

Riassunto

La partenocarpia può essere definita come la produzione di frutti senza seme in assenza di impollinazione e/o fecondazione. Questo processo è stato studiato in maniera estensiva in pomodoro (*Solanum lycopersicum* L.) poiché rappresenta un metodo per superare le avverse condizioni ambientali responsabili di una ridotta produzione di polline, deiscenza delle antere e di conseguenza dell'allegagione.

Tra le diverse fonti di partenocarpia genetica descritte in pomodoro, la mutazione *parthenocarpic fruit* (*pat*), oggetto di studio della presente tesi, è di particolare interesse in quanto presenta una forte espressività del carattere ed è responsabile di un'elevata allegagione con la produzione di frutti qualitativamente migliori.

Studi precedenti hanno caratterizzato la mutazione *pat* sia da un punto di vista genetico che biochimico. Mentre, ricerche più recenti descrivono la complessità della sindrome *pat,* che associa al carattere di partenocarpia un complesso fenotipo fiorale legato allo sviluppo degli stami (lunghezza ridotta e caratteristiche carpelloidi) e degli ovuli (perdita di vitalità dovuta ad un arresto della crescita del tegumento).

Attraverso un approccio di clonaggio posizionale, il locus della mutazione *pat* è stato collocato sul braccio lungo del cromosoma 3 e di recente, attraverso un approccio per geni candidati, nove geni sono stati indicati come potenziali responsabili del fenotipo mutante. Quattro di essi, coinvolti in meccanismi riproduttivi, sono stati sequenziati sia nella linea wild type (WT) che nella quasi-isogenica *pat*. Dopo tale sequenziamento, una singola mutazione puntiforme è stata trovata nel gene ortologo di pomodoro ad *ATHB15*, conosciuto anche come *CORONA* (*CNA*) o *INCURVATA4* (*ICU4*), in Arabidopsis. *ATHB15/CNA/ICU4* codifica per un fattore di trascrizione (TF) che appartiene alla classe III della sottofamiglia di proteine HD-Zip. In pomodoro, il gene è stato chiamato *Solanum lycopersicum HB15* (*SlHB15*).

A partire da queste informazioni, la tesi ha avuto come scopo quello di: (i) confermare che *SlHB15* è coinvolto in processi biologici che, se deregolati, inducono partenocarpia; (ii) mettere in evidenza geni differenzialmente espressi nell'ovario WT e *pat* durante il processo di allegagione.

Utilizzando diverse risorse bioinformatiche, la sostituzione amminoacidica presente nella proteina SlHB15, codificata dall'allele *pat,* è stata predetta essere non tollerata per la sua funzione. Inoltre, attraverso un altro approccio *in silico* di tipo comparativo tra *ATHB15/CNA/ICU4* in Arabidopsis e *SlHB15* in pomodoro, sono stati trovati interessanti suggerimenti riguardo al coinvolgimento di tale gene nella regolazione dell'auxina in diversi tessuti e durante differenti processi biologici, come per esempio lo sviluppo fiorale ed l'allegagione (**Capitolo 2**).

Per la conferma genetica della mutazione sono stati eseguiti degli esperimenti di *RNA interference* e complementazione. Finora, tali esperimenti non hanno portato a dei risultati definitivi, anche se l'osservazione promettente di piante putativamente silenziate avvalora l'ipotesi che *SlHB15* possa rappresentare il gene candidato per la mutazione *pat*. Inoltre, per confermare ulteriormente tale ipotesi e cercare delle similarità a livello fenotipico tra *pat* e mutanti singoli per *ATHB15/CNA/ICU4* in Arabidopsis, è stata eseguita una caratterizzazione dei mutanti *cna-1* (*loss-of-function*) e *icu4-1* (*gain-of-function*) per tale gene. È stato molto interessante notare che entrambi i mutanti singoli per *ATHB15/CNA/ICU4* hanno mostrato dei fenotipi paralleli a quelli dalla mutazione *pat* in pomodoro, come ad esempio la deviazione del numero di cotiledoni, ovuli aberranti e partenocarpia (**Capitolo 3**).

Con lo scopo poi di identificare geni differenzialmente espressi (DEGs), nell'ovario WT e *pat*, è stato condotto un esperimento *microarray*. In base al loro pattern di espressione, i DEGs sono stati categorizzati in cinque gruppi di clusters rappresentanti differenti andamenti biologici. Uno dei gruppi che ha destato notevole interesse, definito *'Controlling complex'*, conteneva dei putativi regolatori negativi o positivi dell'allegagione (geni sovra o sotto-regolati allo stadio di pre-antesi nell'ovario WT e deregolati in *pat*). In tale gruppo sono stati trovati geni codificanti in pomodoro per ortologhi a TFs di Arabidopsis coinvolti nella differenziazione del meristema e nello sviluppo degli organi fiorali, come ad esempio SHOOTMERISTEMLESS (STM), BIG PETALp (BPEp), AINTEGUMENTA (ANT) e CRABS CLAW (CRC). Questi risultati rappresentano una novità, poiché tali TFs non erano mai stati associati così direttamente a fenomeni di partenocarpia. L'espressione di questi ed altri geni, selezionati dall'analisi trascrittomica, è stata studiata anche in altri sistemi partenocarpici (*pat-2*, *pat-3/pat-4*, *EMS-iaa9* e *RNAi-ARF7*) con lo scopo di aumentare la comprensione dell'allegagione e trovare omologie tra queste differenti fonti di partenocarpia in pomodoro (**Capitolo 4**).

Infine, è stato condotto uno studio dell'interazione genetica tra *pat* e *Curl* (Cu), una mutazione dominante responsabile per la sovra-espressione del gene *LeT6/TKn2* (ortologo in pomodoro del gene *STM* di Arabidopsis) in organi vegetativi e fiorali. Complessivamente, la caratterizzazione fenotipica e molecolare del doppio mutante *pat Cu* ha confermato dei risultati precedenti che indicavano *LeT6/TKn2* come un importante regolatore negativo dell'allegagione (**Capitolo 5**).

Presi assieme, i risultati ottenuti nella presente tesi hanno aumentato la conoscenza delle basi genetiche e molecolari dell'allegagione e della partenocarpia in pomodoro.

Contents

Chapter 1

General introduction

Tomato (*Solanum lycopersicum* L.) as model species

Tomato (*Solanum lycopersicum* L.) is one of the most consumed vegetables in the world and represents a dietary source of vitamins, minerals and fiber, which are important for human nutrition and health. Second to potato, tomato is the most widely grown vegetable of the Solanceae family. The acid sweet taste and unique flavors account for its popularity and diverse usage (Rubatzky and Yamaguchi, 1997).

Tomato cultivation is adaptable to many environments, so that production is found well distributed from high-elevation regions near the equator to temperate areas far from the equator. Exceptions are the humid tropics because of high disease incidence and temperate regions where low temperatures and short growing seasons limit growth (Rubatzky and Yamaguchi, 1997).

The traditional breeding for pure lines in the cultivated tomato has narrowed its genetic base (Stevens and Rick, 1986). Fortunately, genetic resources from the primary center of diversity provide a wealth of useful genetic traits to improve the crop. All wild tomato species are diploid ($2n = 2x = 24$) and can be crossed (but sometimes with difficulty) to the cultivated tomato. They are of great use in breeding programs as sources of disease resistances and agronomic traits (Stevens and Rick, 1986). The largest and most important collection of wild species genetic resources exists at the Tomato Genetics Resource Center (TGRC, http://tgrc.ucdavis.edu/).

Tomato represents a model organism for studying the genetic and molecular basis of fruit development. Moreover, features that enhance the usefulness of tomatoes for genetic studies are: the naturally occurring variability in the species, self pollination that lead to the expression of recessive mutations, the possibility of controlled hybridization within and among species, the relative short life cycle, the lack of gene duplication, and the possibility to easily identify the 12 chromosomes (Rick, 1978).

In the past decades, there have been great advances in tomato genetics. The variability displayed by the different sources of germplasm available for tomato could be explored to search for new genes or favourable alleles to be transferred by conventional breeding and/or genetic transformation in selected genotypes to obtain new varieties (Di Matteo *et al.*, 2011).

Presently, several resources are available for genetic/genomic research in tomato and include tomato wild species and mutant collections, marker collections, F_2 and permanent recombinant inbred mapping populations, BAC libraries and an advanced physical map, TILLING populations, microarrays, gene silenced tomato lines and VIGS

libraries (reviewed by Barone *et al.*, 2008; 2009). All these tools, used together or separately, are having a great impact on tomato breeding and genetics.

In 2012, the genome *of* the inbred tomato cultivar 'Heinz 1706' was sequenced and assembled using a combination of Sanger and 'next generation' technologies (The Tomato Genome Consortium, 2012). The predicted tomato genome size is approximately 900 megabases (Mb), consistent with previous estimates (Arumuganathan and Earle, 1991), of which 760 Mb were assembled in 91 scaffolds aligned to the 12 tomato chromosomes, with most gaps restricted to pericentromeric regions (The Tomato Genome Consortium, 2012). After the tomato genome release, this species became even more an ideal crop system for genetic/genomic studies in plants.

Tomato reproductive biology

In most tomato cultivars the vegetative phase is short; typically six to 12 leaves are produced below the first inflorescence and the floral transition usually starts when the third leaf is expanding. Contrary to *Arabidopsis thaliana* (Arabidopsis) and *Antirrhinum majus* (Antirrhinum) which present a monopodial growth pattern, tomato shows a sympodial growth habit. While in monopodial species the shoot apical meristem (SAM) is indeterminate and the vegetative or reproductive organs are generated on its flanks, the SAM of tomato is determinate and the primary shoot is completed by the first inflorescence (Lozano *et al.*, 2009). However, the growth habit in tomato can be considered as indeterminate because it continously produce sympodial units.

This growth pattern is repeated by the formation of successive determinate units or sympodial segments, resulting from the newly arisen sympodial meristems. Thus, the 'architecture' of a tomato plant means a regular alternation of vegetative and reproductive phases along the primary and axillary shoots (Atherton and Harris, 1986).

Despite the differences between the monopodial and sympodial systems, genes that maintain the indeterminate state of the shoot apex in Arabidopsis, *TERMINAL FLOWER 1* (*TFL1*), and Antirrhinum, *CENTRORADIALIS* (*CEN*), have an ortholog in the tomato genome, the *SELF PRUNING* (*SP*) gene, which controls the regular vegetative-to-reproductive switch of inflorescence meristems (Pnueli *et al.*, 1998).

Tomato inflorescence has been classically described as a cyme, although available evidences also permit to interpret it as a raceme (Quinet and Kinet, 2007; Lippman *et al.*, 2008). Irrespectively, initiation of reproductive development entails the conversion

of SAM into an inflorescence meristem (IM) from which the floral meristem is produced laterally, giving rise to the first flower. The successive floral meristems developed from the IM are located at the base of each preceding flower bud. This process culminates in the production of a terminal flower, once the determinate inflorescence is composed of about five to ten flowers (Allen and Sussex, 1996). In tomato, the transition to flowering means that the apical meristem is completely consumed in the development of the first inflorescence. In this species, it has been shown that *FALSIFLORA* (*FA*) and *SINGLE FLOWER TRUSS* (*SFT*) are the genes promoting the floral transition (Molinero-Rosales *et al.*, 1999; 2004; Lifschitz *et al.*, 2006), while *SP* regulates this process in the sympodial segments (Pnueli *et al.*, 1998).

At maturity, the hermaphrodite and symmetric flower of tomato consists of four whorls each formed from the outermost by five to six green sepals, which alternate to a similar number of yellow petals at the second whorl, about six stamens displaying anthers forming a cone around the style, and a variable number of fused carpels in the innermost whorl (Lozano *et al.*, 2009). Genetic analyses in Arabidopsis and Antirrhinum have led to propose three main gene functions, A, B and C, each including a low number of genes, which acting alone or in combination determine organ identity in the four floral whorls. The so-called ABC model (Coen and Meyerowitz, 1991; Meyerowitz *et al.*, 1991) has been confirmed in several plant species and assumes that mutations affecting A-, B- and C-class genes promote homeotic changes in the floral organs of two consecutive whorls. Most of the ABC genes belong to the MADS-box family encoding transcription factors (TFs), which are highly conserved among plant species. MADS proteins bind to DNA as multimeric complexes which ultimately control the development of floral organs (Robles and Pelaz, 2005).

Characterization of both homeotic mutants and transgenic plants where homolog ABC genes have been up- or down-regulated confirmed the ABC model in tomato. The *macrocalyx* (*mc*) mutation resides in a homolog to the *APETALA1* (*AP1*), an Arabidopsis class A MADS-box gene (Vrebalov *et al.*, 2002). Expression of *MC* is detected in sepals, petals and carpels while either mutation or gene silencing of *MC* causes homeotic conversion from sepals to leaf-like structures (Rick and Butler, 1956; Vrebalov *et al.*, 2002).

Several class B MADS-box mutants showing partial or complete transformations in the second and third organ whorls have been identified in tomato (Nash et *al.*, 1985; Sawhney, 1992). Among them, *stamenless* (*sl*) and its allelic mutant *corollaless* (*cs*) show sepals instead of petals in the second whorl and stamens replaced by carpels in third whorl. Mutation of *SL* affects a class B MADS-box gene homolog to *DEFICIENS*

(*DEF*) in Antirrhinum and *APETALA3* (*AP3*) in Arabidopsis, both involved in the development of petals and stamens (Lozano *et al.*, 2009).

Regarding tomato class C MADS-box genes, tomato mutants with homeotic changes in both reproductive organs (whorls 3 and 4) have not been described until now. However, *TOMATO AGAMOUS1* (*TAG1*), a tomato ortholog of the Arabidopsis *AGAMOUS* (*AG*) gene has been isolated. Tomato plants expressing sense and antisense *TAG1* transcripts corroborate the role of TAG1 in the specification of stamen and carpel identities (Pnueli *et al.*, 1994a).

Recently, the ABC model has been extended with two new classes of genes (D and E). The class D MADS-box genes control ovule identity and were initially described in Petunia after the functional and molecular analyses of *FLORAL BINDING PROTEIN7* (*FBP7*) and *FBP11* (Angenent *et al.*, 1995; Colombo *et al.*, 1995). The Arabidopsis class D MADS-box gene is *SEEDSTICK* (*STK*) which, like *FBP7* and *FBP11*, is specifically expressed in ovules (Pinyopich *et al.*, 2003). Furthermore, it has been proven that A, B and C genes require an additional function which cooperates with them in the development of the four floral organs. Such function is accomplished by the class E MADS-box *SEPALLATA* (*SEP*) genes. Strong evidence was found to support the formation of multimeric complex involving A, B, C and E (SEP) proteins, as mechanism which triggers the development of floral organs (Robles and Pelaz, 2005).

Current understanding of fruit set and parthenocarpy

Seed and fruit are the key yield components in most crop species. As such, their development has been researched extensively for decades. Upon flower pollination and ovule fertilization, the carpels become a complex organ, forming the mature fruit, thus ensuring seed dispersal and therefore survival of the plants (Lozano *et al.*, 2009).

Mature fruits can be classified generally as either fleshy or dry, which mainly differ in the mechanism achieved to permit seed dispersal. A senescence program leading to fruit dehiscence is needed before some external agent (e.g. wind, rain, and physical contact) can force seeds to be released from dry fruits. However, fleshy fruits have evolved edible components making them attractive for animals, which facilitate dispersion of the seeds without any other requirements (Lozano *et al.*, 2009).

Tomato plants produce fleshy red fruits as result of a developmental process which includes three phases (Gillaspy *et al.*, 1993). The first phase starts just at anthesis with pollination and involves the decision to abort or to proceed with fruit development (i.e.

fruit set). In the second phase, the fruit growth is due primarily to cell division. Concomitantly, during this phase, embryos begin their differentiation and development. In the last phase, the cell division ceases and fruit growth continues by cell expansion until the fruit reaches its final size (Lozano *et al.*, 2009).

Once a fully developed fruit has been formed and seeds are mature, respiration and ethylene synthesis are significantly increased allowing ripening and maturation. As result, biochemical and physiological changes affecting colour, texture, flavor, aroma, nutritional content and susceptibility to opportunistic pathogens are made visible from the onset of ripening (Giovannoni, 2004). Later, a softening process occurs as part of ethylene-induced gene activities which promote degradation of cell walls in different fruit compartments (Giovannoni, 2004). On the other hand, the sharp increase in respiration rate, which usually occurs in combination with elevated ethylene production at the onset of fruit ripening, are considered specific features of climacteric fruits like tomato. Indeed, such features are absent during ripening of non-climateric fruits such as strawberry, grapes, legumes or citrus (Lozano *et al.*, 2009).

As above reported, seed and fruit set are the result of successful pollination and fertilization. However, two biological phenomena, apomixis and parthenocarpy, can lead respectively to the development of seeds and fruits indipendently from these reproductive processes. Apomixis is defined as asexual reproduction through seed (Nogler, 1984), leading to the production of a clonal progeny (Koltunow and Grossniklaus, 2003) and parthenocarpy is the growth of the ovary into a seedless fruit in the absence of pollination and/or fertilization (George *et al.*, 1984; Lukyanenko, 1991). Additionally to parthenocarpy, also another biological mechanism, known as stenospermocarpy, can lead to the formation of seedless fruits. In this process, pollination and fertilization are required, but embryos either do not form or they abort before completion of seed formation. Anyway, in both parthenocarpy and stenospermocarpy, the plant must have an inherent or acquired ability to sustain fruit development in the absence of seed formation.

Parthenocarpy represents an efficient way to improve fruit production under unfavorable conditions for cultivation. Moreover, it can also be beneficial under conditions favourable for fruit set and development because seedless fruits are a commodity for consumers in many species. In addition, parthenocarpic plants often display an early fruit set, taking place before anthesis, that allows early fruit production (e.g. tomato; Falavigna *et al.*, 1978). Moreover, it has been reported that parthenocarpic mutants or varieties in some crops (e.g. tomato, grape) present an improved fruit quality (Varoquaux *et al.*, 2000). For example, studies have shown that

seedless tomato fruits are tastier than the seeded variety, because they exceed seeded fruits in dry-matter content by up to 1%, contain more sugars, less acids and cellulose (Falavigna *et al.*, 1978; Lukyanenko, 1991). At the same time, parthenocarpy might offer the possibility for improving fruit quality and productivity. Finally, parthenocarpy could represent a strategy for seed technology protection (Varoquaux *et al.*, 2000).

Genetic (natural) parthenocarpy has been reported in many species such as tomato, citrus, grape, banana and cucumber (Varoquaux *et al.*, 2000). However, this trait has been so far extensively used only in banana and cucumber. The cultivated bananas (*Musa* spp.) are usually triploid sterile plants that produce parthenocarpic fruits. The parthenocarpic trait in *Musa* spp. is polygenic (Ortiz and Vuylsteke, 1995). In cucumber, parthenocarpy is controlled by a single dominant gene, but also other modifier genes partecipate to the expression of such trait (Pike and Peterson, 1969).

Parthenocarpy may occur naturally or can be induced artificially with the application of various hormones (Gustafson, 1936, 1942; Nitsch, 1952). It is therefore suggested that an hormonal imbalance in the ovary of parthenocarpic plants substitutes for pollination and fertilization and triggers fruit set and development.

Hormonal regulation of fruit set and parthenocarpy

Upon flower pollination and ovule fertilization, fruit and seed undergo concomitant development. Seed development comprises endosperm and embryo differentiation that are thought to by important for fruit intiation (Gillaspy *et al.*, 1993).

Auxin (IAA) and gibberellins (GAs) are the key players in fruit set following fertilization (de Jong *et al.*, 2009a; Hazra *et al.*, 2010). This view is supported by the fact that exogenous application or transgenic elevation of these hormones lead to the uncoupling of fruit set from fertilization, resulting in the development of parthenocarpic fruits (Rotino *et al.*, 1997; Carmi *et al.*, 2003).

Transcriptional regulators from the Auxin Response Factors (ARF) and Auxin/indole acetic acid (Aux/IAA) type of TFs are encoded by two large gene families (Wu *et al.*, 2011; Audran-Delalande *et al.*, 2012) that are known to channel IAA signaling to specific physiological responses (Wang *et al.*, 2005; Guilfoyle and Hagen, 2007; Chaabouni *et al.*, 2009; Deng *et al.*, 2012).

A significant advance in our understanding of the IAA-dependent mechanism underlying fruit set came from the characterization of the *fruit without fertilization* (*fwf*,

also kwown as *arf8-4*) mutant in Arabidopsis (Vivian-Smith *et al.*, 2001; Goetz *et al.*, 2006) or transgenic manipulation of specific *ARF* and *Aux/IAA* genes leading to the development of parthenocarpic fruits in both tomato and Arabidopsis. Specifically, transgenic downregulation of the *INDOLE-3-ACETIC ACID9* (*IAA9*) and *AUXIN RESPONSE FACTOR7* (*ARF7*) in tomato and *ARF8* in both tomato and Arabidopsis, results in uncoupling fruit set from pollination and fertilization, giving rise to parthenocarpy, thus suggesting that these genes encode negative regulators of fruit set (Wang *et al.*, 2005; Goetz *et al.*, 2007; de Jong *et al.*, 2009b).

Although the interaction between ARF and Aux/IAA proteins plays a pivotal role in regulating auxin responses (Dharmasiri and Estelle, 2004; Guilfoyle and Hagen, 2007), it is still not known whether IAA9, ARF7 and ARF8 control fruit set through common or distinct pathways (Ruan *et al.*, 2012). A further investigation should uncover whether heterodimerization between IAA9 and ARF7/ARF8 is part of the control mechanism regulating fruit set (Ruan *et al.*, 2012). Moreover, given that *ARF* genes can be potentially regulated by siRNAs at both the transcriptional and post-transcriptional levels (Wang *et al.*, 2005; Ru *et al.*, 2006), it would be important to know whether the IAA-dependent fruit set is under the epigenetic regulation. If proved, this level of regulation may explain the environmentally induced variation in fruit set and parthenocarpy observed for example in *entire*, a natural tomato mutant impaired in the *IAA9* function (Wang *et al.*, 2005; Zhang *et al.*, 2007).

In support of the multihormonal control of fruit set, there is strong evidence suggesting that the role of IAA is facilitated by synergistic activity with GAs (Serrani *et al.*, 2008; de Jong *et al.*, 2009a). Notably, treatment of unpollinated ovaries with GAs triggers fruit initiation without altering the expression of auxin signaling genes (Vriezen *et al.*, 2008), whereas IAA-induced fruit development is significantly reduced by simultaneous application of GA biosynthesis inhibitors (Serrani *et al.*, 2008). All these data suggest that IAA may act before GAs and that the effect of IAA is mediated at least partly by the GA pathway. Consistent with this hypothesis, GA biosynthesis genes are upregulated after pollination and upon IAA treatment of emasculated flowers (Serrani *et al.*, 2008). However, in tomato, each hormone seems to play a specific role given that IAA application results in a larger number of pericarp cells, whereas treatment with GAs results in fewer pericarp cells but of a larger size (Serrani *et al.*, 2007). Interestingly, concomitant treatment with both hormones results in the formation of seedless fruits similar to those with seeds induced by pollination and fertilization (Serrani *et al.*, 2007), suggesting that IAA and GAs are both required for normal fruit development.

Moreover, Marti *et al.* (2007) silencing the *DELLA* gene in tomato obtained parthenocarpic fruits. The DELLA protein belongs to the GRAS subfamily of plant-specific TFs named after the characterization of the three Arabidopsis members (Pysh *et al.*, 1999): GIBBERELLIC ACID INSENSITIVE (GAI), REPRESSOR of GAI (RGA) and SCARECROW (SCR). These TFs are characterized by the conserved amino acid motif DELLA and are able to repress GA signal transduction (Thomas and Sun, 2004). GA targets DELLA proteins for degradation via ubiquitin-proteasome-mediated proteolysis releasing their repressive action (Fleet and Sun, 2005). In tomato, the *DELLA* gene silencing mimics the degradation of DELLA protein stimulated by the increased GA content observed in pollinated ovaries (Marti *et al.*, 2007).

In several plant species and tissues, IAA stimulates transcription of GA biosynthetic genes (Ross and O'Neill, 2001; Weiss and Ori, 2007) and IAA-induced GA synthesis might lead to an increased GA content. Thus, the increased GA content of the ovary could be caused either by pollen-derived GAs (Nitsch, 1970) and/or by stimulating endogenous GA synthesis and/or inhibiting GA inactivation within fertilized ovules (de Jong *et al.*, 2009a). Furthermore, in Arabidopsis roots, it has been shown that GA-dependent DELLA protein degradation is stimulated by IAA (Fu and Harberd, 2003). Tomato parthenocarpic fruits obtained via *DELLA* silencing are smaller and more elongated compared with either wild type (WT) or *DELLA*-silenced fruits obtained after pollination (Marti *et al.*, 2007). Again, these findings might indicate that, to achieve an optimal fruit set and growth, both IAA and GA signal transduction pathways have to be active.

Fruit set and parthenocarpy at the trascriptome level

Tomato fruit set and early development have also been studied at the transcriptome level. Lemaire-Chamley *et al.* (2005) performed a comparative analysis between the developing fruit and other plant organs, and showed that most genes active in the fruit are not exclusively expressed there, underlining the ontogenetic relationship between fruit and other tissues (Gillaspy *et al.*, 1993). Apparently, tomato fruit development depends on the regulation of gene activity both in time and intensity (Lemaire-Chamley *et al.*, 2005).

Recently, besides the established role of IAA and GA, other studies based on transcriptomic and metabolomic profiling point to the putative involvement of other hormones such as ethylene and abscisic acid (ABA) in regulating fruit set (Vriezen *et*

al., 2008; Pascual *et al.*, 2009; Wang et *al.*, 2009).

Vriezen *et al.* (2008) compared the transcriptomes from pollinated ovaries and GA-treated ovaries, collected three days after pollination or treatment. As it could be expected, genes triggered by pollination were not largely overlapping those activated by the GA_3 application. Several genes involved in the cell cycle were more rapidly induced by GA application than by pollination. Possibly, this difference can be explained by the time that pollen tubes require in order to reach the ovules, what would suggest that the induction of fruit growth does not take place prior to fertilization (Vriezen *et al.*, 2008), and that the growth substances, which are present in the pollen (Mapelli *et al.*, 1978), are only released after the pollen tubes have reached the ovules and delivered the sperm nuclei to the embryo sac (de Jong *et al.*, 2009a). Moreover, the comparative analysis of Vriezen *et al.* (2008) showed that mRNA levels of several ethylene biosynthesis genes and genes involved in ethylene signalling decreased after pollination. At the same time, genes related to ABA biosynthesis decreased and the opposite behavior was found for ABA degradation-related genes (Nitsch *et al.*, 2009). These findings suggest that normal fruit development depends on induction of IAA and GA responses, whereas ethylene and ABA responses are attenuated. By contrast, exogenous application of citokinins can induce parthenocarpic fruit formation in a range of agricultural species, but the mechanism by which this hormone may interact with IAA and/or GA during fruit set remains to be elucidated (Ruan *et al.*, 2012).

Interestingly, in another study, comparing ovaries from WT and *IAA9*-silenced plants, it has been shown that not only IAA, GA and ethylene signaling, but also photosynthesis and sugar metabolism may represent major events of the fruit set program (Wang *et al.*, 2009). These authors showed that in pollinated fruits almost 5% of the differentially expressed genes are related to hormone response and metabolism. In the same study, *Aux/IAA* and *ARF* genes showed a dramatic shift in their expression levels across natural fruit development, suggesting that these TFs play an active role in this developmental process. Moreover, downregulation of *IAA9* results in feedback regulation of several *Aux/IAA* and *ARF* genes (Wang *et al.*, 2009). In keeping with the importance of IAA, recent transgenic works have implicated the auxin receptor homolog TIR1 in tomato fruit set (Ren *et al.*, 2011). Downregulation of the expression of IAA-related negative regulators of fruit set genes occurs earlier than that of ethylene-related genes, suggesting the existence of a temporal dependence on hormone action for the flower-to-fruit transition to proceed (Ruan *et al.*, 2012).

Recently, additionally to the consolidated role of IAA9, ARF7 and ARF8 in regulating fruit set, it has been shown that also PIN4, a member of the PIN-FORMED (PIN) auxin

efflux transport protein family, could act as a negative regulator of fruit set in tomato (Mounet *et al.*, 2012). These authors, using *PIN4*-silenced lines, showed that a parthenocarpic fruit development can be achieved by modifying the polar auxin transport. Indeed. phenotypes observed in *PIN4* knockout plants were fully consistent with the effects showed by the application of polar auxin transport inhibitors in tomato (Serrani *et al.*, 2010). Interstingly, in this study, by a TF profiling approach, it has also been shown that *PIN4*-silenced lines presented a deregulation of several TFs belonging to the MADS-box protein family responsible, as above described, for the specification of the identity of floral organs (Coen *et al.*, 1991).

Parthenocarpy and development of floral organs

Seed and fruit set are the result of successful pollination and fertilization, which in turn depend on the proper development and functioning of male and female reproductive organs (Mazzucato *et al.*, 2003).

Parthenocarpy has often been observed in mutants lacking a correct differentiation of floral organs. For example, parthenocarpy has been described in apple cultivars that produce flowers lacking petals and stamens, and presenting two whorls of sepals and up to 15 styles (Tobutt, 1994). Yao *et al.* (2001), through forward genetics, identified the *Malus domestica PISTILLATA* (*MdPI*) gene as responsible for this phenotype. *MdPI* corresponds to the apple ortholog of the class B MADS-box *PISTILLATA* of Arabidopsis required for both petal and stamen identity specification (Goto and Meyerowitz, 1994).

In tomato, parthenocarpy has been observed in male sterile mutants displaying deficiencies in stamen formation and/or anther dehiscence which result in the failure of fertilization. The mutation of genes involved in stamen identity specification was responsible for occasional parthenocarpy in male sterile mutants, such as *stamenless* (Gomez *et al.*, 1999) and *pistillate* (Olimpieri and Mazzucato, 2008). Interestingly, also the functional male sterile mutant *positional sterile-2* affected in anther dehiscence (Atanassova, 1999), under inductive environmental conditions, shows occasional parthenocarpy producing seedlees fruits reduced in size (Ruiu, 2006). All these findings and observations suggest that parthenocarpy can be triggered by the absence of the normal synchronized development of male and female organs.

Parthenocarpic fruit development has also been described in transgenic tomato lines down-regulated for the *SEP* genes *Tomato MADS-box 5* (*TM5*, Pnueli *et al.*, 1994b)

and *TM29* (Ampomah-Dwamena *et al.*, 2002) or *TM8* (Lifschitz *et al.*, 1993), a MADS-box gene of uncertain classification (Hileman *et al.*, 2006). SEP TFs are class E MADS-box members that, based on the ABC (DE) model for the specification of floral organs, are involved in the control of organ identity in all floral whorls (Honma and Goto, 2001; Pelaz *et al.*, 2000).

A direct evidence that parthenocarpy can be associated to alterations of floral organs is represented by the *parthenocarpic fruit* (*pat*) mutation in tomato (Bianchi and Soressi, 1969; Mazzucato *et al.*, 1998). The *pat* mutant, object of the thesis, shows malformed stamens with carpelloid features and aberrant ovules lacking the growth of the integument (Mazzucato *et al.*, 1998). Recently, it has been shown that the *Pat* locus is not allelic to any known mutation of class B or E MADS-box genes in tomato (Mazzucato *et al.*, 2008). However, the expression of the *Solanum lycopersicum DEFICIENS* (*SlDEF*) gene in the WT ovary at anthesis and its differential transcription in the *pat* ovary suggests that this class B MADS-box gene plays a role in the control of ovary growth (Mazzucato *et al.*, 2008). Accordingly, when compared to its near-isogenic WT line, the gene was also differentially expressed in the *parthenocarpic fruit-2* (*pat-2*) mutant, that is not allelic to *pat* and has normal ovule development (Mazzucato *et al.*, 2008). Altogether these results indicated that in tomato *SlDEF* plays a role in the control of ovary growth and it has been proposed that the *pat* mutation is located upstream of this regulatory cascade (Mazzucato *et al*., 2008). In addition, when the *pat* mutant expressivity is high, the fruit set is 100% and the aberrancy of stamens and ovules reachs the maximum level (Mazzucato *et al.*, 2003). Again, this indicates a strong relationship between fruit set and development of floral organs.

Recently, other studies suggest that, as in the *pat* mutant, alterations of the ovule integument(s) could be related to parthenocarpy (Lora *et al.*, 2011; Tiwari *et al.*, 2011). In particular, Lora *et al.* (2011) showed that the seedlessness of the spontaneous parthenocarpic mutant (Thai seedless) in *Annona squamosa* (sugar apple) could be addressed to the lack of ovule integuments. At molecular level, authors associated the parthenocarpic phenotype with the deletion of the *A. squamosa INNER-NO-OUTER* (*INO*) gene (Lora *et al.*, 2011). The Arabidopsis *INO* gene encodes a member of the YABBY family proteins and is essential for the formation and asymmetric growth of the outer ovule integument (Villanueva *et al.*, 1999). Consistent with this finding, also the loss-of-function mutant for the *DNA methyltransferase* (*MET1*) gene in Arabidopsis, shows an enhanced cell proliferation in ovule integuments which in turn results in a parthenocarpic fruit initiation (FitzGerald *et al.*, 2008). Furthermore, parthenocarpy observed in the *arf8-4* mutant is also significantly enhanced by integument defects in

the double mutant background *ats arf8-4* (Vivian-Smith *et al.*, 2001). In Arabidopsis, mutants for the *ABERRANT TESTA SHAPE* (*ATS,* also known as *KANADI4*) gene, enconding a member of the KANADI family protein, produce a single integument instead of two integuments developed normally by WT ovules (McAbee *et al.*, 2006). However, the single *ats* mutant, as also other ovular mutants in Arabidosis, does not show an indipendent-fertilization fruit growth (Vivian-Smith *et al.*, 2001).

Finally, it is well accepted that a successful fertilization triggers not only fruit growth, but also the senescence of the floral organs. In this regard, the mechanical deletion of outer floral organs enhances the parthenocarpy observed in the *fwf/arf8-4* mutant in Arabidopsis and therefore suggesting that these influence fruit initiation and growth (Vivian-Smith *et al.*, 2001).

Main sources of natural parthenocarpy in tomato

Normally, the tomato plant produces seeded fruits after pollination and fertilization. However, these processes depend on narrow environmental constrains (Picken 1984). Good pollen production is permitted by night temperatures ranging between 15 and 21°C and air circulation is necessary to ensure pollen shedding. These conditions are not often met in unheated greenhouses or tunnels during winter or early spring cultivations. In this regards, parthenocarpy has been extensively studied in tomato because it offers a method to overcome the unfavourable environmental conditions that reduce pollen production, anther dehiscence and, as a consequence, fruit set (Mazzucato *et al.*, 1998). In addition, parthenocarpic mutants, which are able to set fruits in absence of pollination and fertilization, offer suitable experimental systems to identify genes involved in fruit set and early ovary development.

Over the years, different sources of natural (genetic) parthenocarpy have been described in tomato (reviewed by Lukyanenko, 1991; reviewed by Gorguet *et al.,* 2005). These natural sources conferring parthenocarpy can be referred to as the *pat* series. Within this series, the three main sources of natural parthenocarpy are *pat* (Bianchi and Soressi, 1969)*, pat-2* (Philouze and Maisonneuve, 1978) and *pat-3/pat-4* (Philouze, 1983), but also other lines showing a considerable parthenocarpic potential have been described and are *pat-5* (Zijlstra, 1985), *pat-6/pat-7* (Gorguet *et al.*, 2008) and *pat-8/pat-9* (Zijlstra, 1985; Gorguet *et al.*, 2008).

The pat *mutant*

The *pat* mutation, object of this thesis, was obtained by mutagenesis with ethyl methanesulfonate in the late 60's (Bianchi and Soressi, 1969). This mutant is characterized by a parthenocarpic phenotype with high penetrance and expressivity (Fig. 1.1A-D), that also entails earlier ripening and enhanced fruit quality (Fig. 1.1E and F; Falavigna *et al.,* 1978; Mazzucato et *al.*, 1999; F. Ruiu and A. Mazzucato, unpublished).

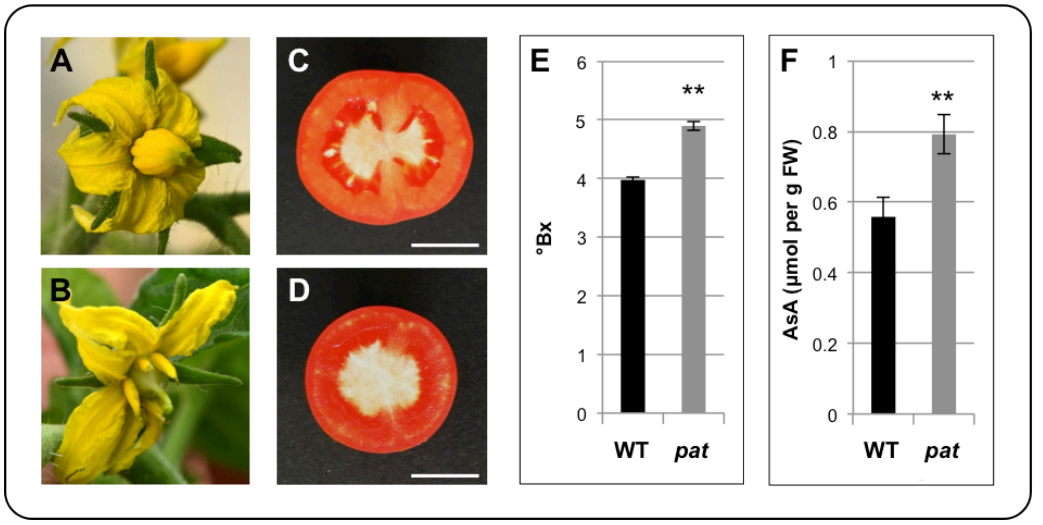

Fig. 1.1. (A) WT flower at anthesis. (B) *pat* flower at anthesis showing the precocious and pollination-indipendent ovary growth, indicating a high expressivity of parthenocarpy. (C) Transversal section of a WT red ripe fruit. (D) Transversal section of a *pat* red ripe fruit displaying a complete seedlessness, indicating a high expressivity of parthenocarpy. (E and F) Degrees Brix (°Bx) and Ascorbic Acid (AsA) content of WT and *pat* mature fruits, respectively. Scale bar indicates 2 cm (C and D). In E and F (**, P≤0.01).

As a pleiotropic effect, *pat* flowers display aberrant androecia and ovules, and therefore reduced male and female fertility (Mazzucato *et al.*, 1998). Specifically, the androecium of *pat* flowers is formed by short, irregular and apparently unfused anthers showing adaxial-abaxial polarity defects (Mazzucato *et al.*, 1998). In addition, the aberrations described for male *pat* organs show similarities with those found in some male sterile tomato mutants (*sl*, *sl-2*, *ms15*, *ms33*) which produce shrunken stamens, bearing carpel-like structures with often external ovules (Sawhney, 1994). The *pat* allele also affects ontogenetic processes during development of female reproductive organs. Therefore, the production of seeds in *pat* plants is very low also under different growth conditions (Mazzucato *et al.*, 1998). The low seed production observed in the *pat* mutant is due not only to the exerted position of the stigma and anticipated ovary growth, which hamper pollination and fertilization (Bianchi and Soressi, 1969), but also

to aberrations in ovule development (arrested integument growth and loss of viability), which reduce the production of viable female gametes (Mazzucato *et al.*, 1998).

In the *pat* mutant, the first evidence of an autonuomous ovary growth occurs one to three days before anthesis at the opening flower stage (Stage 3; according to Mazzucato *et al.*, 1998). In fact, at Stage 3, *pat* ovaries are significantly bigger than those presented by WT flowers, indicating that in the mutant the complete machinery for fruit set is switched on before of and independently from pollen shedding, pollination and fertilization (Mazzucato *et al.*, 1998).

A transcriptomic analysis, using the mRNA differential display approach (Liang and Pardee, 1992), was performed to identify differentially expressed genes in WT and *pat* ovaries at Stage 3, when the mutant ovary starts its autonomous growth (Testa *et al.*, 2002). Following this approach, three differentially expressed genes were identified. Among them, one transcript named 'Clone 91' showed a strong upregulation in the *pat* ovary at Stage 3. This transcript displayed a high homology with the *GAD3* gene encoding a short-chain alcohol dehydrogenase (Testa *et al.*, 2002). Interestingly, this enzyme was found to play an important role in developmental pathways controlled by GAs. Therefore, this early report indicated that the *pat* phenotype could be due to an increase of the GA content (Testa *et al.*, 2002).

A further characterization of the *pat* mutant phenotype described that other pleiotropic effects are associated with the *pat* mutation (defects in cotyledon number and morphology, higher frequency of compound inflorescences, earlier flowering time, lower number of flowers per inflorescence and increased number of carpels per ovary; Olimpieri *et al.*, 2007). In the same study, the expression analysis of genes encoding key enzymes involved in GA biosynthesis showed that the transcriptional regulation of the *GA 20-oxidase1* (*GA20ox1*) gene was enhanced in the *pat* mutant ovary at the pre-anthesis stage. In addition, expression levels of genes involved in the control of GA synthesis (*KNOX* genes such as *LeT6/TKn2*, *LeT12* and *LeCUC2*) and response (*SPY*) were also altered in the *pat* ovary. These findings suggested that the *pat* mutation affects a regulatory gene located upstream of the control of fruit set exerted by GAs (Olimpieri *et al.,* 2007).

Successively, by a positional cloning approach, the locus of the *pat* mutation was mapped on the long arm of chromosome 3 (Beraldi *et al.*, 2004). Recently, through a candidate gene approach the tomato ortholog of *ATHB15* in Arabidopsis, also known as *CORONA* (*CNA*) or *INCURVATA4* (*ICU4*), was indicated as the gene candidate for the *pat* mutation (Selleri, 2010). *ATHB15/CNA/ICU4* is a TF belonging to the class III HD-Zip subfamily protein. Accordingly to this finding, in tomato, we named this gene

Solanum lycopersicum HB15 (*SlHB15*). Details regarding steps torward the positional cloning and the identification of *SlHB15* as the gene candidate for the *pat* mutation are given in Chapter 2.

The pat-2 *mutant*

Another important source of parthenocarpy has been described in the tomato cv Severianin. Philouze and Maisonneuve (1978) and Nuez *et al.* (1986) showed that the single recessive *pat-2* gene is responsible for parthenocarpy showed by this cultivar. The *pat-2* mutation is of particular interest because of its strong expressivity, its facultative character, and its simple genetic control (Philouze and Maisonneuve, 1978).
The quantification of endogenous GA levels in developing tomato ovaries showed an accumulation of very large amounts of GA_{20} in *pat-2* ovaries before anthesis (Fos *et al.*, 2000). This result suggests that the parthenocarpic behaviour showed by the *pat-2* mutant may be the result of the accumulation of GA_{20} in the parthenocarpic ovaries, leading to an early higher synthesis of active GA in the absence of pollination and fertilization (Fos *et al.,* 2000). Consistent with this finding, the *SlGA20ox1* gene was found highly expressed at the pre-anthesis stage in the ovary of both *pat* (Olimpieri et al., 2007) and *pat-2* (Serrani *et al*., 2007) mutants.
Moreover, a further characterization indicated that the parthenocarpic ability of the *pat-2* mutant depends also on elevated levels of polyamines in unpollinated mutant ovaries (Fos *et al.*, 2003).

The pat-3/pat-4 *mutant*

The *pat-3/pat-4* source of parthenocarpy (RP75/59) was described in a progeny from a cross between *Atom x Bubjekosko* (Philouze, 1983). Studies of RP75/59 have finally led to the acceptance of a genetic model with two genes involved, *pat-3* and *pat-4* (Nuez *et al.,* 1986).
Fos *et al.* (2001) investigated the role of GAs in the induction of the parthenocarpic fruit set in the German line RP75/59 in comparison with the near-isogenic WT line (cv Cuarenteno). The quantification of endogenous GAs showed that *pat-3/pat-4* developing ovaries at the pre-anthesis stage showed higher content of GA_1 and GA_3 compared to the WT line. These results suggested that also the parthenocarpic behaviour of *pat-3/pat-4* ovaries is the result of a higher content of active GAs in the absence of pollination and fertilization (Fos *et al.,* 2001). However, the change of GA metabolism produced by *pat-3/pat-4* is different respect to that found in the *pat*

(Olimpieri *et al.,* 2007) and *pat-2* (Fos *et al.,* 2000) mutants that is associated to an increase of GA_{20}.

Anyway, also the parthenocarpic phenotype showed by the *pat-3/pat-4* tomato mutant depends on GAs, but in contrast to the *pat* and *pat-2* mutants, the entire 13-hydroxylation pathway is enhanced in this mutant, resulting in a high content of GA_1 and GA_3 in the ovary before pollination (Fos *et al.,* 2001).

Objectives and outline of the thesis

This thesis aimed to the functional characterization of the *parthenocarpic fruit* mutation in tomato. The first goal of the research was to proof that the *SlHB15* gene, indicated in a previous study as the candidate for the *pat* mutation (Selleri, 2010), could be involved in biological processes that, if deregulated, lead to parthenocarpy. The second was to highlight differentially expressed genes in the WT and *pat* ovary during fruit set, in order to add information regarding molecular mechanisms underlying the parthenocarpic phenotype showed by this mutant.

In **Chapter 2**, using different bioinformatic tools, the amino acid substitution found in the SlHB15 protein encoded by the *pat* allele (Selleri, 2010) was predicted to be not tolerated for the protein function. As above reported, *SlHB15* is the tomato ortholog of the *ATHB15/CNA/ICU4* gene in Arabidopsis. In such a species, this TF is one of the five HD-Zip III members. Following blast and phylogenetic analyses, HD-Zip III ortholog genes were identified also in tomato and interesting cues regarding their expression were obtained by the RNA-seq experiment reported in the paper presenting the tomato genome (The Tomato Genome Consortium, 2012). According to these data, *SlHB15* was found as highly expressed in flower and fruit tissues during fruit set indicating its role in this process. Furthermore, following an *in silico* comparative approach, between *ATHB15/CNA/ICU4* in Arabidopsis and *SlHB15* in tomato, interesting highlights about its involvement in the regulation of IAA homeostasis in plant tissues and biological processes (e.g. flower development and fruit set) were found.

In **Chapter 3**, RNA interference and complementation experiments, for the genetic confirmation of the mutation, were pursued. So far, unfortunately, these approaches were not definitive due to different reasons, but promising observations of putatively *SlHB15*-silenced plants reinforced the hypothesis that *SlHB15* underlies the *pat* mutation. Furthermore, in order to find phenotypic similarities between *pat* and single mutants for its ortholog *ATHB15/CNA/ICU4 in* Arabidopsis, a characterization of the

cna-1 (loss-of-function) and *icu4-1* (gain-of-function) mutants for this gene, was performed. Interestingly, pleiotropic effects showed by *pat* (e.g. deviation of the number of cotyledons and aberrant ovules) associated to parthenocarpy, were also observed in these mutants, indicating again that *SlHB15* could represent the locus of the *pat* mutation.

In Chapter 4, a microarray experiment was performed in order to identify differentially expressed genes (DEGs) in the WT and *pat* ovary during fruit set. Based on their expression pattern, the DEGs were categorized in five group of clusters representing different biological trends. One of the most interesting group was named 'Controlling complex' and contained putative negative or positive regulators of fruit set (genes up- or down-regulated at pre-athesis in the WT ovary and deregulated in the *pat* mutant). Interesting genes belonging to this group encoded tomato orthologs of Arabidopsis TFs regulating the meristem differentiation and development of floral organs, such as SHOOTMERISTEMLESS (STM), BIG PETALp (BPEp), AINTEGUMENTA (ANT) and CRABS CLAW (CRC). These findings represented new insights, because so far these genes belonging respectively to the KNOX, bHLH, AP2/ERF and YABBY families of TFs had never been so directly associated to parthenocarpy. Finally, these TFs and other selected genes were studied also in other pathenocarpic systems (*pat-2*, *pat-3/pat-4*, *EMS-iaa9* and *RNAi-ARF7*) in order to increase the understanding of parthenocarpy in tomato and to find homologies between these different sources for such an agronomically important trait.

In **Chapter 5**, a genetic interaction study between *pat* and *Curl* (*Cu*), a mutation responsible for the overexpression of the gene *LeT6/TKn2* (tomato ortholog of *STM* in Arabidopsis) in vegetative and floral organs, was performed. Overall, the phenotypic and molecular characterization of the *pat Cu* double mutant confirmed findings previously reported (Olimpieri *et al.*, 2007) and indicated that KNOX family members, such as LeT6/TKn2, may act as negative regulators of the fruit set.

In the general discussion and conclusions (**Chapter 6**), results obtained during this project are discussed with regards to the highlighted role of *SlHB15* in flower development and fruit set. Moreover, the transcriptomic characterization performed comparing WT and *pat* ovaries during fruit set and the study of deregulated genes in *pat* also in other parthenocarpic systems, allowed us to propose an integrated model for partenocarpy in tomato that could be eventually extended also to other species.

Chapter 2

Bioinformatic characterization of *SlHB15*: the candidate gene underlying the *parthenocarpic fruit* mutation in tomato

Abstract

Currently, bioinformatics represents an integral part of many biological studies. In specific fields, such as genetics and genomics, it aids in annotating genomes and detecting DNA polymorphisms. Moreover, in structural biology, it might be usefull for the prediction of protein structures and molecular interactions. A previous research indicated *SlHB15* as the candidate gene underlying the *parthenocarpic fruit* (*pat*) mutation. SlHB15 is the tomato ortholog of the Arabidopsis transcription factor (TF) ATHB15, also known as CORONA (CNA) or INCURVATA 4 (ICU4). This TF is a member of the class III HD-Zip protein subfamily. In this Chapter, in order to predict the severity of the lesion found in the *SlHB15* allele of the *pat* mutant line and to gain information regarding the biological function of *SlHB15*, several bioinformatic approaches were used. *In silico* characterization, using different tools, predicted the G583R amino acid substitution occurring in the *pat* line to be not tolerated for the protein function, being responsible, as shown in the predicted 3D model, of an altered protein folding. The multiple protein alignment generated comparing SlHB15 with other 120 HD-Zip III sequences present in different databases, as depicted in the WebLOGO, highlighted a high conservation of G583 in HD-Zip III proteins and consequentely suggested its importance for a correct protein functionality. Using protein sequences of the five Arabidopsis HD-Zip III members, six ortholog genes in tomato were identified. The phylogenetic analysis indicated that the relationship among HD-Zip III members in Arabidopisis is conserved also in tomato and additionally showed that *SlHB15* has a paralogous gene that we named *SlHB15*-like. Furthermore, RNA-seq data were used to investigate the expression of the six identified tomato HD-Zip III members in different plant tissues and during flower/fruit development. This approach provided interesting cues regarding the expression of these genes in tomato.
In addition, the bioinformatic platform GeneMANIA, integrating genomics and proteomics data from Arabidopisis, was used to generate the functional association network of *ATHB15/CNA/ICU4*. Interestingly, this analysis highlighted relationships between this gene and TFs involved in the regulation of auxin (IAA) homeostasis during different developmental processes (i.e. flower development and fruit set). Among them, members of the Auxin Response Factors (ARF), Auxin/indole acetic acid (Aux/IAA), PIN-FORMED (PIN) and LIKE AUXIN RESISTANT (Aux/LAX) TF families were present. Because *SlHB15* and *ATHB15/CNA/ICU4* share 83.7% of identity at the amino acid level, it can be hypothesized that most of TFs interacting in Arabidopsis with *ATHB15/CNA/ICU4* could represent those interacting with *SlHB15* in tomato.

Introduction

The *parthenocarpic fruit* (*pat*) mutant phenotype was firstly ascribed to the action of two tightly linked genes, named *sha* for '*short anthers'* and *pat* for '*parthenocarpic fruit'* (Soressi and Salamini, 1975). The discovery of a spontaneous *sha-pat* mutation in the line "Montfavet 191" (Pecaut and Philouze, 1978) proved that the previously described phenotype was caused by a single recessive mutation with pleiotropic effects and the mutation was finally named *pat* (Philouze and Pecaut, 1986).

The *Pat* locus was mapped on the long arm of chromosome 3 and its position located in a genetic window spanning 1.2 centiMorgan (cM) between the conserved orthologous set (COS) sequences T0796 and T1143 (Beraldi *et al*., 2004) of the EXPEN2000 genetic map available at the Sol Genomics Network (SGN, http://www.sgn.genomics.net/; Fulton *et al*., 2002).

Recently, through genetic and physical mapping approaches, the genomic region between these two COS markers, was refined with new anchor-points and the *Pat* locus was confined within a region of about 0.2 cM between two internal BAC-developed markers named T17 and T20 (Selleri, 2010). The publication of the tomato genome sequence allowed the fine analysis of this target region and the integration of the two closest markers flanking *pat* (T17 and T20, corrisponding respectively to the *Solyc03g120880* and *Solyc03g120980* according to the gene nomenclature recently adopted by the SGN) into the scaffold sc03701 of the Tomato WGS Scaffolds Release (SL2.31) at the SGN website (Selleri, 2010). According to both this and last release (SL2.40), the genomic region defined by the T17 and T20 markers contains nine genes (from *Solyc03g120890* to *Solyc03g120970*). Among them, four genes involved in tomato reproductive processes and thus putatively responsible for the *pat* mutant phenotype were sequenced in the cv Chico III (WT) and in the near-isogenic *pat* line. In particular, the genomic DNA was sequenced for the *Solyc03g120910* (SGN description: Class III homeodomain-leucine zipper involved in the polarity of plant and floral organs; Prigge *et al.*, 2005; Bowman and Floyd, 2008), *Solyc03g120930* (SGN description: Avr9/Cf-9 rapidly elicited protein 146 involved in plant-microbe and putatively in pollen-pistil interactions; Rowland *et al.*, 2005; var der Hoorn *et al.*, 2005), *Solyc03g120960* (SGN description: STIG1 involved in pollen-pistil interaction; Goldman *et al.*, 1994; Tang *et al.*, 2004) and *Solyc03g120970* (SGN description: Gibberellin 2-beta-dioxygenase 2 involved in the gibberellin catabolism in plant and floral organs; Hu *et al.*, 2008; Rieu *et al.*, 2008a). After sequencing, a single point

mutation was found only in the coding DNA sequence (CDS) of the *Solyc03g120910*. Specifically, the *pat*-mutated allele presented a guanine (G) to adenine (A) transition in the CDS position 1747 of the tomato ortholog of *ATHB15,* also known as *CORONA* (*CNA*) or *INCURVATA4* (*ICU4*), in Arabidopsis (Selleri, 2010). The found mutation was in agreement with the action of the ethyl methanesulfonate (EMS), the chemical mutagen used by Soressi to induce the *pat* line (Bianchi and Soressi, 1969). This gene is composed by 18 exons and the G1747A nucleotide substitution in the *pat* allele is located in the exon 14th (Selleri, 2010). This lesion affects the first position of the codon 583 and is responsible of an amino acid change from glycine (Gly, G) to arginine (Arg, R) at the protein level (Selleri, 2010). In tomato, following these findings, the *Solyc03g120910* was named *Solanum lycopersicum HB15* (*SlHB15*).

ATHB15/CNA/ICU4 belongs to the class III Homeodomain-Leucine Zipper (HD-Zip III) subfamily of transcription factors (TFs) that in Arabidopsis comprises other four members named *ATHB8*, *ATHB9*/*PHAVOLUTA (PHV)*, *ATHB14*/*PHABULOSA* (*PHB*) and *INTERFASCICULAR FIBERLESS1 (IFL1)*/*REVOLUTA* (*REV*).

The HD-Zip III represents a subfamily of the HD-Zip family that in turn belongs to the HD-containing protein superfamily. The latter comprises other TF families such as, the knotted related homeobox (KNOX), plant homeodomain associated to a finger domain (PHD), BELL (named after the distinctive Bell domain), Wuschel related homeobox (WOX) and zinc finger associated to a homeodomain (ZF-HD). A schematic representation of the domains found in each family of HD-containing proteins is presented in Fig. 2.1 (Ariel *et al.*, 2007).

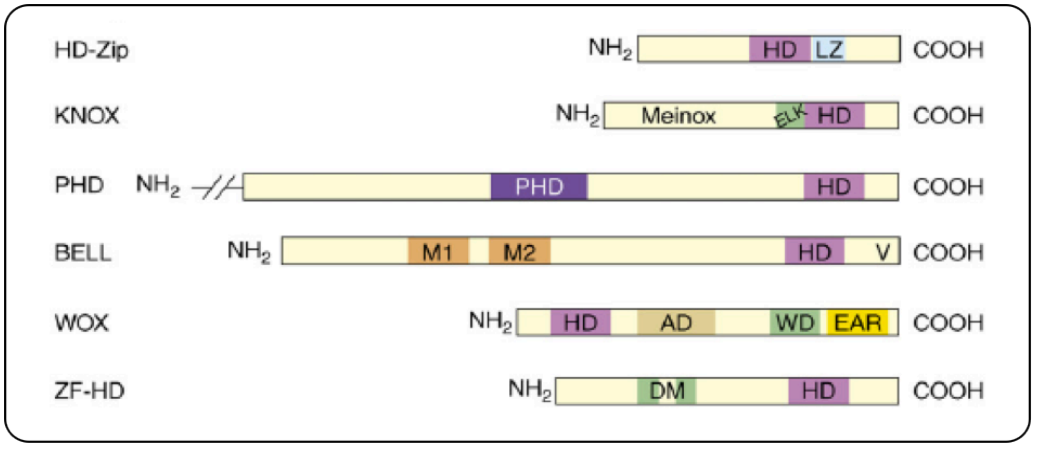

Fig. 2.1. Schematic representation of the distinctive domains exhibited by each family of HD-containing proteins. Abbreviations: AD, acidic domain; DM, dimerization motif; EAR, amphiphilic repression motif; ELK motif, named after the three conserved amino acids Glu, Leu and Lys in the one letter code; HD, homeodomain; LZ, leucine zipper; M1 and M2 conform the Meinox (association between MEIS and KNOX domains) interaction domain (MID); PHD, plant homeodomain; V, 'VSLTLGL' box; WD, WUS domain (from Ariel *et al.*, 2007).

Structurally, HD-containing proteins differ not only for the sequence encoding the HD, but also for their size and HD association with other domains. Moreover, they participate in a wide variety of processes during plant growth and development (Ariel *et al.*, 2007; Elhiti and Stasolla, 2009).

The HD-Zip family is characterized by the presence of two functional domains; the HD responsible for DNA binding and the LZ, located immediately C-terminal to the homeodomain, involved in protein-protein interaction. These two domains are also present in TFs of species belonging to other eukaryotic kingdoms, but their association in a single protein is unique to plants (Schena and Davis, 1992). HD-Zip proteins bind to DNA as homo- or heterodimers, and the absence of LZ absolutely abolishes their protein binding ability, which indicates that the relative orientation of the monomers, driven by this motif, is crucial for an efficient recognition of DNA (Ariel *et al.*, 2007). The classification of HD-Zip proteins in four subfamilies is supported by the following four distinguishing characteristics: (i) conservation of the HD-Zip domain that determine DNA-binding specificities, (ii) genes structures, (iii) additional conserved motifs and (iv) functions (Ariel *et al.*, 2007). A schematic representation of the four HD-Zip subfamilies is presented in Fig. 2.2 (Ariel *et al.*, 2007).

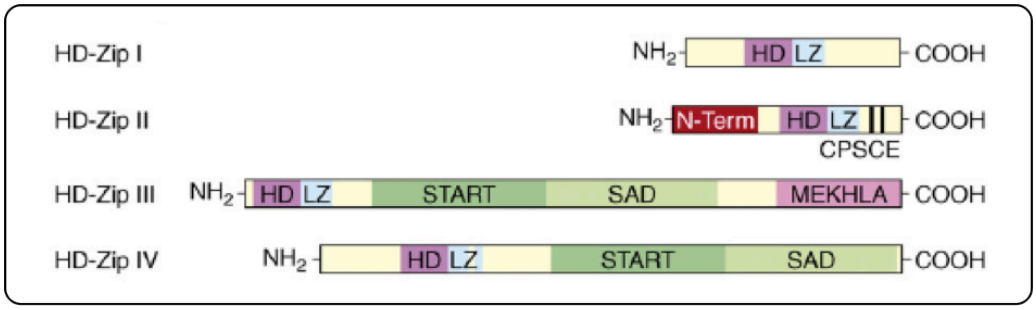

Fig. 2.2. Schematic representation of the distinctive features exhibited by each HD-Zip subfamily. Abbreviations: MEKHLA domain, named after the highly conserved amino acids Met, Glu, Lys, His, Leu, Ala in the one letter code; N-term, N-terminus consensus; SAD, START-adjacent domain; START, steroidogenic acute regulatory protein-related lipid transfer domain (from Ariel *et al.*, 2007).

In Arabidopsis, the HD-Zip I subfamily comprises 17 members encoding proteins of similar size (~35 kDa) including a well conserved HD domain and a less conserved LZ motif (Fig. 2.2). HD-Zip I proteins are generally involved in responses to abiotic stresses, abscisic acid and blue light and in de-etiolation and embryogenesis (Elhiti and Stasolla, 2009). HD-Zip II subfamily is composed of nine members (*ATHB2*/*HAT4*, *ATHB4*, *HAT1-HAT3*, *HAT9*, *HAT14*, *HAT17* and *HAT22*) in Arabidopsis (Tron *et al.*, 2002), characterized by the presence of a third domain, known as 'CPSCE', located downstream of the LZ motif and involved in cellular redox status perception (Fig. 2.2).

HD-Zip II TFs participate in light response, shade avoidance and auxin signalling (Elhiti and Stasolla, 2009). HD-Zip IV comprises 16 members in Arabidopsis and despite lacking a MEKHLA domain (described below), members of this group have a START and SAD motifs (Fig. 2.2; described below). HD-Zip IV proteins play significant roles during anthocyanin accumulation, differentiation of epidermal cells, trichome formation and root development (Elhiti and Stasolla, 2009).

HD-Zip III members present an additional loop formed by four amino acids between the HD and LZ domains. Among these TFs, more than a half of the amino acids are conserved and exhibit a common steroidogenic acute regulatory protein related lipid transfer (START) domain followed by an adjacent conserved region called START-adjacent domain (SAD). Although many START-containing proteins found in the animal kingdom have been well characterized, up to now no lipid ligands have been identified in plants (Schrick *et al.*, 2004). However, the high conservation of this motif achieved throughout evolution indicates that it likely plays a significant role in the regulatory activity (Ariel *et al.*, 2007). Additionally, all HD-Zip III members present a conserved domaim at the C-terminus, called MEKHLA that is a member of the Per-ARNT-Sim (PAS) domain superfamily (Magnani and Barton, 2011). PAS domains are signal sensors that regulate a wide range of signal transduction pathways in all kingdoms of life (Mukherjee and Bürglin, 2006). They respond to a variety of chemical and physical stimuli and regulate the activity of covalently linked effector domains, such as kinases, cyclases, ion channels and transcription factors (Magnani and Barton, 2011). The interaction between HD-Zip III and DNA is less studied than in the case of the other three HD-Zip subfamilies. Nonetheless, GTAAT(G/C)ATTAC was determined to be the extended sequence for which ATHB9 has the highest affinity *in vitro* (Elhiti and Stasolla, 2009). HD-Zip III proteins are known to play a role in many processes, such as meristem formation and regulation, embryonic shoot and root development, leaf polarity, vascular tissue establishment, plant architecture, lateral root primordia initiation, auxin transport and signaling (Zhong and Ye, 2001; Eshed *et al*., 2001; Emery *et al*., 2003; Prigge *et al*., 2005; Ochando *et al*., 2006; Scarpella *et al*., 2006; Izhaki and Bowman, 2007).

Starting from this background and in order to gain more information about the biological role of *SlHB15* and its codified protein in tomato, this chapter was developed with multiple aims: (i) to *in silico* predict the severity of the G583R amino acid substitution occurred in the SlHB15 protein codified by the *pat*-mutated allele, (ii) to highlight the HD-Zip III phylogenetic relationship in tomato and (iii) to hypothesize the involvement of HD-Zip III proteins in the regulation of flower development and fruit set.

Materials and methods

In silico *prediction of the* pat *mutation severity*

SlHB15 protein sequences encoded by both WT (cv Chico III) and *pat* alleles, previously deduced by sequencing (Selleri, 2010), were scanned using the Eukariotic Linear Motif (ELM) server (Dinkel *et al.*, 2012; http://elm.eu.org/) searching for putative functional protein sites. To predict the effect of the G583R amino acid change found comparing the SlHB15 from WT ($SlHB15^{WT}$) and from *pat* ($SlHB15^{pat}$) protein sequences, the Sorting Intolerant From Tolerant (SIFT) software was used (Kumar *et al.*, 2009; http://sift.jcvi.org/). This program was also adopted to generate a SlHB15 multiple protein alignment to highlight the degree of amino acid conservation by using the WebLOGO software (Crooks *et al.*, 2004; http://weblogo.berkeley.edu/). The 3D protein structure prediction server I-TASSER was adopted to generate the predicted molecular models of $SlHB15^{WT}$ and $SlHB15^{pat}$ proteins (Roy et *al.*, 2010; http://zhang.bioinformatics.ku.edu/ITASSER/).

Phylogenetic and transcriptomic analysis of HD-Zip III *genes in tomato*

HD-Zip III tomato genes were identified by the BLASTP tool available at the SGN (Bombarely *et al.*, 2011; http://solgenomics.net/) using Arabidopsis HD-Zip III protein sequences as queries against the last release (SL2.40) of the ITAG Release 2.3 predicted proteins database. Full-lenght protein sequences of the HD-Zip III in Arabidopsis were downloaded from The Arabidopsis Information Resource website (TAIR; http://www.arabidopsis.org/) and can be found in the Arabidopsis Genome Initiative (AGI) database under the following accession numbers: ATHB8 (At4g32880); ATHB9/PHV (At1g30490); ATHB14/PHB (At2g34710); ATHB15/CNA/ICU4 (At1g52150); IFL1/REV (At5g60690). The five HD-Zip III protein sequences from Arabidopsis and the six identified trough blasting in the tomato database were aligned by Geneious 5.6.3 (http://www.geneious.com/) and a phylogenetic tree was generated with the same software using Jukes-Cantor and Neighbor-Joining as genetic distance model and tree building method, respectively. The phylogentetic analysis was performed according to 1000 bootstrap replicates. Furthermore, in order to gain more information about the expression of the HD-Zip III genes in tomato, a transcriptomic investigation was performed according to RNA-seq data reported in the Supplementary Table 1 of the paper presenting the tomato genome (The Tomato Genome Consortium, 2012).

In silico *prediction of the* SlHB15 *functional association network*

The GeneMania web interface (Warde-Farley *et al.*, 2010; http://www.genemania.org/) was used to obtain information about molecular interactions and biological functions of *ATHB15/CNA/ICU4*. Currently, this bioinformatic platform integrates genomics and proteomics data from six model organisms (*Arabidopsis thaliana*, *Caenorhabditis elegans*, *Drosophila melanogaster*, *Mus musculus*, *Homo sapiens* and *Saccharomyces cerevisiae*). Considering that ATHB15/CNA/ICU4 and SlHB15 proteins are identical for the 83.7%, it can be hypothesized that most of the genes present in the functional association network, generated quering the platform with the Arabidopsis *ATHB15/CNA/ICU4* gene, could putatively represent those interacting with *SlHB15* in tomato.

Results and discussion

Severity prediction of the G583R amino acid substitution occurring in the SlHB15 *gene encoded by the* pat *allele*

As previously described by Selleri (2010), the CDS of the *SlHB15* gene encoded by the *pat* allele compared to WT showed a G1747A transition in the 14th exon (Fig. 2.3A). At the protein level, this point mutation is responsible for the G583R amino acid change located between SAD and MEKHLA domains (Fig. 2.3B). G583R belongs to a sequence of three highly conserved amino acids (SGF) in other 120 putative HD-Zip III proteins found by SIFT in protein databases. The multiple protein alignment generated by SIFT was used to define the degree of amino acid conservation in the SlHB15 protein as depicted by using the WebLOGO software (Fig. 2.3C).

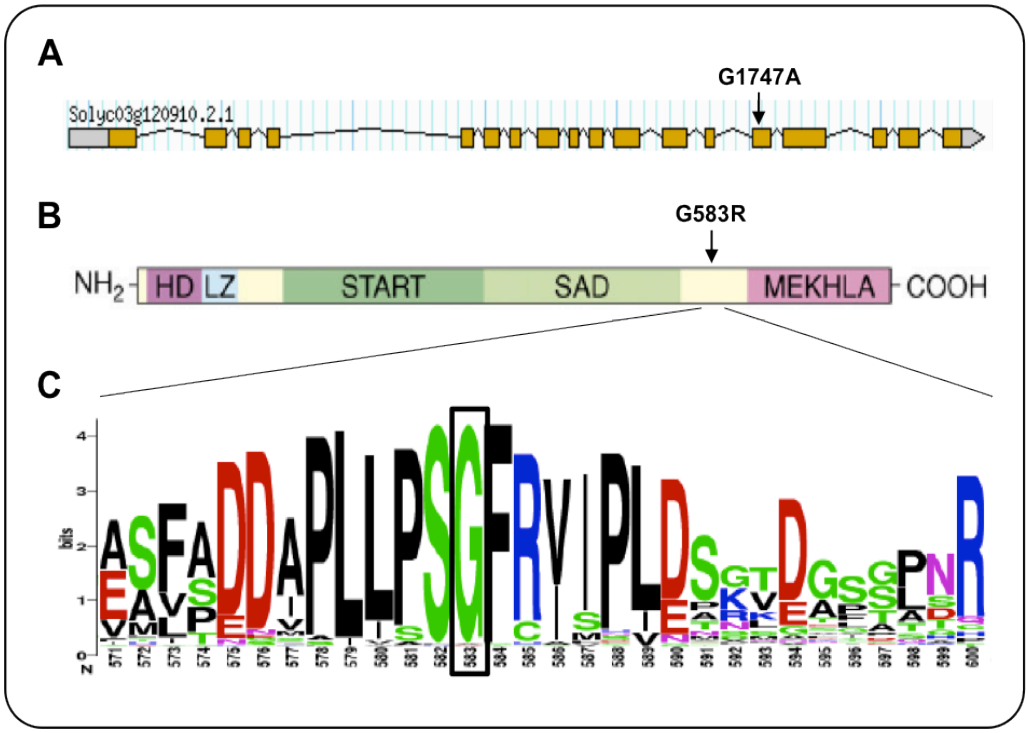

Fig. 2.3. (A) *SlHB15* gene model (Solyc03g120910.2.1) as reported at the SGN website. Grey boxes indicate 5' and 3' UTRs. Yellow boxes and black horizontal lines represent exons and introns, respectively. The arrow points the G1747A transition found in the 14th exon of the *SlHB15 pat* allele. (B) Schematic representation of HD-Zip III proteins (from Ariel *et al.*, 2007). HD, LZ, START, SAD and MEKHLA represent the five HD-Zip III characteristic domains (see text). The arrow points the G583R amino acid change occurring in the SlHB15 protein encoded by the *pat* allele. (C) WebLOGO of a 30 aa-portion between SAD and MEKHLA domains of the SlHB15 WT protein showing the high degree of conservation of G583 (black square; see text). Amino acids have different colors according to their chemical properties (Crooks *et al.*, 2004 and reference therein).

The G583R substitution was predicted as deleterious for the SlHB15 TF activity using the SIFT software (not shown). SIFT does not account for active or conserved domains, but bases its prediction on amino acid physical properties and on the level of conservation of each amino acid in the sequence after an alignment search in different protein sequence databases (Kumar *et al.*, 2009).

The 3D structure of the SlHB15 WT protein (SlHB15^{WT}) and its G583R mutated *pat* variant (SlHB15^{pat}) was predicted using the I-TASSER server (Roy *et al.*, 2010). Comparison of these 3D models, distinguishing WT and *pat* genotypes, highlighted structural differences between SlHB15^{WT} and SlHB15^{pat} (Fig. 2.4). The protein folding of SlHB15^{pat} was notably destructurated compared to the prediction of the SlHB15^{WT} protein (Fig. 2.4).

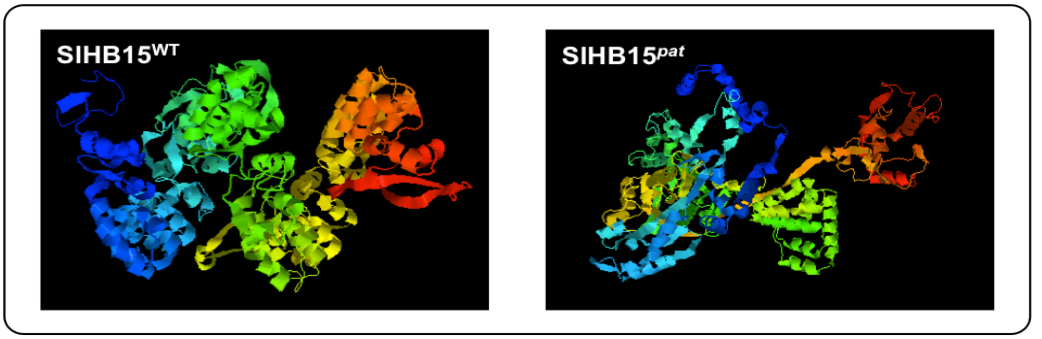

Fig. 2.4. I-TASSER prediction of the 3D structure models of SlHB15^{WT} and SlHB15^{pat} proteins.

Putatively, structural modifications occuring in the SlHB15^{pat} mutated protein, altering important domains (i.e. HD, LZ and START) for its TF activity, could be responsible for a reduction of protein functionalities, such as interaction with the DNA of target gene promoters and/or homo-heterodimerization.

SlHB15^{WT} and SlHB15^{pat} protein sequences were scanned using the ELM software for the presence of short linear motifs (SLiMs) that are protein regulatory modules spanning three to 11 contiguous amino acids (Dinkel *et al.*, 2012). This analysis showed several hits for both proteins (not shown). In SlHB15^{WT} the only motif spanning G583 was the GlcNHglycan (aa 581-584, PSGF) known to be important for cell communication and playing a role during morphogenesis and development in animal kingdoms such as Metazoa (Perrimon and Bernfield, 2001). In plants, these motifs are present in arabinogalactan proteins that have been involved in plant reproductive development, pattern formation, and somatic embryogenesis, as well as in the underlying processes of cell division, cell expansion, and cell death (Nothnagel, 1997; Estévez *et al.*, 2006).

After submitting the SlHB15^{pat} protein to the same analysis, results highlighted interesting cues. Indeed, the G583R substitution was predicted to be responsible for the lost of the GlcNHglycan motif and at the same time for the formation of three additional SLiMs (originated by the G583R aa change) not present in SlHB15^{WT}.
Specifically, the first "gained" motif by the SlHB15^{pat} protein was Scr-homology 3 (SH3, aa 578-583, PLLPSR). This domain has been characterized in Arabidopsis as involved in protein-protein interaction and vescicle trafficking (Lam and Blumwald, 2002 and reference therein). The second was represented by the SPAK-OSR1 docking motif (aa 583-587, RFRII). SPAK (Ste20/Sps1-related proline/alanine-rich kinase) and OSR1 (oxidative stress-responsive-1) are related kinases belonging to the GCK-VI subfamily of Ste20 group kinases (Lee *et al.,* 2009). In plants, SPAK and OSR1 transducer kinases are downstream interacting proteins of WNK (with no lysine = K) kinase *osmosensors* controlling osmotic homeostasis (Kahle *et al.*, 2008). In addition, WNK kinases were recently characterized in Arabidopsis as important regulators of flowering time by modulating the photoperiod pathway (Wang *et al.*, 2008). The last "new" formed motif in SlHB15^{pat} is the Protein Kinase B (PKB, aa 583-591, RFRIISLES). PKB proteins are mainly described in animals (Anthony *et al.*, 2004), but they share high similarities with AGC (cAMP-dependent protein kinase A/cGMP-dependent protein kinase G/protein kinase C) kinases found in plants and described to regulate important developmental processes and defense responses (Hirt *et al.*, 2011). Despite interesting cues obtained by the ELM analysis, being *pat* a mutation inherited as recessive, there is not evidence that the three SLiMs formed by chance in the SlHB15^{pat} protein could have a role in the expression of the mutant phenotype.
Overall, predictions conducted with SIFT and I-TASSER bioinformatic tools, together with the high G583 conservation level highlighted by the multiple protein alignment with other 120 putative HD-Zip III proteins, suggest that the *pat* mutant phenotype could be caused by a modification of the SlHB15^{pat} protein functionality.

Phylogenetic and transcriptomic analysis of the HD-Zip III protein subfamily in tomato

To our knowledge, members of the HD-Zip III protein subfamily has never been studied in tomato. This is the first time that HD-Zip III members are described in this species. Blast analyses conducted at the SGN website clearly indicated that a tomato ortholog gene exists for all the five HD-Zip III Arabidopsis members. Identified tomato HD-Zip III genes are reported in Table 2.1.

Table 2.1. Arabidopsis and tomato HD-Zip III genes paired according to their protein sequence similarity.

Arabidopsis			Tomato			Pairwise Identity (%)
Gene name	**TAIR locus ID**	**Protein length (aa)**	**Gene name**	**SGN locus ID**	**Protein length (aa)**	
ATHB8	*At4g32880*	833	*SlHB8*	*Solyc08g066500*	827	78.9
ATHB9/PHV	*At1g30490*	841	*SlHB9*	*Solyc02g069830*	842	73.7
ATHB14/PHB	*At2g34710*	852	*SlHB14*	*Solyc02g024070*	851	78.3
ATHB15/CNA/ICU4	*At1g52150*	837	*SlHB15**	*Solyc03g120910*	836	83.7
			SlHB15-like	*Solyc12g044410*	837	81.5
IFL1/REV	*At5g60690*	842	*SlIFL1*	*Solyc11g069470*	841	80.9

* Candidate gene underlying the *pat* mutation in tomato.

HD-Zip III genes found in the tomato genome were named according to their degree of homology with Arabidopsis members. Loci of the six HD-Zip III tomato genes reside in different chromosomes, except *SlHB9* (*Solyc02g069830*) and *SlHB14* (*Solyc02g024070*) that are both located on chromosome 2. In tomato, *SlHB15* (*Solyc03g120910*) presents a parologous gene with a different chromosomal location that we named S*lHB15*-like (*Solyc12g044410*).

Arabidopsis and tomato HD-Zip III full-lenght protein sequences were aligned to study their phylogenetic relationship by drawing a dendrogram (Fig. 2.5). The alignment highlighted that, as already reported (Ariel *et al.*, 2007; Elhiti and Stasolla, 2009 Mukherjee *et al.*, 2009), HD-Zip III proteins are remarkably well conserved and display the five characteristic domains (not shown). The dendrogram resulting from the Arabidopsis and tomato sequences comparison highligthed that the phylogentic relationship among HD-Zip III in Arabidopsis is conserved also in tomato (Fig. 2.5).

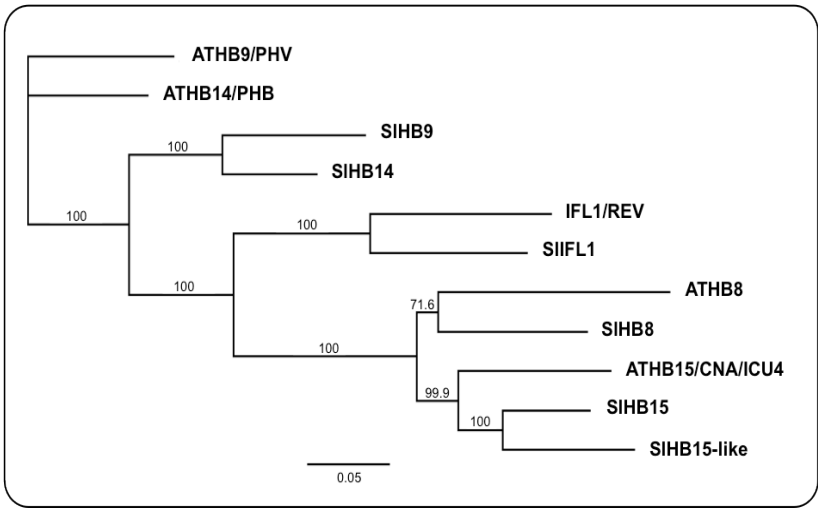

Fig. 2.5. Phylogenetic tree of tomato and Arabidopsis HD-Zip III proteins. Neighbour-joining tree based on full-length protein alignment that shows percentage bootstrap support at each node (n = 1000). Scale bar = number of amino acid substitutions per site.

A further investigation on tomato HD-Zip III genes was performed according to the transcriptomic analysis conducted on the cv Heinz 1706 (tomato genome reference line) and reported in the Supplementary Table 1 of the paper presenting the tomato genome (The Tomato Genome Consortium, 2012). Relative expression of the six tomato HD-Zip III genes, according to the RNA-seq experiment performed in different plant tissues and during different stages of flower and fruit development, was evaluated and reported in Table 2.2.

Table 2.2. Normalized expression of the six tomato HD-Zip III genes based on RNA-seq data reported in the Supplementary Table 1 of the paper presenting the tomato genome (The Tomato Genome Consortium, 2012). Data are the mean ± SEM of the relative expression assayed in two biological replicates.

Gene name	RNA-seq normalized expression (mean ± SEM)							
	Leaf	**Root**	**Flower bud**	**Fully open flower**	**1 to 3 cm fruit[a]**	**MG[b] fruit**	**B[c] fruit**	**B + 10[d] fruit**
SlHB8	8.4 ± 0.1	44.9 ± 2.6	4.5 ± 0.2	5.7 ± 0.1	7.6 ± 3.5	1.7 ± 0.2	0.1 ± 0.0	0.2 ± 0.1
SlHB9	4.4 ± 0.1	10.9 ± 0.6	3.6 ± 0.2	3.4 ± 0.1	4.9 ± 0.6	4.2 ± 0.1	3.9 ± 0.4	10.3 ± 0.0
SlHB14	8.4 ± 0.1	17.5 ± 0.6	15.1 ± 0.3	4.0 ± 0.3	3.0 ± 0.8	0.5 ± 0.1	0.2 ± 0.0	0.1 ± 0.0
SlHB15	10.1 ± 0.2	26.5 ± 1.2	15.3 ± 1.0	19.9 ± 0.3	22.9 ± 9.4	23.7 ± 0.7	9.2 ± 0.1	6.6 ± 0.3
SlHB15-like	15.8 ± 0.4	30.5 ± 0.6	13.2 ± 0.8	14.3 ± 1.0	7.0 ± 0.1	11.0 ± 0.0	4.2 ± 0.1	25.4 ± 1.3
SlIFL1	13.6 ± 0.3	50.6 ± 1.1	9.8 ± 0.3	14.7 ± 0.7	14.8 ± 0.9	12.0 ± 0.1	8.2 ± 0.8	14.0 ± 1.1

[a] Data obtained using the three means of 1, 2 and 3 cm fruit stages obtained respectively with RNA-seq normalized expression values from the two biological replicates per stage (1, 2 and 3 cm, respectively). The SEM is relative to the mean of the value obtained from the three different stages. [b] MG stands for mature green stage. [c] B stands for breaker (early ripening) stage. [d] B + 10 stands for 10 days post breaker (red ripe) stage.

According to this transcriptomic analysis, *SlHB15* shows the highest expression level compared to the other HD-Zip III genes during flower and early fruit development (Table 2.1). This finding could suggest that among the HD-Zip III members, *SlHB15* plays the major role during tomato fruit set and that functional alterations of this gene could lead to parthenocarpy as hypothesized in the *pat* mutant where the functionality of its protein has been predicted to be altered by bioinformatic means.

SlHB8 together with *SlHB15*-like and *SlIFL1* present the highest expression levels in leaves and roots. Except *SlHB8* and *SlHB14*, all the others HD-Zip III TFs show a considerable expression during fruit ripening (Table 2.1). Notably, *SlHB15*-like peaks at the red ripe fruit stage, indicating a putative role in the regulation of ripening-associated metabolic processes (Table 2.1). In tomato, all these transcriptomic cues regarding HD-Zip III genes represent a novelty, because up to now this HD-Zip subfamily has been never characterized in this species.

In silico *prediction of the* SlHB15 *functional association network*

As reported in Table 2.1, *SlHB15* and its ortholog *ATHB15/CNA/ICU4* in Arabidopsis share 83.7% of identity at the amino acid level. Starting from this observation and considering that in the GeneMANIA a *Solanum lycopersicum* transcriptomic and proteomic database is not implemented, we used *ATHB15/CNA/ICU4* as query gene on this bioinformatic platform (Warde-Farley *et al.*, 2010). Following this comparative approach, the *ATHB15/CNA/ICU4* functional association network was generated (Fig. 2.6). Thus, it was possible to hypothesize that a similar molecular network could be present in tomato for *SlHB15*.

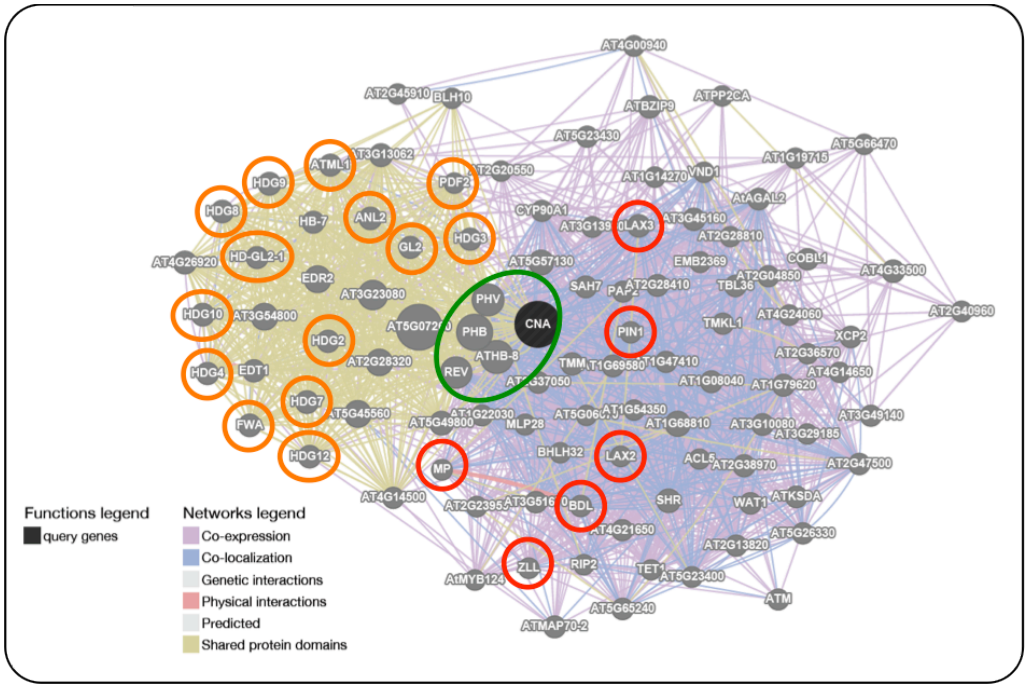

Fig. 2.6. GeneMANIA functional association network generated using *ATHB15/CNA/ICU4* as query. A hundred genes are presented in the molecular network. HD-Zip III protein family members are circled in green and HD-Zip IV (sharing protein domains) are circled in orange. Red-circled genes are those related with auxin metabolism/response (see text).

The GeneMANIA software, integrating genomics and proteomics data from Arabidopisis, was queried to generate a network with 100 genes related to *ATHB15/CNA/ICU4* for different factors (co-expression, co-localization, genetic interactions, physical interactions, predicted and sharing protein domains).

As expected, all the five members of the Arabidopsis HD-Zip III protein subfamily were present in the network since they share protein domains and are both co-expressed and co-localized in Arabidopsis tissues such as the shoot apical meristem (SAM), leaf

primordia, vasculature and ovules (Fig. 2.6; Green *et al.*, 2005; Prigge *et al.*, 2005 Williams *et al.*, 2005; Kelley *et al.*, 2009). Additionally to HD-Zip III proteins, members of the HD-Zip IV subfamily were also greatly represented in the network (Fig. 2.6) as having in common with ATHB15/CNA/ICU4 four (except the MEKHLA) of the five HD-Zip III domains (Fig. 2.2; Ariel *et al.*, 2007).

In the network, *ATHB15/CNA/ICU4* was found to be co-expressed and/or co-localized with many auxin (IAA)-related genes such as *MONOPTEROS* (*MP*, also known as *ARF5* and *IAA24*) and *BODENLOS* (*BDL*, also known as *IAA12*) belonging respectively to the Auxin Response Factors (ARF) and Aux/indole acetic acid (Aux/IAA) protein families. In Arabidosis, these two TFs physically interact at the protein level and are both involved in the formation of vascular bundles and in the initiation of the embryo body axis (Hardtke and Berleth, 1998; Hamann *et al.*, 1999; 2002). Notably, expression of *MP* was also observed in immature ovules and gynoecium vascular tissues during flower development (Hardtke and Berleth, 1998).

Interestingly, other IAA-related genes involved in auxin signaling and transport were present in the network. Specifically, the ARGONAUTE (AGO) family member *ZWILLE* (*ZLL,* also known as *PINHEAD* and *AGO10*), *PIN-FORMED1* (*PIN1*), *LIKE AUXIN RESISTANT2* (*Aux/LAX2*) and *LAX3*.

ZLL encodes AGO10, a member of the elongation Initiation Factor 2C (eIF2C) protein family. Along with *WUSCHEL* (*WUS*) and *CLAVATA* (*CLV*) genes, controls the relative organization of the central and peripheral zone cells in meristems (Tucker *et al.*, 2008). Acts in embryonic provascular tissue potentiating the WUS function during meristem development in the embryo (Moussian *et al.*, 1998; Tucker *et al.*, 2008). AGO10 specifically sequesters miR165/166 (targeting HD-Zip III genes) to regulate the SAM development (Tucker *et al.*, 2008). *PIN1* encodes an auxin efflux carrier involved involved in the maintenance of the auxin gradient in all developing plant tissues (Petrášek and Friml, 2009). Loss-of-function severely affects organ initiation, *pin1* mutants show an inflorescence meristem that does not initiate any flowers, resulting in the formation of a naked inflorescence stem (Vernoux *et al.*, 2000). *LAX2* and *LAX3* encode auxin influx carriers that are respectively required for vascular patterning in cotyledons and promotion of lateral roots emergence (Péret *et al.*, 2012; Swarup *et al.*, 2010).

PIN and Aux/LAX protein families have been recently described to regulate in tomato the polar auxin transport within specific flower and fruit tissues (Pattison and Catalá, 2012). A regular spatial and temporal IAA accumulation leading to fruit initiation is achieved only after pollination and fertilization. Mounet *et al.* (2012), specifically

silencing the *SlPIN4* family member in tomato obtained plants setting seedless fruits, indicating that altering the function of specific members of such families could lead to parthenocarpy.

In tomato, considering these observations and findings, one could hypothesize that *SlHB15* is implyed in a similar functional association network. Consistent with this hypothesis, in the *pat* mutant some pleiotropic effects such as an altered number of cotyledons (Olimpieri *et al.*, 2007), aberrations of stamens and ovules (Mazzucato *et al.*, 1998), and parthenocarpy could be strongly associated with an altered polar auxin transport.

Chapter 3

Functional characterization of the *HB15* gene in tomato and Arabidopsis

Abstract

In order to confirm that *SlHB15* is the gene underlying the *pat* mutation in tomato, two functional approaches were pursued. The first was the obtainment of *SlHB15*-silenced plants by RNA interference (RNAi) with the attempt to phenocopy the mutant phenotype and the second was the genetic complementation of the *pat* mutant with the CDS of the WT allele of *SlHB15*. So far, results obtained through RNAi and complementation experiments are not definitive due to different reasons, such as difficulty of genetic transformation and gene structure complexity for making constructs associated to the complex biological scenario in which the gene is involved. Phenotypic observations of putatively RNAi-*SlHB15* silenced regenerants suggested that *SlHB15* is plausibly the candidate gene underlying the *pat* mutation, but at the same time paved the way for the use of more specific silencing approaches (e.g. use of tissue-specific or inducible promoters) for its genetic confirmation. Presently, despite transgenic experiments have not been definitive yet, comparative phenotypic studies conducted on Arabidopsis single *ATHB15/CNA/ICU4* loss- and gain-of-function mutants reinforced the hypothesis that the mutation found in its tomato ortholog *SlHB15* is responsible for the *pat* mutant phenotype. Indeed, alterations of plant organs together with the parthenocarpic behavior, displayed by *cna-1* (loss-of-function) and *icu4-1* (gain-of-function) single mutants for *ATHB15/CNA/ICU4* in Arabidopsis, recall pleiotropic effects and parthenocarpy-associated traits exhibited by the *pat* mutant in tomato.

Introduction

Over the years, it has been determined that different subsets of genes encoding for the HD-Zip III subfamily proteins are involved in different developmental events, playing overlapping, antagonistic or distinct roles in Arabidopsis (Prigge *et al.*, 2005). In general, HD-Zip III transcription factors (TFs) are functionally well characterized as developmental regulators of the shoot apical meristem (SAM), leaf polarity, vasculature development, auxin signaling and transport (Zhong and Ye, 2001; Emery *et al*., 2003; Prigge *et al*., 2005; Scarpella *et al*., 2006; Izhaki and Bowman, 2007). Their expression patterns have been fully described, and are in complete agreement with the roles they play (Prigge *et al.*, 2005).

HD-Zip III genes such as *INTERFASCICULAR FIBERLESS1* (*IFL1*)/*REVOLUTA* (*REV*), *ATHB9/PHABULOSA* (*PHB*) and *ATHB14/PHAVOLUTA* (*PHV*) control the pattern of apical formation during embryo development (Prigge *et al.*, 2005; Izhaki and Bowman, 2007). Mutant analyses demonstrated the role of *REV* and *PHB* in regulating SAM maintenance and lateral organ initiation (Otsuga *et al.*, 2001). Regulation of these morphogenic processes might be caused by changes in auxin flow, since several HD-Zip III members have been implicated in events leading to changes of polar auxin transport (Bowman and Floyd, 2008).

Several studies have elucidated the mode of action of *REV*, *PHB* and *PHV*, together with *KANADI* family genes in controlling abaxial-adaxial patterning of lateral organs (Emery *et al.*, 2003). The abaxilation process and phloem differentiation are initiated by *KANADI* genes which also repress the expression of *REV*, *PHB* and *PHV*. This repression is gradually released and expression of these genes inhibits *KANADI* through feedback mechanisms resulting in the adaxilation of the lateral organ and xylem formation (Bowman and Floyd, 2008). *ATHB8* is also implicated in the vasculature development (Baima *et al.*, 2001). Indeed, production of xylem is significantly increased in Arabidopsis plants overexpressing this gene, suggesting its role in inducing the differentiation of xylem elements (Baima *et al.*, 2001). *ATHB8*, together with *ATHB15,* also known as *CORONA* (*CNA*) or *INCURVATA4* (*ICU4*), downregulates the action of *REV* in lateral shoot meristems as well as during floral meristem formation (Ariel *et al.*, 2007). The plant stature is redundantly regulated by each of the five HD-Zip III proteins, although it remains unclear how this is achieved (Prigge *et al.*, 2005; Prigge and Clark, 2006).

All five HD-Zip III genes are both transcriptionally and post-transcriptionally regulated. Their mRNAs are targets of the miRNAs miR165 and miR166 (Byrne, 2006; Zhong and Ye, 2007). In Arabidopsis plants overexpressing these miRNAs, *PHB*, *PHV* and *ATHB15/CNA/ICU4* have been shown to be downregulated (Kim *et al.*, 2005; Williams *et al*., 2005). Accordingly, when their target sequences are mutated in the *PHB, PHV* and *ATHB15/CNA/ICU4* mRNAs, a gain-of-function of these genes is observed, revealing their participation in the leaf polarity determination and meristem maintenance (McConnell *et al.*, 2001; Mallory and Vaucheret, 2006; Ochando *et al.*, 2006). Besides, miRNA targeting to the *PHB* transcript also influences the methylation status of the *PHB* locus (Bao *et al.*, 2004). Considering that the *PHV* gene is also methylated in the 3' region, one might expect that all HD-Zip III genes are regulated at multiple levels (Byrne, 2006; Ariel *et al.*, 2007).

Different *ATHB15/CNA/ICU4* single mutants have been characterized. The *corona-1* (*cna-1*) loss-of-function mutant was isolated after an EMS-mutated population screening and described as an enhancer of the phenotype showed by *clavata* (*clv*) mutants (Green *et al.*, 2005). The *CLV* gene was described to regulate the size of the SAM and floral meristem (Clark *et al.*, 1997). In the *clv-1 cna-1* double mutant, the meristem crown developed around the main SAM and showed an increased size, hence the name '*corona*'. The *cna-1* mutated allele carries a point mutation responsible for the amino acid substitution from alanine to valine at the position 606 of the protein in a domain of unknown function, between SAD and MEKHLA (Green *et al.*, 2005).

The *cna-2* null mutant was obtained by T-DNA insertion in the CDS region encodying the leucine zipper domain of the protein (Prigge *et al.*, 2005). Its mutant phenotype was mainly characterized for the alteration of vascular bundles (Prigge *et al.*, 2005).

The *incurvata4-1* (*icu4-1*) gain-of-function mutant resulted from a point mutation altering the sequence of the mRNA complementary to miRNA165/166 (Ochando *et al.*, 2006). This mutant showed an altered vegetative phenotype with curved leaves, having an excess of stomates and smaller epidermal cells (Ochando *et al.*, 2006).

Another recently isolated mutant for *ATHB15/CNA/ICU4* is *hoc.* This mutation causes the replacement of the highly conserved serine 701 with a cysteine in the MEKHLA domain (Duclercq *et al.*, 2011). Among all the single *ATHB15/CNA/ICU4* mutants described so far, *hoc* displays the most dramatic vegetative phenotype (Catterou *et al.*, 2002). This mutant is bushy due to extra rosette leaves developing from early axillary meristems and it has the ability to regenerate whole plants *in vitro* without added phytohormones (Duclercq *et al.*, 2011). In this characterization, these authors studied

also knockout lines for T-DNA insertion, mainly affected in the gene promoter region, and interestingly observed that each one of them showed a different, but nearly-normal WT vegetative phenotype, indicating that a dissimilar alteration of *ATHB15/CNA/ICU4* could produce different phenotypes.

Recently, despite their recognized role for the regulation of the vegetative plant development, *ATHB15/CNA/ICU4, PHB*, *PHV* and *REV* have been described to play a fundamental role in the formation of ovule integuments (Kelley *et al*., 2009). Indeed, both the single *phv-1d* gain-of-function and triple *cna phb phv* loss-of-function mutants mutants showed aberrant ovules with a not properly formed integuments and an exposed nucellus (Kelley *et al*., 2009), reminding *pat* in tomato (Mazzucato *et al*., 1998).

The *pat* mutant displays, besides parthenocarpy, pleiotropic effects that involve anther and ovule phenotypes. In *pat* mutant flowers, the anthers show partial homeotic transformation into carpel-like structures, seldom bearing external ovules, whereas ovules in the ovary show arrested integument growth with the absence of meiosis and consequent non-viability (Mazzucato *et al.*, 1998).

Other pleiotropic effects associated with the *pat* phenotype involve cotyledons. In fact, nearly all the seedlings of the near-isogenic WT line show normal cotyledon number and morphology; conversely, in the *pat* mutant line, about one-fourth of the seedlings displays cotyledon phenotypes deviating from the normality. Among such deviations, the most common is the presence of tricots; but tetracots and fused cotyledons are also observed (Olimpieri *et al.*, 2007).

Experiments reported in this Chapter were performed in order to confirm that the G583R amino acid substitution found in the SlHB15 protein encoded by the *pat* allele (see Chapter 2) is responsible for the mutant phenotype. Moreover, considering all the above reported studies, we decided to perform a phenotypic characterization of Arabidopsis single mutants for *ATHB15/CNA/ICU4* in order to search for similarities with phenotypes displayed by *pat* in tomato. In particular, we focused on vegetative and reproductive traits of *cna-1* (Green *et al.*, 2005) and *icu4-1* (Ochando *et al.*, 2006), respectively loss- and gain-of-function mutants for this gene in Arabidopis.

Materials and methods

Preparation of RNAi and complementation constructs

For the gene silencing approach, an *in silico* analysis was conducted to select the most appropriate region of the *SlHB15* gene (*Solyc03g120910*) for the RNAi targeting purpose. The full-length cDNA was blasted using BLASTX against the release SL2.31 of the Tomato Whole Genome Sequence Chromosomes database at the SGN (Bombarely *et al.*, 2011; http://www.solgenomics.net/). This analyisis was performed to select a region with low degree of homology with other tomato sequences to avoid the silencing of other genes. The *SlHB15* cDNA was also scanned for the presence of restriction sites targeted by cloning enzymes using NEBcutter V2.0 (http://tools.neb.com/NEBcutter2/). After these analyses, an *SlHB15* target region suitable for RNAi was identified and a fragment of 249 bp was amplified by polymerase chain reaction (PCR) from the cDNA extracted from WT (cv Chico III) ovaries at the flower bud stage (Stage 2; Mazzucato *et al.*, 1998). cDNA was prepared according to Materials and Methods presented in Chapter 4. At both fragment extremities, a sequence recognized by two different pairs of restriction enzymes was introduced by PCR using the following primers: forward (5'-TCTAGA*CTCGAG*ATGGAGTGTGCCTG AGTC-3'; *XbaI* and *XhoI* restriction sites underlined and italic, respectively) and reverse (5'-ATCGAT*GGTACC*CCATTCCATCACTATCCAGCA-3'; *ClaI* and *KpnI* restriction sites underlined and italic, respectively). PCR amplification was performed in a 50 µl of total volume, containing 5 µl of ten-fold diluted cDNA, 0.5 µM of each primers, 200 µM of dNTPs, 1X DreamTaq Buffer, and 1 U of DreamTaq DNA polymerase (Fermentas). The amplification was conducted with an initial step of 4 min at 94°C that was followed by 36 cycles of 1 min at 94°C, 30 s at 58°C and 30 s at 72°C, plus 7 min of final extension at 72°C. The amplicon was purified from 1.5% agarose gel using the GFX PCR DNA and Gel Band Purification Kit (GE Healthcare, Little Chalfont, Buckinghamshire, UK) and ligated into the TA site of the pGEM-T easy system (Promega) using the T4 DNA Ligase (Fermentas) following manufacturer's instructions. The ligation reaction was used to transform *Escherichia coli* DH5α competent cells. Plasmid minipreparations of colonies positive for the presence of the target RNAi fragment, assessed by PCR using universal T7 and SP6 primers, were cut with different combinations of restriction enzymes. Two consecutive digestions with *XhoI-KpnI* and *XbaI-ClaI* were performed to obtain the sense (S) and antisense (AS) arm, respectively. The cloning vector pKANNIBAL for RNAi application was obtained

from the Australian Plant Industry Company CSIRO (http://www.csiro.au/). This vector carries the *Cauliflower Mosaic Virus* (*CaMV*) 35S promoter and the *octopine synthase* (*OCS*) terminator separated with the *pyruvate orthophosphate dikinase* (*Pdk*) intron flanked by two polylinkers. Each polylinker contains the restriction sites for the introduction respectively of the sense and antisense arm (Wesley *et al.*, 2001). This vector was firstly opened with *XhoI-KpnI* to accept the S arm. After transformation and confirmation of transformed DH5α compentent cells, this intermediate construct (pKANNS-*SlHB15*) was opened to accept the AS arm with *XbaI-ClaI* for the obtainment of the complete RNAi vector (pKANNSAS-*SlHB15*). The entire RNAi cassette was then excised from this vector using *NotI* and introduced in the binary vector *pART27* (Gleave, 1992) previously linearized with the same restriction enzyme. This final RNAi construct (pARTSAS-*SlHB15*) was sequence verified and used to transform *Agrobacterium tumefaciens* competent cells of the strains GV3101 and EHA105. Positive colonies were checked by PCR and used for plant transformation experiments.

For the complementation assay, the full-length CDS of the *SlHB15* gene (2511 bp) was amplified from the cDNA of WT ovaries at opening flower stage (Stage 3). cDNA preparation is described in Materials and Methods of Chapter 4. At both extremities of the CDS, a sequence recognized by two different restriction enzymes was introduced by PCR using the following primers: forward (5'-CCCGGGATGGCTTCCTGCAAGGATGG-3'; *SmaI* restriction site underlined) and reverse (5'-GAGCTCTTAGACAAATGACCAGTTGAC-3'; *SacI* restriction site underlined). PCR amplification was performed in a 50 µl of total volume, containing 5 ul of ten-fold diluted cDNA, 0.4 µM of each primer, 200 µM of dNTPs, 1X FastStart High Fidelity Reaction Buffer, and 2.5 U of FastStart High Fidelity *Taq* DNA polymerase (Roche). The amplification was conducted with an initial step of 2 min at 95°C that was followed by 36 cycles of 30 s at 95°C, 30 s at 60°C and 3 min at 72°C, plus 7 min of final extension at 72°C. The PCR product was purified from 0.8% agarose gel using the GFX PCR DNA and Gel Band Purification Kit (GE Healthcare, Little Chalfont, Buckinghamshire, UK) and ligated into the TA site of the pGEM-T easy system (Promega) using the T4 DNA Ligase (Fermentas) following manufacturer's instructions. The ligation reaction was used to transform *Escherichia coli* DH5α competent cells. Positive plasmid minipreparations were cut with *SacI* and *SmaI* to recover from 0.6% agarose gel the full-length *SlHB15* CDS to be introduced into the pBI121 vector under the control of the *CaMV* 35S promoter and the *nopaline synthase* (*NOS*) terminator (Chen *et al.*, 2003). Before cloning SlHB15 complementation construct the *β-glucoronidase* (*GUS*) gene was removed from the

pBI121 vector using *SacI* and *SmaI*. The obtained final construct (pBI121-*SlHB15*) was sequence verified and used to transform *Agrobacterium tumefaciens* competent cells of the strains GV3101 and EHA105. Positive colonies were screened by PCR and used for plant transformation experiments.

Plant material and transformation

Agrobacterium tumefaciens GV3101 and EHA105 strains were transformed with the RNAi (pARTSAS-*SlHB15*) and complementation (pBI121-*SlHB15*) constructs. For silencing, WT cotyledons of the tomato cv MicroTom (MT-WT) were used. Conversely, for complementation experiments, cotyledons of the *pat* mutant line in the cv Chico III (near-isogenic WT background of *pat*) were employed. The protocol used for plant genetic transformation was based on those described by Sun *et al.* (2006) and de Jong *et al*. (2009b).

Phenotypic characterization of Arabidopsis ATHB15/CNA/ICU4 *mutants and comparison with* pat *in tomato*

A phenotypic characterization of single mutant lines for *ATHB15/CNA/ICU4*, the Arabidopsis ortholog of *SlHB15* (see Chapter 2), was performed in order to understand if lesions in this gene could lead to altered floral phenotypes similar to those displayed by *pat* in tomato. Phenotypic analyses were conducted comparing mutant lines with their respective WT genotypes: *cna-1* (loss-of-function allele; Green *et al.*, 2005) and its Col-0 WT background were kindly provided by G. Morelli, INRAN, Italy; *icu4-1* (gain-of-function; Ochando *et al.*, 2006) and its En-2 WT background were kindly supplied by J.L. Micol, Universidad Miguel Hernández, Spain. Twenty plants of each genotype were cultured at 24 ± 2°C in a growth chamber under 16 h of light and 8 h of dark. By stereomicroscopy, five-d-old seedlings were scored for the presence of cotyledon alterations. The general plant size and leaf morphology was evaluated at 15, 25 and 40 days after germination (DAG). Twelve plants of each genotype were used to estimate the flowering time, according to the DAG until emergence of the first inflorescence. For comparison, the flowering time was also evaluated in six WT and *pat* tomato plants grown in open field during summer at the experimental station of the Tuscia University (Viterbo, Italy), scoring the DAG until the first flower of the first floral truss was fully opened. By stereomicroscopy, from the same 12 plants used to evaluate the flowering time, data regarding the size and/or morphology of flowers at anthesis, mature siliques and ovules, were collected. The remaining eight plants, of each genotype, were used

for an emasculation experiment in order to study the parthenocarpic behaviour of their siliques. Materials and Methods used to evaluate the parthenocarpic behaviour of WT and *pat* ovaries in tomato are reported in Chapter 5. At maturity, seed size and morpholgy was also evaluated. All the collected data are presented as mean ± standard error of the mean (SEM). Statistical significance was assessed by the Student's *t* test. Finally, because mutants of the HD-Zip III subfamily in Arabidopsis display vasculature alterations (Prigge *et al.*, 2005), we evaluated this trait also in WT and *pat* tomato plants to see if similar alterations could be present. This characterization was carried out using 30-d-old plants. Six individuals from both genotypes were cultured at 24 ± 2°C in a growth chamber under 16 h of light and 8 h of dark. To study the plant vasculature, hand made cross-sections of hypocotyl and epicotyl, respectively 1 to 2 cm below and above cotyledons, were stained in a phlorogluginol-satured solution 20% HCl in the dark (Jensen, 1962) and after 10-15 min immediately photographed at the stereomicroscope.

Results and discussion

Silencing of SlHB15 *by RNA interference*

Five different RNAi transformation experiments were performed using MT-WT seeds. Overall, we tried to genetically transform about 800 cotyledons with the pARTSAS-*SlHB15* RNAi construct (Fig. 3.1). In these experiments, two different *Agrobacterium tumefaciens* strains (GV3101 and EHA105) were employed.

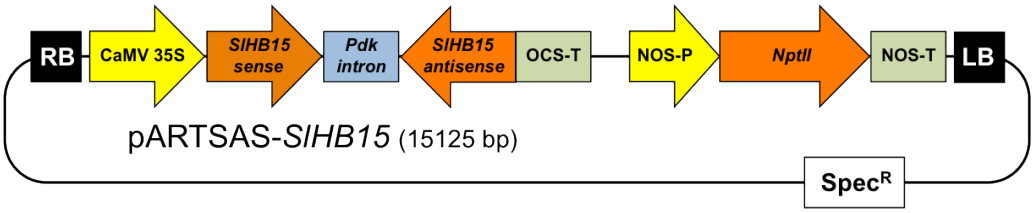

Fig. 3.1. Schematic representation of the T-DNA region of the RNAi construct pARTSAS-*SlHB15* (15125 bp). RB and LB represent right and left T-DNA borders, respectively; CaMV 35S and OCS-T, represent respectively promoter and terminator driving the RNAi cassette (*SlHB15* sense arm - Pdk intron - *SlHB15* antisense arm); NOS-P and NOS-T, represent respectively the promoter and terminator driving the *nopaline phosphotrasferase II* (*nptII*) gene conferring resistance to Kanamycin.

The first two trials, using 320 cotyledonary explants (240 and 80 in the first and second, respectively) failed to give any putative transformant. In both experiments, after one month, explants from positive control plates (C+, no co-cultivation without kanamycin) formed shoots, conversely to cotyledons from both negative control (C-, no co-cultivation with kanamycin) and co-cultivated (CO-C, co-cultivated with Agro GV3101 harbouring the pARTSAS-*SlHB15* with kanamycin) plates (Fig. 3.2).

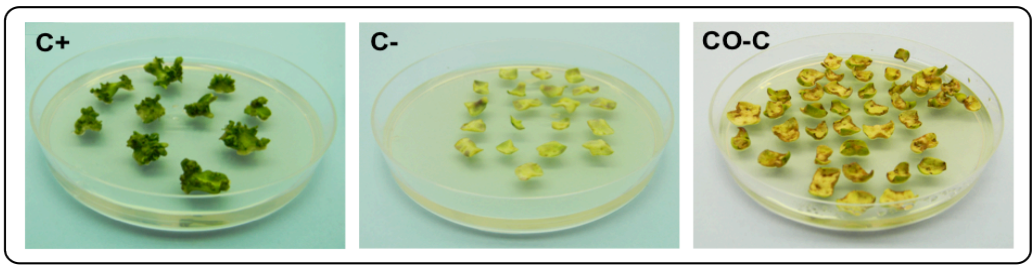

Fig. 3.2. Phenotype of explants from positive control (C+), negative control (C-) and co-cultivated (CO-C) plates after one month of transformation experiment (see text).

On the one hand, this first result suggested that there could be some problems related to the co-cultivation phase, but on the other hand, indicated that the employed transformation medium had the right composition, because C+ explants were able to develop shoots (Fig. 3.2).

In the third trial (120 explants), changing the Agro concentration for co-cultivation, putatively T_0 transformed plants or tissues were obtained. One putative primary *SlHB15*-silenced plant was able to form roots in the selective medium containing kanamycin. It exhibited a disorganized plant development, a reduced leaf complexity, thick and/or hairy roots (Fig. 3.3A) compared to *in vitro* MT-WT control plants (not shown). These vegetative alterations might be due to a constitutive silencing of *SlHB15.* In fact, its ortholog *ATHB15/CNA/ICU4* in Arabidopisis has been described to be important for the differentiation of plant organs (Green *et al.*, 2005; Prigge et al., 2005; Ochando *et al.*, 2006; Duclercq *et al.*, 2011). In addition, this putative transformed plant showed also a reduction of leaf complexity reminding the tomato mutant *entire* (Dengler, 1984) and knockout plants for the gene *SlIAA9* (Wang *et al.*, 2005). Interestingly, these genotypes confer the competence to set parthenocarpic fruits (Wang *et al.*, 2005; Zhang *et al.*, 2007).

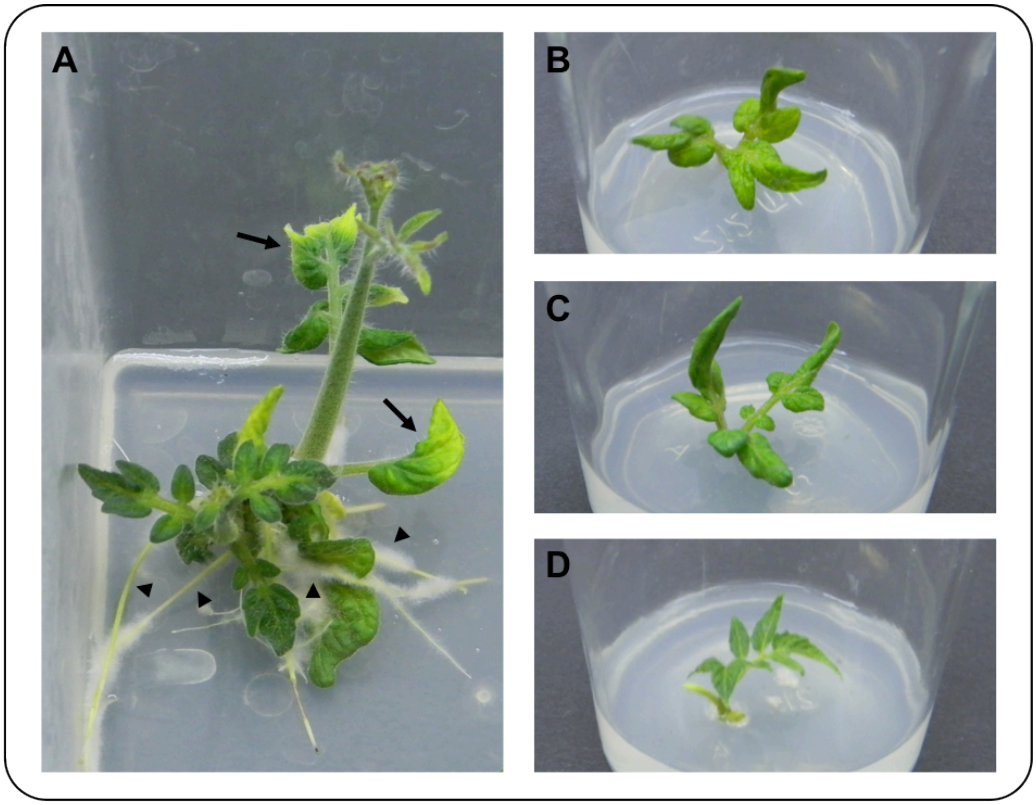

Fig. 3.3. (A) Phenotype of the putative RNAi-*SlHB15* transformed plant, showing *entire*-like leaves (*arrows*) and thick and/or hairy roots (*arrowheads*). (B and C) *entire*-like phenotype showed by leaves respectively of two explants, derived from the plant showed in A, which lost their rooting capability in the selecting medium after two sub-cultivation cycles. (D) Normal compound leaf phenotype of an *in vitro* cultured MT-WT explant.

Explants derived from this plant, after two sub-cultivation cycles, lost their capacity of rooting in the selective medium, but were still showing *entire*-like leaves (Fig. 3.3B and C) compared to normal compound leaves produced *in vitro* by MT-WT explants (Fig. 3.3D). Their loss of rooting capacity could be attributed to the fact that the initial plant presented chimeric tissues.

In the same trial, independent calli from other co-cultivated plates developed vegetative meristems lacking shoot and leaf primordia (Fig. 3.4A-C). Putatively, this phenotypic observation suggested that the silencing of *SlHB15* driven by the constitutive promoter *CaMV* 35S could be too strong for a correct plant development. Another possibility might be that the *SlHB15* fragment selected for RNAi was able to silence also other tomato HD-Zip III members leading to the production of lethal phenotypes. Consistent with this idea, the quintuple mutant for all the five HD-Zip III members in Arabidopsis is seedling lethal (Prigge *et al.*, 2005).

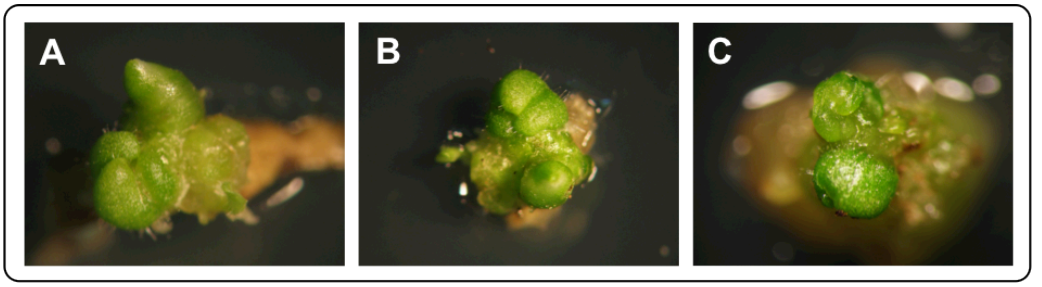

Fig. 3.4. (A, B and C) Meristems lacking shoot and leaf promordia developed by independent calli from different co-cultivated plates with the Agro GV3101 strain harbouring the RNAi pARTSAS-*SlHB15* construct.

In the same transformation trial, another putative transformed explant organized a floral meristem able to accomplish its developmental process and to set a single flower. Surprisingly, if compared with a flower set *in vitro* by a MT-WT plant (Fig. 3.5A-D), it presented features phenocopying the *pat* mutant (Fig. 3.5E; Mazzucato *et al.*, 1998), producing an enlarged ovary (Fig. 3.5F), malformed stamens (short and carpelloid) lacking pollen sacs (Fig. 3.5G) and aberrant ovules (Fig. 3.5H).

The phenotype showed by this single flower, produced by putatively silenced tissues, suggested that *SlHB15* represents the gene underlying the *pat* mutation. Unfortunately, it was not possible to replicate and confirm at molecular level this promising observation because, again, the last two transformation trials (300 explants), using both Agro GV3101 and EHA105 strains, harbouring the pARTSAS-*SlHB15* construct, failed to give any putative *SlHB15*-silenced plant.

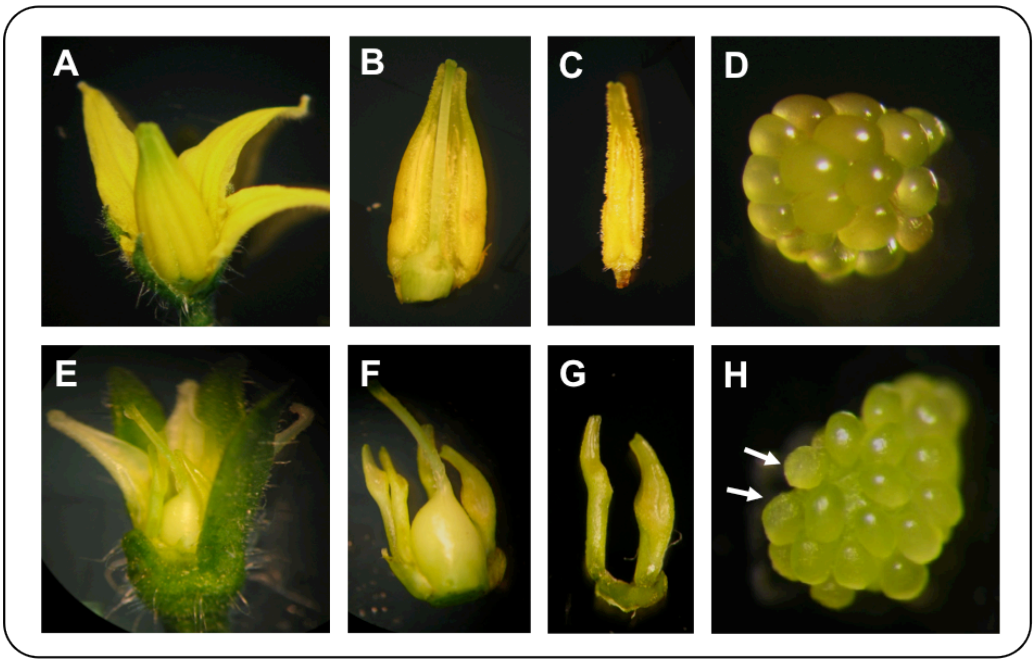

Fig. 3.5. (A) Flower set *in vitro* by a MT-WT plant. (B, C and D) WT phenotype showed by the ovary, anther and ovules of this flower. (E) Phenotype of the single flower produced *in vitro* by a floral meristem putatively transformed with the pARTSAS-*SlHB15* construct. (F, G and H) Enlarged ovary, malformed stamens and aberrant ovules (*arrows*), respectively showed by this flower (see text).

Complementation of the pat *mutant line with the* SlHB15 *WT allele*

The pBI121-*SlHB15* construct obtained for the complementation approach is presented in Fig. 3.6. So far, it was possible to carry out only one preliminary transformation experiment. In this trial, 120 cotyledonary explants of the *pat* mutant line were employed. Unfortunately, also in this case, we could not recover any putative complemented transformed plants.

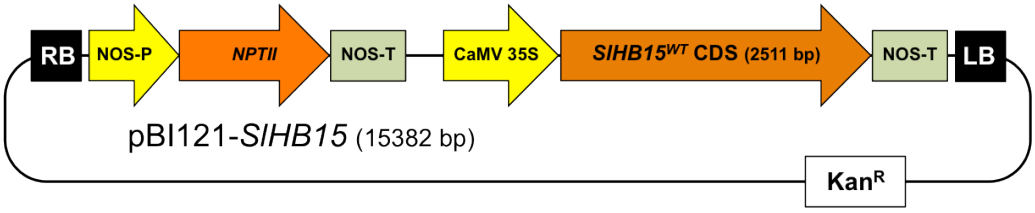

Fig. 3.6. Schematic representation of the T-DNA region of the complementation construct pBI121-*SlHB15* (15382 bp). RB and LB represent right and left T-DNA borders, respectively; CaMV 35S and NOS-T, represent respectively promoter and terminator driving the *SlHB15*^{WT} CDS (2511 bp); NOS-P and NOS-T, represent respectively the promoter and terminator driving the *nopaline phosphotrasferase II* (*nptII*) gene conferring resistance to Kanamycin.

In conclusions, despite promising phenotypic observations obtained in one silencing transformation trial, RNAi and complementation experiments were not successful due to technical and/or biological reasons putatively related to the role of this gene for the

differentiation of plant organs. To exclude technical problems, other experiments using both the developed RNAi (Fig. 3.1; pARTSAS-*SlHB15*) and complementation (Fig. 3.6; pBI121-*SlHB15*) constructs have to be performed. They could provide the definitive proof that *SlHB15* represent the *Pat* gene and eventually give interesting insights about the function of *SlHB15* for plant development in tomato. Simultaneously, it could be useful to follow other transgenic approaches (e.g. use of tissue-specific or inducible promoters) for gene confirmation.

Phenotypic characterization of Arabidopsis ATHB15/CNA/ICU4 *single mutants: looking for similarities with* pat *in tomato*

Unequivocally, blast and phylogenetic analyses conducted in Chapter 2 indicated that *SlHB15,* the gene identified as candidate for the *pat* mutation (Selleri, 2010)*,* is the tomato ortholog of the HD-Zip III gene *ATHB15/CNA/ICU4* in Arabidopsis.

The vegetative phenotype of single mutants affected in this gene, such as *cna-1*, *cna-2*, *icu4-1* and *hoc*, has been characterized in different studies (Green *et al.*, 2005; Prigge *et al.*, 2005; Ochando *et al.*, 2006; Duclercq *et al.*, 2011), but reproductive traits of such mutants have never been described in detail.

In tomato, the *pat* mutant shows aberrant ovules lacking the growth of the single integument (Fig. 3.7A; Mazzucato *et al.*, 1998). Recently, it has been determined that different HD-Zip III members (i.e. *ATHB15/CNA/ICU4, PHB, PHV* and *REV*) in Arabidopsis are important for the adaxial-abaxial definition of the ovule integuments primordia (Kelley and Gasser, 2009). Consistent with these findings, the single *phv-1d* gain-of-function mutant exhibited aberrant ovules (Fig. 3.7B; Kelley *et al.*, 2009), strongly reminding those set by *pat* in tomato. Previously, a similar phenotype was also described in onother gain-of-function HD-Zip III mutant (*phb-1d*)*.* In *phb-1d* ovules, the timing of the initiation and growth of both integuments is disrupted, producing ovules with elongated inner integument (McConnell and Barton, 1998). Interestingly, this mutant showed also abaxial-adaxial polarity defects of stamens (McConnel and Barton, 1998), as *pat* anthers do in tomato (not swown; Mazzucato *et al.*, 1998). Because both *phb-1d* and *phv-1d* dominant mutations represent miRNA-resistant alleles of *PHB* and *PHV*, these data imply that a proper regulation of *PHB* and *PHV* expression patterns via miR165/166 action is required for the normal development of ovule integuments (Kelley *et al.*, 2009). Additionally, these phenotypes were similar to those observed in the triple *cna phb phv* loss-of-function mutant (Fig. 3.7C; Kelley *et al.*, 2009), suggesting that a deviation from the normal level of adaxializing activity

produced by *PHB*, *PHV* and *CNA* may directly influence integument morphogenesis (Kelley *et al.*, 2009). Parallel thoughts can be made for the *pat* mutant in tomato, where a predicted reduction/modification of the SlHB15^{pat} protein functionality (see Chapter 2) and/or a reduction of the gene expression (see Fig. 4.5 in Chapter 4), due to disrupted positive feedback regulation mechanisms, could lead to the formation of aberrant ovules.

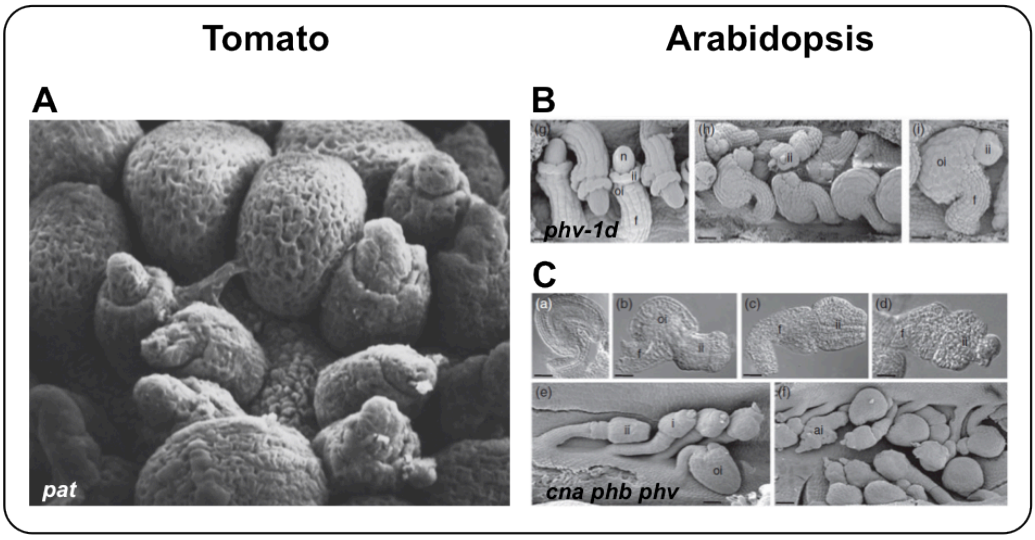

Fig. 3.7. (A) Normal and aberrant *pat* ovules impaired in the growth of the single integument in tomato (from Mazzucato *et al.*, 1998). (B and C) Normal, nearly-normal and aberrant ovules produced respectively by the *phv-1d* (single gain-of-function) and *cna phb phv* (triple loss-of-function) mutants in Arabidopsis (from Kelley *et al.*, 2009).

Moreover, Kelley *et al.* (2009) showed that *ATHB15/CNA/ICU4*, *PHB* and *PHV* act in concert with *ABERRANT TEST SHAPE* (*ATS*, also known as *KANADI4*) and *REV* to regulate the differentiation of ovule integuments. By the characterization of quadruple *cna phb phv ats* and *cna phb phv rev/+* mutants, it has been hypothesized that loss of *ATHB15/CNA/ICU4* activity may be a predominant component of the mutant phenotype (Kelley *et al.*, 2009).

Starting from these observations and in order to evaluate if also single mutants for this gene could produce similar ovular phenotypes to those showed by *pat* in tomato and by the above described HD-Zip III mutants in Arabidopsis, we performed a phenotypic characterization of the single mutants *cna-1* (Green *et al.*, 2005) and *icu4-1* (Ochando *et al.*, 2006).

Interestingly, defects of cotyledons (tricots), similar to those observed in *pat* (Fig. 3.8A), were present in about 10% of five-d-old seedlings produced by the *icu4-1* gain-of function mutant (Fig. 3.8B).

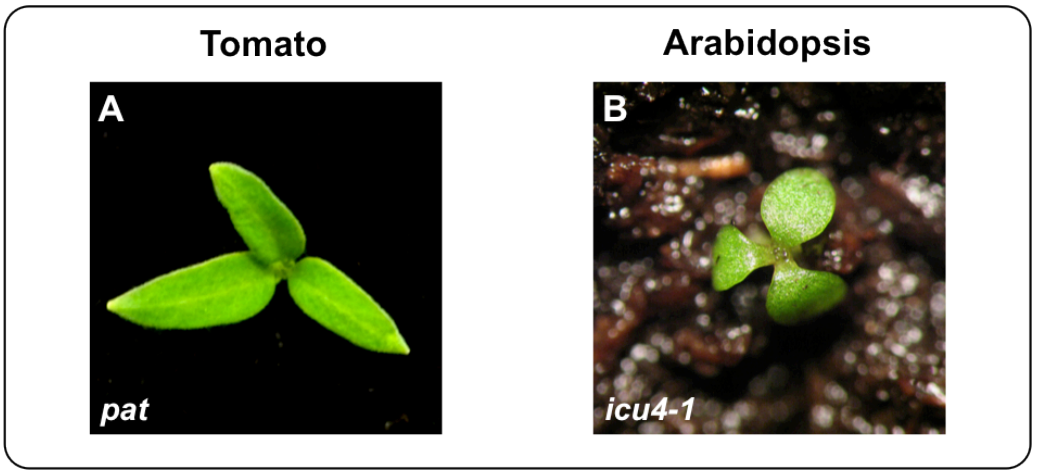

Fig. 3.8. (A and B) *pat* and *icu4-1* seedlings producing tricotyledons in tomato and Arabidopsis, respectively.

As already reported, *icu4-1* presented also other vegetative alterations such as curved (Fig. 3.9E; Ochando *et al.*, 2006) and supernumerary rosette leaves (Fig. 3.9F) compared to its En-2 WT counterpart (Fig. 3.9D and F, respectively).

Apparently, cotyledon alterations were not displayed by the *cna-1* loss-of-function mutant (not shown), but a general reduction of the plant size (Fig. 3.9B) and the number of rosette leaves (Fig. 3.9C) was evident, if compared to the Col-0 WT background (Fig. 3.9A and C, respectively).

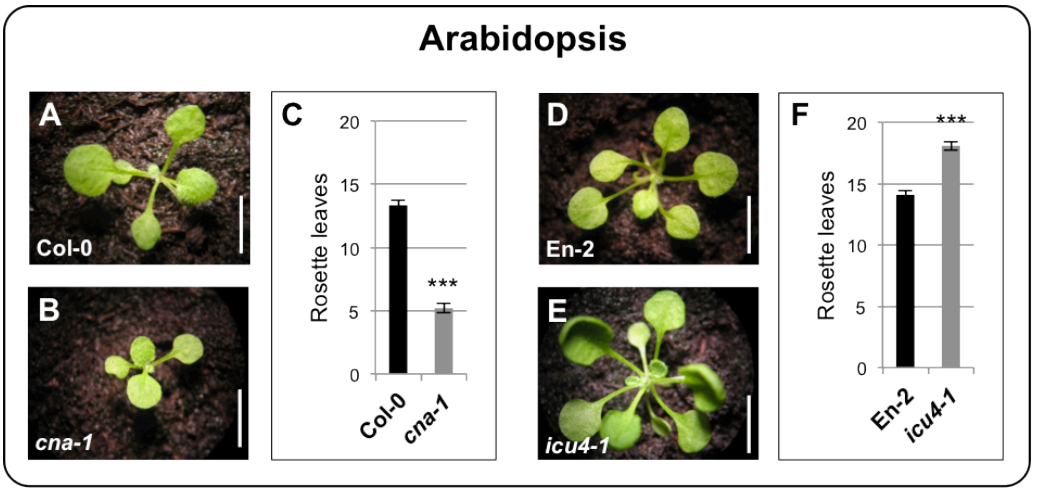

Fig. 3.9. (A and B) Plant phenotype of Col-0 and *cna-1* at 15 days after germination (DAG). (C) Number of rosette leaves in Col-0 and *cna-1* at 25 DAG. (D and E) Plant phenotype of En-2 and *icu4-1* at 15 DAG. (F) Number of rosette leaves in En-2 and *icu4-1* at 25 DAG. Scale bars indicate 1 cm (A, B, D and E). In C and F, the statistical significance was assessed by Student's *t* test (n = 12). ***, P≤0.001.

In tomato, the *pat* mutant set flowers earlier than its near-isogenic WT line (Fig. 3.10A). Interestingly, as *pat*, the *cna-1* mutant in Arabidopsis, when compared to Col-0 plants,

showed a similar phenotype (Fig. 3.10B). Conversely, *icu4-1* did not display a significant reduction of the flowering time compared to the En-2 WT background (Fig. 3.10C).

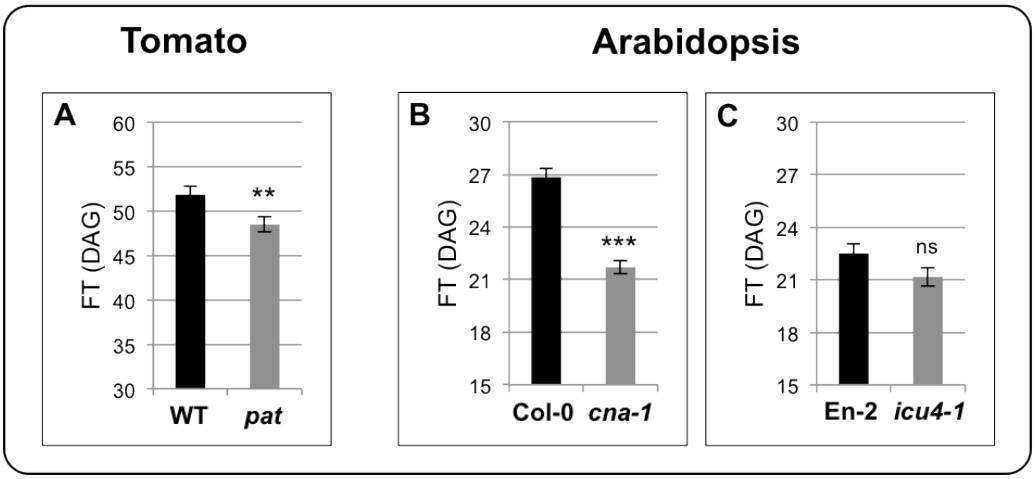

Fig. 3.10. (A) Flowering time (FT) in WT and *pat* tomato plants. (B) FT in Col-0 and *cna-1* loss-of-function mutant plants. (C) FT in En-2 and *icu4-1* gain-of-function mutant plants. DAG stands for days after germination. Statistical significance was assessed by Student's *t* test between genotypes (A, WT vs *pat*; B, Col-0 vs *cna-1*; C, En-2 vs *icu4-1*). In A (n = 6), B and C (n = 12). ^{ns}, not significant; **, P≤0.01; ***, P≤0.001.

The characterization of these vegetative traits, in both *cna-1* and *icu4-1* single mutants, highlighted alterations similar to those displayed by *pat* in tomato and reinforced the hypothesis that *SlHB15* could be the real gene for the mutation. Moreover, these findings indicated that *ATHB15/CNA/ICU4* alone, if mutated, could affect the plant stature (*cna-1*) and cotiledonary development (*icu4-1*). Deviations of cotyledons were often associated to a deregulation of the polar auxin transport, as observed in other Arabidopsis mutants, such as *cup-shaped cotyledon1* (*cuc1*) and *cuc2* (Takada *et al.*, 2001). Notably, as *pat* in tomato, the *cuc1 cuc2* double mutant displays aberrant ovules lacking the growth of the outer ovule integument (Ishida *et al.*, 2000).

In tomato, the size of the WT ovary at anthesis (Fig. 3.11A) is significantly smaller when compared to *pat* (Fig. 3.11B). At this developmental stage, the WT ovary has just started its differentiation and growth program triggered by pollination and ovule fertilization. Conversely, the *pat* ovary has already started its autonumous parthenocarpic ovary growth and figures bigger. Interestingly, a similar phenotype was observed in pistils at anthesis of both *cna-1* and *icu4-1* mutants, that appeared respectively thicker (Fig. 3.11D) and longer (Fig. 3.11F) than their Col-0 (Fig. 3.11C) and En-2 (Fig. 3.11E) WT counterparts.

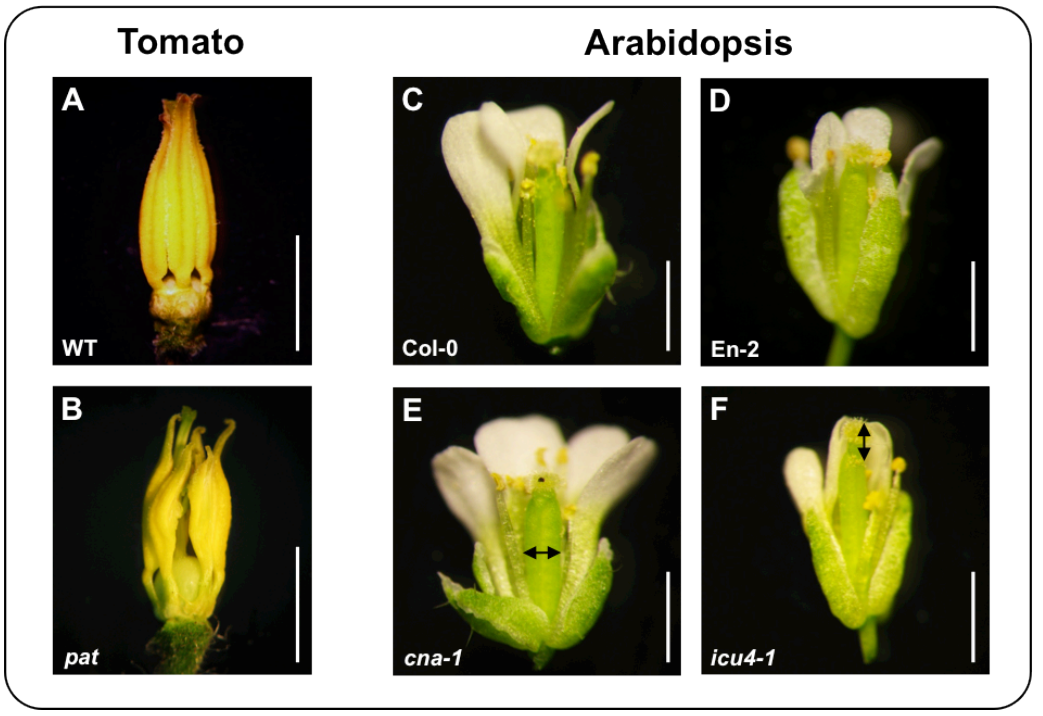

Fig. 3.11. (A) WT anther cone at anthesis showing the ovary size in WT flowers. (B) *pat* anther cone at anthesis highlighting the bigger size of the *pat* ovary compared to WT. (C) Col-0 flower and pistil at anthesis. (D) *cna-1* flower at anthesis showing a thicker pistil (*horizontal double arrowheads*). (E) En-2 flower and pistil at anthesis. (F) *icu4-1* flower at anthesis showing a longer pistil (*vertical double arrowheads*). Scale bars indicate 5 mm (A and B) and 1 mm (C-F).

This first evidence of a parthenocarpic tendency showed by *cna-1* and *icu4-1* pistils at anthesis was confirmed by an emasculation experiment. Indeed, emasculated not-pollinated flowers of these two genotypes developed, in eight d, parthenocarpic siliques significantly longer than those produced by their respective WT counterparts (Table 3.1).

Table 3.1. Parthenocarpic behaviour showed by *cna-1* and *icu4-1* single mutants for *ATHB15/CNA/ICU4* in Arabidopsis. Values are the mean ± SEM of the silique lenght in mm (n = 3-6). Student's *t* test between genotypes (Col-0 vs *cna-1* and En-2 vs *icu4-1*, respectively) within traetment. **, P≤0.01; ***, P≤0.001.

Treatment	Ecotype or mutant background			
	Col-0	***cna-1***	**En-2**	***icu4-1***
8 DPE[a]	2.16 ± 0.07	3.98 ± 0.24***	2.48 ± 0.09	5.23 ± 0.33**

[a] DPE stands for Days Post Emasculation.

Parthenocarpic *cna-1* and *icu4-1* siliques were respectively about 40% and 30% shorter than siliques formed after self-pollination (not shown), suggesting that in both mutants pollination, fertilization and processes associated with seed formation contribute to final silique size.

The same parthenocarpic behaviour was exhibited by emasculated not-pollinated *pat*

flowers that, in 11 d, conversely to WT flowers that undergo flower abortion, were able to develop seedless fruitlets independently from pollination and ovule fertilization (see Chapter 5). At maturity, self-pollinated siliques of both *cna-1* (Fig. 3.12C) and *icu4-1* (Fig. 3.12D) mutants were smaller than those of their respective WTs (Fig. 3.12C and D, respectively). A similar phenotype was observed in tomato comparing mature *pat* fruits (Fig. 3.12A) to those set by the near-isogenic WT line (Fig. 3.12B).

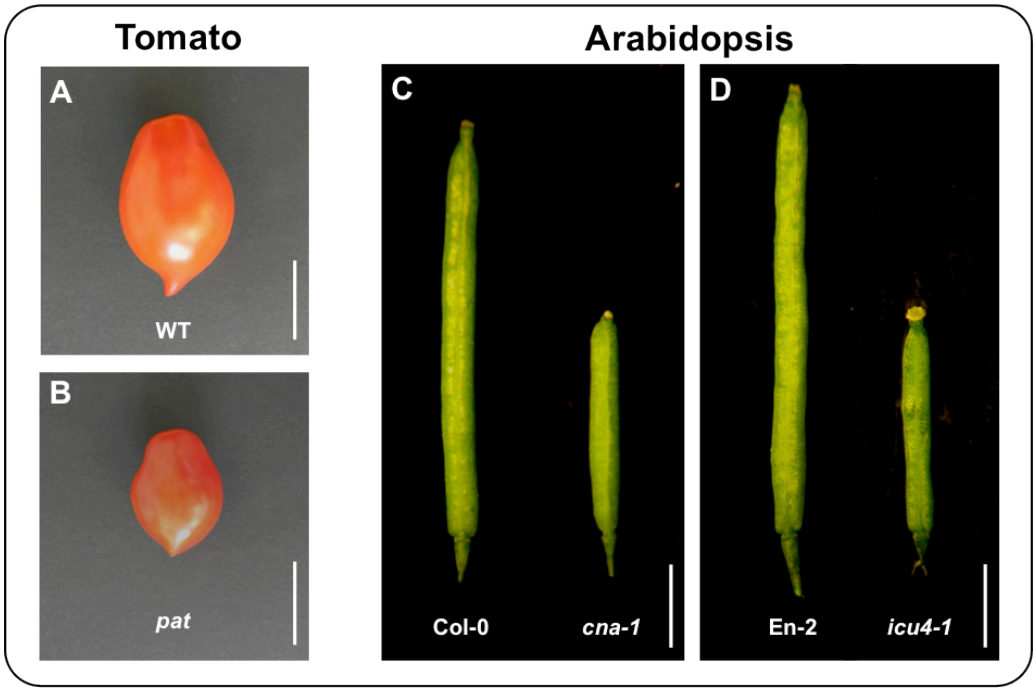

Fig. 3.12. (A and B) Fruit phenotype respectively of WT and *pat* plants at mature stage. (C) Phenotype of the mature silique in Col-0 and *cna-1* mutant. (D) Phenotype of the mature silique in En-2 and *icu4-1* mutant. Scale bars indicate 5 cm (A and B) and 2 mm (C and D).

As previously described in this Chapter, a pleiotropic effect distinguishing *pat* from other parthenocarpic mutants in tomato (see Table 4.1 in Chapter 4), is the occurrence of aberrant ovules with impaired integument growth (Fig. 3.13B). Their frequency in the *pat* mutant ovary was positively correlated with a high expressivity and penetrance of the parthenocarpic fruit set (Mazzucato *et al.*, 1999). Interestingly, the lack of ovule integuments or their modification in carpel-like structures was also associated to the production of seedless fruits, respectively in *Annona squamosa* (sugar apple; Lora *et al.*, 2011) and *Capsicum annuum* (sweet pepper; Tiwari *et al.*, 2011).

In Arabidopsis, several single mutants displaying ovular defects have been identified. Among them, *aintegumenta* (*ant*) lacks inner and outer integuments, *aberrant testa shape* (*ats*) shows a single integument, *inner no outer integument* (*ino*) presents the

absence of the outer integument growth in ovule primordia, *short integuments1* (*sin1*) displays short integuments, and *bel1* and *apetala2* (*ap2*) (Lang *et al.*, 1994; Baker *et al.*, 1997; Colombo *et al.*, 2008; Kelley and Gasser, 2009). In the latter two loss-of-function mutants, ovule integuments are converted into carpel-like structures (Modrusan *et al.*, 1994; Ray *et al.*, 1994; Pinyopich *et al.*, 2003). Interestingly, two specific mutants have been reported to affect parthenocarpic fruit development of the Arabidopsis *fruit without fertilization* (*fwf*) mutant. First, the *ats-1/kan4-1* loss-of-function mutation enhances the *fwf* parthenocarpic phenotype, suggesting that modification of the ovule integument structure influences parthenocarpic fruit growth (Vivian-Smith *et al.*, 2001). Second, parthenocarpic fruit development was also enhanced in the *bel1-1 fwf-1* double mutant, and at the same time a higher frequency of carpelloid structures was observed compared to the *bel1-1* single mutant. This suggests on the one hand that carpelloid structures enhance parthenocarpic fruit development, and on the other hand that the development of carpelloid structures is enhanced in the absence of seed set (Vivian-Smith, 2001).

Notably, ovular aberrations paralleling those showed by *pat* in tomato (Fig. 3.13B), compared to WT (Fig. 3.13A), and by the above described mutants in Arabidopsis, were also observed in both *cna-1* (Fig. 3.13D) and *icu4-1* (Fig. 3.13F) single mutants when compared to their Col-0 (Fig. 3.13C) and En-2 (Fig. 3.13E) WT backgrounds.

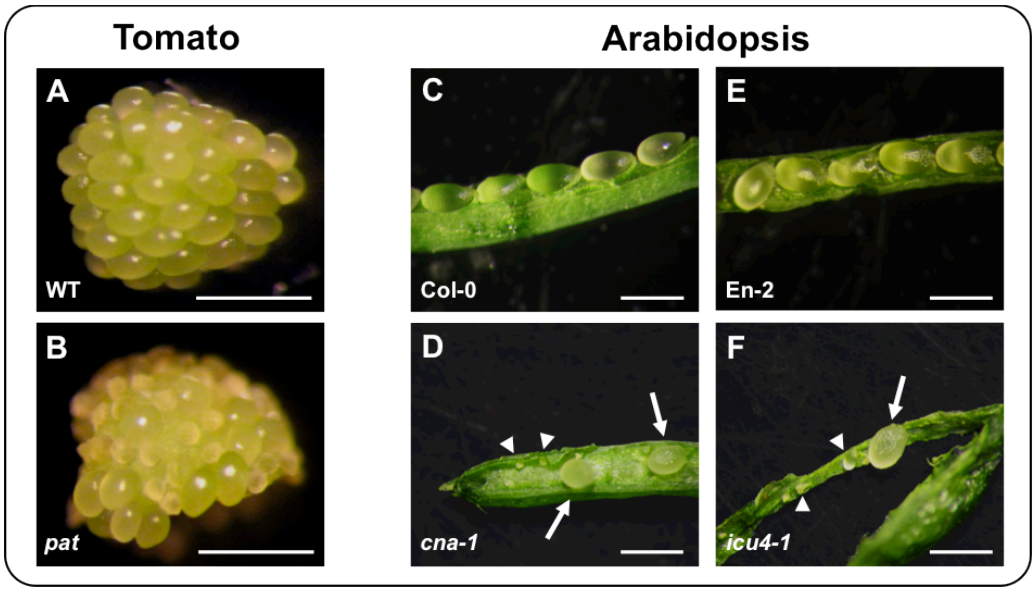

Fig. 3.13. (A) Normal ovules in the WT ovary at anthesis. (B) Normal and aberrant ovules impaired in the growth of the single integument within the *pat* ovary at anthesis. (C) Normal ovules in the Col-0 silique at 7 days post anthesis (DPA). (D) Subnormal (*arrows*) and aberrant ovules (*arrowheads*) in the loss-of-function *cna-1* mutant silique at 7 DPA. (E) Normal ovules in the En-2 silique at 7 DPA. (F) Subnormal (*arrow*) and aberrant ovules (*arrowheads*) in the loss-of-function *cna-1* mutant silique at 7 DPA. Scale bars indicate 1 mm (A and B) and 0.5 mm (C-F).

This result supports the idea proposed by Kelley *et al.* (2009) that *ATHB15/CNA/ICU4*, among the HD-Zip III members (*PHB*, *PHV* and *REV*) involved in the differentiation of ovule integuments, could represent the main regulator of this trait. Moreover, this result indicates that both the loss- and gain-of-function of this gene could lead to a production of aberrant ovules, positively associated with a parthenocarpic silique development. So far, this association has never been described before for other HD-Zip III mutants in Arabidopsis.

The ovule phenotype of the four Arabidopsis genotypes presented in Fig. 3.13 (C-F), was evaluated in self-pollinated siliques at 7 DPA. Deviations presented by aberrant *cna-1* and *icu4-1* ovules were observed also in pistils at anthesis (not shown). At the stereomicroscope, aberrations of integuments presented by both mutants appeared similar between them, but to determine if they actually reflect those showed by other Arabidopisis mutants, a SEM analysis is required.

Aberrant integuments formation in ovules of *cna-1* and *icu4-1* gived rise to subnormal seed sometimes not viable (Fig. 3.14D and F, respectively) compared to their relative Col-0 (Fig. 3.14C) and En-2 (Fig. 3.14E) WTs. In tomato, a similar phenotype is observed for *pat* (Fig. 3.14B) when seed is produced. Mainly, *pat* seeds appear smaller than those produced by its near-isogenic WT line (Fig. 3.14A), but viable after all.

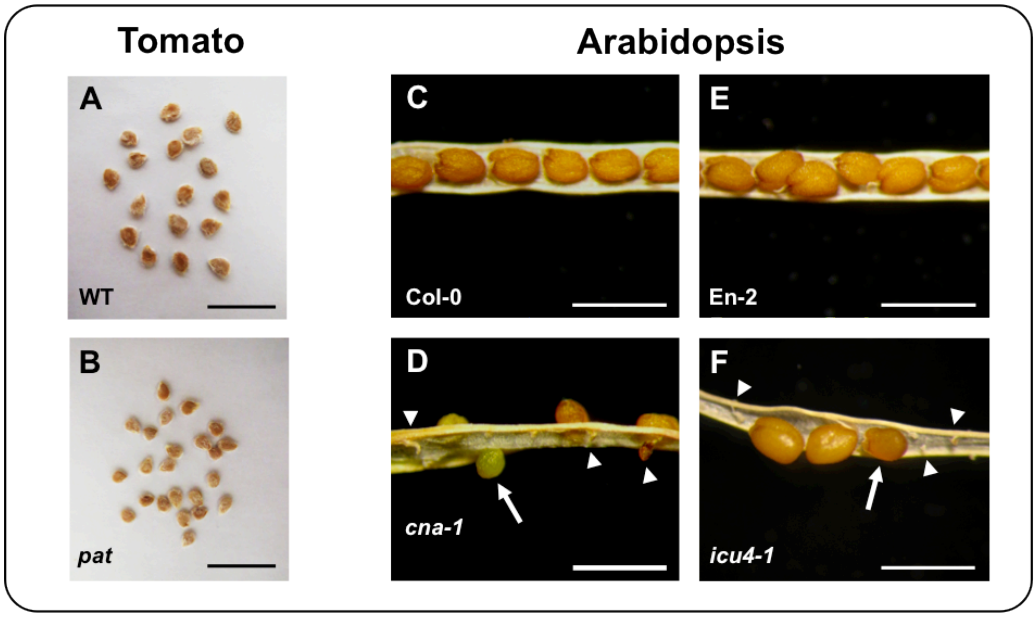

Fig. 3.14. (A) Phenotype of WT tomato seeds. (B) Phenotype of *pat* seeds produced by partially seeded fruits. (C) Normal seeds in Col-0 dried siliques. (D) Subnormal (*arrow*) and aborted (*arrowheads*) seeds in *cna-1* dried siliques. (E) Normal seeds in En-2 dried siliques. (F) Subnormal (*arrow*) and aborted (*arrowheads*) seeds in *icu4-1* dried siliques. Scale bars indicate 1 cm (A and B) and 1 mm (C-F).

In Arabidopsis, different single, double and triple HD-Zip III loss-of-function mutants display alterations of the vasculature (Fig. 3.15E; Prigge *et al.*, 2005). In order to investigate if the *pat* mutant in tomato presents similar alterations, an histochemical staining of lignin with phloroglucinol-HCl was employed and the arrangement of vascular bundles, in hypocotyls and epicotyls of 30-d-old WT and *pat* plants, was determined. Hypocotyl hand made cross-sections of *pat* plants showed a disorganized vasculature (Fig. 3.15B) compared to the one produced by WT plants (Fig. 3.15A), although the symmetry of the vascular bundles appeared to be conserved between the two genotypes. Vascular bundles disposition was different between hypocotyl and epicotyl, but the disorganization of the *pat* vasculature scored in the hypocotyl was reflected at the epicotyl level (Fig. 3.15D) compared to WT plants (Fig. 3.15C).

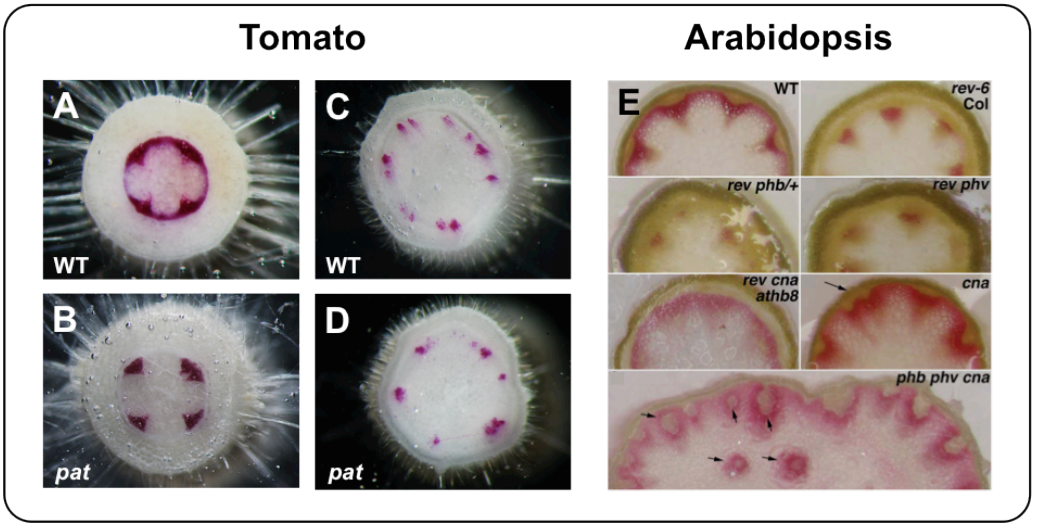

Fig. 3.15. (A and B) Arrangement of the vasculature in the hypocotyl of WT and *pat* 30-d-old plants, respectively. (C and D) Organization of vascular bundles in the epicotyl of WT and *pat* 30-d-old plants, respectively. (E) Inflorescence stem vasculature in *er-2* (WT), and single (*cna-2* and *rev-6* indicated in the figure as *cna* and *rev-6* Col, respectively), double (*rev-6 phb-13/+* and *rev-6 phv-11* indicated in the figure as *rev phb/+* and *rev phv*, respectively), triple (*rev-6 cna-2 athb8-11* and *phb-13 phv-11 cna-2* indicated in the figure as *rev cna athb8* and *phb phv cna*, respectively) HD-Zip III loss-of-function mutants in Arabidopsis. In *cna*, the arrow points irregularly spaced vascular bundles. In *phb phv cna*, arrows indicate vascular bundles internal to the inflorescence stem (from Prigge *et al.*, 2005).

Taken together, all the similarities found comparing *pat* vegetative and reproductive phenotypes with those presented by *cna-1* and *icu4-1*, respectively single loss- and gain-of-function mutants for *ATHB15/CNA/ICU4* in Arabidopsis, strongly suggest that *SlHB15* is the gene underlying the *pat* mutation in tomato. In addition, all the produced data regarding reproductive traits in *cna-1* and *icu4-1* represent novel insights, because all the studies reported so far about these two mutants took into consideration only aspects related to their vegative development.

Chapter 4

Differentially expressed genes in the wild type and *parthenocarpic fruit* ovary during fruit set

Abstract

The *pat* mutation in tomato associates a strong competence for parthenocarpy (seedless fruit production) with homeotic transformation of anthers (reduced length and carpelloidy) and aberrancy of ovules (arrested integument growth and loss of viability). To dissect this complex floral phenotype and to detect genes involved in the pollination-independent fruit set of the *pat* mutant, a transcriptomic approach was used. Two pre- and one post-anthesis stage were selected to monitor and compare the expression profile of genes in the WT and mutant ovary during flower-to-fruit transition. A customized microarray platform, designed on Tomato Gene Index Version 11 (LeGI v.11) tentative consensus (TC) sequences, was used in this study. Normalized microarray expression data were subjected to one-way ANOVA and 3,627 transcripts showed significant expression differences ($P \leq 0.01$). Among them, 1,714 displayed a greater than 3-fold change in at least one of the pair-wise comparisons analyzed between genotypes and stages. By clustering analysis, co-expressed genes were grouped into 20 clusters and those developmentally regulated in the WT ovary during fruit set and deregulated in the mutant were highlighted. These genes are putatively involved in the determination or in the expression of the parthenocarpic phenotype showed by the mutant. Clusters showing a specific expression pattern in the WT and/or in mutant ovary were statistically grouped according to their centroid expression graph and based on their putative biological function. Using this approach, five biological trends were identified and clusters classified as Controlling complex (CC), Fruit growth-related (FG), Pollination-dependent (PD), Always different (AD) and Always similar (AS). CC clusters contained putative negative or positive regulators of fruit set (genes up- or down-regulated at pre-athesis in the WT ovary and deregulated in the *pat* mutant). Interesting genes belonging to this group encoded orthologs of Arabidopsis TFs regulating the meristem differentiation and development of floral organs, such as SHOOTMERISTEMLESS (STM), BIG PETALp (BPEp), AINTEGUMENTA (ANT) and CRABS CLAW (CRC). These findings represented new insights, because so far these genes belonging respectively to the KNOX, bHLH, AP2/ERF and YABBY families of TFs had never been so directly associated to parthenocarpy. Their expression profile was confirmed by real-time PCR, which was also extended to other TFs already known to be involved in controlling tomato fruit set, such as AUXIN RESPONSE FACTOR7 (ARF7), ARF8 and INDOLE-3-ACETIC ACID9 (IAA9). Finally, selected genes showing a deregulated expression pattern in *pat*

compared to the WT were also studied in other parthenocarpic genotypes (*pat-2*, *pat-3*/*pat-4*, *EMS-iaa9* and *RNAi-ARF7*). This comparative approach raised interesting cues for improving the present molecular understanding of fruit set and parthenocarpy in tomato.

Introduction

Fruit set is a complex developmental process related to many molecular and physiological aspects of plant growth. The obtainment of a high fruit set is strongly dependent on optimal flower pollination and ovule fertilization. An important role for the correct accomplishment of this process is played by favorable environmental conditions being fundamental for pollination and cross-talk occurring between ovule and ovary placental tissues during flower-to-fruit transition. However, the occurrence of fruits without seeds (parthenocarpic fruits) indicates that flower pollination and ovule fertilization are not absolute prerequisites for ovary development (Dorcey *et al*., 2009).

In tomato, as in other species, it has been shown that auxin (IAA) and gibberellins (GAs) play a crucial role in the fruit set process (de Jong *et al.*, 2009a), although it appears that other growth regulators might also be implicated, such as cytokinins (García-Martínez and Carbonell, 1980), ethylene (Vriezen *et al.*, 2008) and polyamines (Antognoni *et al.*, 2002; Fos *et al.*, 2003). The implication of these hormones in fruit set has been shown by the measurement of their endogenous levels in pollinated ovaries of wild type (WT) plants, in unpollinated ovaries of parthenocarpic genotypes and by exogenous application (Mapelli *et al*., 1978; Gillaspy *et al*., 1993; Vivian-Smith and Koltunow, 1999; Balbi and Lomax, 2003; Ozga and Reinecke, 2003; Srivastava and Handa, 2005; de Jong *et al.*, 2009a).

Endogenous bioactive GAs have been recently shown to play a fundamental role in Arabidopsis early stages of fruit development. The GAs biosynthetic enzymes GA 20-oxidases and GA 3-oxidases are required for silique elongation (Hu *et al*., 2008; Rieu *et al*., 2008b), and blocking GA inactivation, by knocking out the five catabolic enzymes GA 2-oxidases, led to the formation of parthenocarpic fruits in absence of fertilization (Rieu *et al*., 2008a). The role of IAA in promoting fruit set and development has been described since long time (Gustafson, 1937; 1939) and recently has been supported by molecular work in Arabidopsis and tomato, where key regulatory elements in IAA signaling with a function in fruit initiation and development have been identified. In tomato, loss-of-function of the *INDOLE-3-ACETIC ACID9* (*IAA9*) gene, encoding a nuclear-localized Aux/IAA protein, or of the *AUXIN RESPONSE FACTOR7* (*ARF7*) resulted in plants producing parthenocarpic fruits, suggesting that both IAA9 and ARF7 TFs inhibit ovary growth in absence of ovule fertilization (Wang *et al*., 2005; de Jong *et al*., 2009b). Furthermore, in Arabidopsis a loss-of-function allele of *ARF8* (*fruit without fertilization*, *fwf* or *arf8-4*) also provokes parthenocarpic fruit development (Vivian-Smith *et al*., 2001; Goetz *et al*., 2006). Proteins of the Aux/IAA and ARF families interact to

mediate IAA signaling (Dharmasiri and Estelle, 2004), which leads to the hypothesis that both Arabidopsis and tomato possess ARF8- and IAA9-related proteins that physically interact to regulate fruit set (Dorcey *et al.*, 2009).

In the past decade, transcriptomic approaches to identify genes involved in tomato fruit set and parthenocarpic ovary development have been pursued (Testa *et al.*, 2002; Lemaire-Chamley *et al.*, 2005; Vriezen *et al.*, 2008; Wang *et al.*, 2009; Martinelli *et al.*, 2009; Pascual *et al.*, 2009; Mounet *et al.*, 2012). These studies described several genes whose differential regulation suggested different functions in the control of tomato fruit set. Many of these genes were related to the regulation of hormonal homeostasis in the ovary. For example, Vriezen *et al.* (2008) showed that genes controlling ethylene and abscisic acid (ABA) metabolism are also involved in this process and proposed their role as antagonist of IAA and GAs to keep the pre-anthesis unpollinated ovary in a temporally protected and dormant state. An opposite role for the ethylene in the fruit set was highlighted by another transcriptomic work comparing ovaries from a WT line with those from the *pat-3/pat-4* natural mutant (Pascual *et al.*, 2009). In fact, these authors found that both GA and ethylene synthesis genes were activated in the ovary at anthesis of the parthenocarpic line. Accordingly with these findings, it has been proposed that this hormone could mimic pollination signals, activating IAA synthesis and a response, proper of the pollination-dependent fruit set (Pascual *et al.*, 2009).

In tomato, parthenocarpic transgenic plants were also obtained expressing genes for IAA synthesis (*iaaM* from *Agrobacterium tumefaciens*) or responsiveness (*rolB* from *A. rhizogenes*) driven by *DefH9* (from Antirrhinum) and *INO* (from Arabidopsis) ovule-specific promoters (Martinelli *et al.*, 2009). This study showed that the *INO* promoter from Arabidopsis fused with both *iaaM* or *rolB* genes effectively induced parthenocarpy in tomato. Changes between transgenic parthenocarpic and WT fruits, at the breaker stage, were detected at both transcriptomic and metabolomic levels. Significant differences were observed in gene expression of several differentially regulated genes, such as those involved in the cell wall, hormone metabolism and response (IAA in particular), and metabolism of sugars and lipids (Martinelli *et al.*, 2009).

Furthermore, Wang *et al.* (2009) using a combined transcriptomic and metabolomic approach for studying *IAA9* knockout parthenocarpic plants obtained by antisense technology, identified other IAA and ethylene signaling components. In addition, these authors gave importance to the photosynthetic process and sugar metabolism, hypothesizing their regulatory role for the flower-to-fruit transition (reviewed by Ruan *et al.*, 2012). Mounet *et al.* (2012) specifically silencing in tomato (*SlPIN4*), a member of

the PIN-FORMED (PIN) auxin efflux transport protein family, demonstrated its specific involvement as negative regulator of fruit set. Indeed, down-regulation of *SlPIN4* in transgenic lines led to the formation of parthenocarpic fruits due to precocious ovary growth before fertilization. In this work, a TF profiling approach revealed important downstream targets involved in IAA-dependent fruit set regulation in tomato.

Previously, molecular insights for the implication of polar auxin transport in tomato fruit set were highlighted by application of auxin transport inhibitors (Serrani *et al.*, 2010) and by characterization of *AUCSIA*-silenced plants generally setting parthenocarpic fruits and showing a reduction of auxin transport in roots (Molesini *et al.*, 2009). In WT tomato flowers, after ovule fertilization, the ovary undergoes cell division and expansion occurring in the carpel wall and in the placental tissue surrounding seeds (Gillaspy *et al.*, 1993). There are early evidences that developing seeds are the main sources of IAA during fruit initiation and development (Gustafson, 1939; Nitsch, 1950; Ozga *et al.*, 2002).

Recently, Pattison and Catalá (2012) unraveled the timing and mechanisms of the IAA gradient and distribution during tomato fruit set characterizing two important IAA-related families of genes (*PIN* and *Aux/LAX*). PIN and Aux/LAX proteins control cellular auxin efflux and influx respectively (Vanneste and Friml, 2009). These authors, using an IAA-responsive reporter construct (*DR5rev::mRFPer*; Gallavotti *et al.*, 2008), found that before anthesis the IAA signal is localized in vascular strands of the ovary, as well as in the embryo sac. At anthesis, the IAA distribution was widespread throughout the ovules and was no longer confined to the embryo sac. Whereas, after anthesis, the IAA signal was strongly detected in the funiculus and in the outer layers of the placenta that surrounds developing seeds (Pattison and Catalá, 2012).

In tomato, the natural *parthenocarpic fruit* (*pat*) mutant shows a strong compentence for parthenocarpy associated with stamen and ovules aberrations (Bianchi and Soressi, 1969; Mazzucato *et al.*, 1998). To dissect this complex floral phenotype and to detect genes involved in the pollination-independent fruit set displayed by this mutant, a microarray approach was used. Selected deregulated genes in the *pat* ovary during flower-to-fruit transition were also studied in other four parthenocarpic systems. This comparative transcriptomic approach represents a novelty and was performed in order: (i) to highlight similar mechanisms between different sources of parthenocarpy in tomato and (ii) to increase the knowledge about the molecular regulation of such an agronomically important trait.

Materials and methods

Plant material and phenotypic analysis

In spring 2011, WT (cv Chico III) and mutant plants from the near-isogenic *pat* line were grown with standard horticultural practices in an unheated tunnel under environmental light conditions at the experimental station of the Tuscia University (Viterbo, Italy). During flowering, ovaries from different plants of both genotypes, were sampled from the 2nd to the 4th inflorescence at flower developmental Stage 2 (9-12 mm flower bud corresponding to 5 Days Before Anthesis, DBA), 3 (opening flower, 2 DBA) and 5 (2 Days Post Anthesis, DPA) (flower stadiation according to Mazzucato *et al.*, 1998). Such flower developmental stages were selected in order to study and compare key molecular events occurring during fruit set in the WT and *pat* mutant ovary. Other parthenocarpic mutants were also used in this study: *pat-2* (mutant line in cv Early Mech background; Philouze, 1991), *EMS-iaa9* (loss-of-function TILLING mutant line loss of function for *SlIAA9* in cv Red Setter background; A. Mazzucato and F. Carriero, unpublished) and *RNAi-ARF7* (T_2 RNAi-silenced line for *SlARF7* in cv Money Maker backgroud; de Jong *et al.*, 2009b).

Parthenocarpic mutants with their respective near-isogenic WT lines (hereafter referred to as *pat*, *pat-2*, *EMS-iaa9* and *RNAi-ARF7* systems) were grown in the same conditions, except for the *pat-3/pat-4* system for which plant material was not available. Sixteen plants (eight from WT and eight from parthenocarpic mutant lines) were grown to evaluate the expressivity of parthenocarpy and to observe floral phenotypes and dissect ovaries for transcriptomic analyses at Stages 2, 3 and 5. In each parthenocarpic system, specific mutation expressivity was evaluated comparing the fresh weight of mutant and WT ovaries at anthesis and scoring the percentage of seedless fruits at maturity. Other flower phenotypic traits, such as stamen and ovule aberrations were also evaluated in two flowers at anthesis (Stage 4) collected from the 1st or 2nd inflorescence of all the WT and mutant plants of each parthenocarpic system. Similarly, the fruit weight and the percentage of seedlessness was scored on 16 red ripe fruits (two per plant) harvested from the 1st or 2nd inflorescence of all the WT and mutant plants of each parthenocarpic system. Statistical significance for data within the parthenocarpic system was assessed by Student's *t* test using Microsoft Excel 2011.

Custom oligoarray construction

Tentative consensus (TC) sequences of the Tomato Gene Index Version 11 (LeGI v.11) released from the Dana Farber Cancer Institute (DFCI, Boston, MA; http://www.danafarber.org/) were used for custom oligoarray construction. Agilent aArray v.4.5 tool was used to design the microarray platform with 60-mer probes of the 41,425 tomato unigenes (21,550 contigs and 19,875 singletons). This online array creation software removed 112 sequences for various reasons such as repeated sequences and 41,313 probes were consequently installed on the oligoarray (4x44K format, Agilent Technologies).

RNA isolation, cDNA labeling and array hybridization

All samples for RNA preparation were quick-frozen in liquid nitrogen and ground to a powder with a mortar and pestle. Total RNA from 100 mg of ovaries (without style) at Stages 2, 3 and 5 was extracted using TRIzol reagent (Invitrogen, Carslbad, CA, USA) according to the manufacturer's protocol. The yield and purity of RNA samples were assessed by determination of absorbance (Abs) at 260 nm and 280 nm using the Agilent RNA 6000 Nano Kit with an Agilent 2100 Bioanalyzer (Agilent Technologies). RNA integrity was checked by 1% (w/v) agarose gel and RNA was only used when the ratio Abs260 nm/Abs280 nm was higher than 1.8. Two biological replicates were used for each genotype and stage. Reverse transcription of mRNA in the total RNA samples (500-ng aliquots) and composition of labeled cDNA was performed using the Quick Amp Labeling Kit, One-Color (Agilent Technologies) according to the manufacturer's instructions. Labeled cDNA samples were hybridized against the oligoarray slides using the Gene Expression Hybridization Kit (Agilent Technologies). After hybridization, arrays were washed with Gene Expression Wash Buffer (Agilent Technologies) according to the manufacturer's instructions. The dried slides were scanned with an Agilent scanner (Agilent Technologies) and raw data from the array scanning were captured using Agilent Feature Extraction Ver. 10.7.1.1.

Microarray procedures and data analysis

Normalized microarray expression data were processed using the software MeV 4.8 of the TM4 suite specifically developed for microarray analysis (Saeed *et al*., 2003; http://www.tm4.org/). One-way ANOVA with a p-value<0.01 was applied to select genes with significant differences in expression. Then, only transcripts whose change in abundance was greater than 3-fold in at least one of the pair-wise comparisons

analyzed between genotypes and stages, were considered for further analyses (referred to as Differentially Expressed Genes, DEGs).

Venn diagrams were generated using the web application tool GennVenn (Pirooznia *et al.*, 2007; http://genevenn.sourceforge.net/) to highlight overlapping genes between the pair-wise comparisons. MeV 4.8 was also used for the clustering analysis performed according to the K-Means (KMC) method (Soukas *et al.*, 2000). Before clustering, normalized microarray values were transformed using the mean and the standard deviation of the row of the matrix to which the value belonged, using the following formula: Value = [(Value) – Mean (Row)]/[Standard deviation (Row)]. This further transformation was applied in order to group genes with a similar expression pattern but showing high differences in absolute expression values. The appropriate number of clusters (K) to be generated with the KMC method was estimated through the Figure of Merit (FOM) analysis (Yeung *et al.*, 2001). By observing in the expression centroid graphs (Supplementary Fig. S2) the six consecutive data points (Stages 2, 3 and 5 in the WT and *pat* ovary), the gene expression pattern identifying each cluster was determined considering differentially expressed those points exceeding the preceding point by more than 3-time its own standard deviation (σ, Supplementary Fig. S2). Clusters were pooled, when showing the same expression pattern, into five groups of clusters (Controlling complex, CC; Pollination-dependent, PD; Fruit growth-related, FG; Always different, AD; Always similar, AS) representing different biological trends.

Functional categorization of genes was performed using the Blast2GO software (Conesa *et al.*, 2005; http://www.blast2go.com/) and crossing references from Gene Ontology (GO) Consortium (http://www.geneontology.org/), Sol Genomics Network (SGN, http://solgenomics.net/) and The Arabidopsis Information Resource (TAIR, http://www.arabidopsis.org/). The composition of DEGs in each group of clusters in terms of GO annotations was reported including the first more abundant 25 level-3-GO terms for the Biological process vocabulary and the first 20 level-3-GO terms for the Molecular Function vocabulary. GO functional enrichment analysis was performed by the Chi-square (χ^2) test for homogeneity for the four groups of clusters (CC, PD, FG and AD) representing trends distinguishing WT and *pat*.

Real-time PCR and microarray validation

Real-time PCR (qRT-PCR) analysis was applied to ten DEGs selected in order to sample the group of clusters of genes putatively involved in the control of fruit set and to investigate other six genes previously described to be associated with a

parthenocarpic tomato fruit development or related to the hyphothesis of *SlHB15* as the gene underlying the *pat* mutation (Supplementary Table S1).

cDNA samples were synthesized from 3 µg of two independent RNA preparations using the SuperScript II RNase-H Reverse Transcription Kit (Invitrogen, Carslbad, CA, USA) following the manifacturer's protocol. Ten-fold dilutions of the resulting first strand cDNA were used for qRT-PCR experiments. Duplicate quantitative assays for each sample were performed with the SensiMix Capillary Kit (Bioline, Luckenwalde, Germany) in the LightCycler 2.0 system (Roche Applied Science) according to the manufacturer's instructions. Primer sets used to analyze the expression pattern of these genes by qRT-PCR are reported on the Supplementary Table S1. To evaluate the gene expression level, results were normalized using the house-keeping (HK) gene *CAC* (SGN-U314153) recently found to provide excellent transcript normalization in tomato development studies (Expósito-Rodríguez *et al*., 2008). Relative expression for each gene in each sample was calculated with the single DCt method as follow: $2^{[(Ct\ value\ of\ target\ gene)-(Ct\ value\ of\ HK\ gene)]}$. The statistical significance within stage was assessed by Student's *t* test using Microsoft Excel 2011.

The validation of microarray data was performed by correlation (r) analysis in Microsoft Excel 2011 comparing qRT-PCR and microarray expression values of ten DEGs selected from interesting group of clusters. In addition, the expression patterns of *LeT6*/*TKn2*, *SlBPEp*, *SlCRC*, *SlDEF*, *SlHB15, SlARF8* and *SlIAA9* were also analysed in ovaries at Stages 2, 3 and 5 of the *pat-2*, *EMS-iaa9* and *RNAi-ARF7* parthenocarpic systems. cDNA samples from ovaries of WT and *pat-3/pat-4* mutant plants (RP75/59 mutant line; Pascual *et al.*, 2009; hereafter referred to as *pat-3*/*pat-4* system) could also be included in the analysis. Expression data from these samples were treated as those obtained for the *pat* system and presented as log2Ratio of the fold change (FC) calculated with the DDCt method as follow: $2^{[(DCt\ value\ of\ target\ gene\ in\ the\ mutant)-(DCt\ value\ of\ the\ target\ gene\ in\ the\ WT)]}$.

Results and discussion

Phenotypic analysis of parthenocarpic systems and pat *microarray experimental design*

In order to evaluate the expressivity of the different parthenocarpic mutations in the lines used in this work, a phenotypic characterization of reproductive traits related to the expression of parthenocarpy was performed. The ovary weight at anthesis and the percentage of seedless fruits at maturity were used as indicators of the strength of parthenocarpy expression.

WT and mutant plants of all the parthenocarpic systems (except *pat-3/pat-4* for which plant material was not available) were grown during spring in a tunnel under natural environmental conditions. In this season, as previously described by Mazzucato *et al.* (1998; 1999), the expressivity of the *pat* mutation reached the maximum level. Indeed, the *pat* ovary weight at anthesis was significantly higher than WT and *pat* flowers showed typical percentages of homeotic transformations of stamen and ovule aberrations (Table 4.1; Mazzucato *et al.*, 1998; 1999). As expected, at maturity, fruits of the *pat* line were smaller than WT (Bianchi and Soressi, 1969; Falavigna *et al.*, 1978) and showed complete seedlessness in agreement with previous reports (Table 4.1; Mazzucato *et al.*, 1998; 1999).

Table 4.1. Flower- and fruit-related phenotypic traits in the different parthenocarpic systems. For aberrations of floral organs, values represent the mean ± SEM of 16 flowers. Student's *t* test within parthenocarpic system (**, P≤0.01; ***, P≤0.001). For fruit weight and percentage of seedless fruits, values represent the mean of 16 ripe fruits.

Parthenocarpic system	Phenotype[a]	Aberrant floral organs (%)		Ovary weight (mg)	Fruit weight (g)	Seedless fruits (%)
		Stamens	Ovules			
pat	pat+ *pat*	0 69.9 ± 3.8	0 38.4 ± 3.6	3.4 ± 0.1 8.2 ± 0.3***	59.1 34.2	0 100
pat-2	pat-2+ *pat-2*	0 10.7 ± 3.0	0 0	5.2 ± 0.2 8.0 ± 0.5***	62.3 49.5	0 45.0
pat-3/pat-4[b]	pat-3/pat-4+ *pat-3/pat-4*	0 0	0 0	17.8 18.9	47.2 36.4	0 64.1
EMS-iaa9	iaa9+ *iaa9*	3.1 ± 2.3 34.1 ± 3.5	0 0	5.2 ± 0.2 7.5 ± 0.7**	62.7 55.3	0 66.7
RNAi-ARF7	arf7+ *arf7*	0 0	0 0	3.6 ± 0.1 5.8 ± 0.2***	71.5 45.9	0 34.4

[a] + indicates the WT lines near-isogenic to the mutants.

[b] Phenotypic data regarding the *pat-3/pat-4* parthenocarpic system were extrapolated from literature: stamen and ovule aberrations have never been described in this mutant (Philouze and Maisonneuve, 1978; Nuez *et al.*, 1986); ovary weight at anthesis in the WT tomato line Cuarenteno (pat-3/pat-4+) and its near-isogenic mutant line Par40-10 (*pat-3*/*pat-4*, derived from RP75/59) is reported in Fos *et al.* (2001), fruit weight and seedlessness percentage were calculated from data reported in Ferrando *et al.* (1987).

With the exception of *pat-3*/*pat-4*, all the parthenocarpic mutants showed a higher ovary weight at anthesis compared to their respective WT lines (Table 4.1). However, regarding the production of seedless fruits, the other mutants showed an expressivity lower than *pat*. The *EMS-iaa9* TILLING line produced 66.7% of seedless fruits, followed by *pat-3/pat-4* (64.1%), *pat-2* (45.0%) and *RNAi-ARF7* (34.4%). In this experimental material, fruit weight at maturity was reduced in the mutant lines respect to their WT counterparts in all the parthenocarpic systems although a statistical analysis on this trait was not performed (Table 4.1). Interestingly, as in the *pat* mutant, homeotic transformation of stamens (mainly carpelloidy) was also present in *pat-2* and *EMS-iaa9* mutants (Table 4.1). Ovular defects were only observed in the *pat* mutant, indicating this as a specific phenotypic trait of this tomato parthenocarpic mutant (Table 4.1).

In order to study and compare molecular events during flower-to-fruit transition in WT and *pat* ovaries, flower developmental Stages 2, 3 and 5 (according to Mazzucato *et al.*, 1998) were selected for the microarray experiment (Fig. 4.1A).

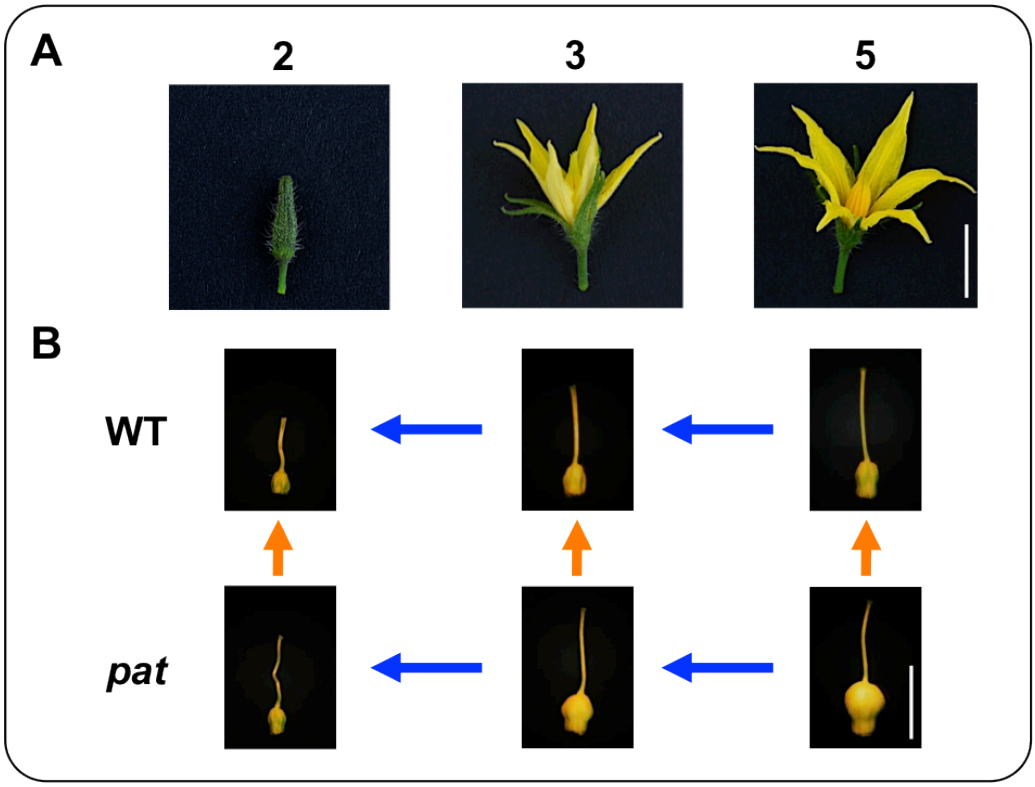

Fig. 4.1. (A) Flower developmental stages selected for the *pat* microarray experiment (according to Mazzucato *et al.*, 1998). Stage 2 (9-12 mm flower bud), 3 (opening flower) and 5 (2 days post anthesis). (B) Phenotype of the ovary in the pair-wise comparisons considered for the transcriptomic analysis among different stages within genotype (blue *arrows*) and between genotypes within the same stage (orange *arrows*). Scale bars indicate 1 cm (A) and 5 mm (B).

Based on such flower development time course, at Stage 4 pollination occurs. Ovary size is not significantly different in WT and *pat* flowers until Stage 2, but it begins to be consistently higher in *pat* from Stage 3 onwards (Fig. 4.1B). Stage 5 marks the beginning of ovary growth in the WT. At the mature fruit stage, the fruit weight becomes higher in the WT (Table 4.1; Mazzucato *et al.*, 1998).

Differentially expressed genes in the WT and pat *ovary during fruit set*

Normalized microarray expression values were subjected to one-way ANOVA by using the application MeV 4.8 of the TM4 software suite (Saeed *et al.*, 2003). Expression profiling of genes in WT and *pat* ovaries at Stages 2, 3 and 5 yielded 3,627 transcripts showing significant differences in expression (P≤0.01). Among them, 1,714 differentially expressed genes displayed a greater than 3-fold change (DEGs) in at least one of the pair-wise comparisons analyzed (Fig 4.1B) and were used as dataset for further investigations. Comparing the number of DEGs from Stage 3 to 2 and 5 to 3 in WT and *pat* (Fig. 4.2A and B, respectively), it was evident that a developmentally complex event was on going in the pre-anthesis WT ovary (388 DEGs), that was not paralleled in the mutant (156 DEGs).

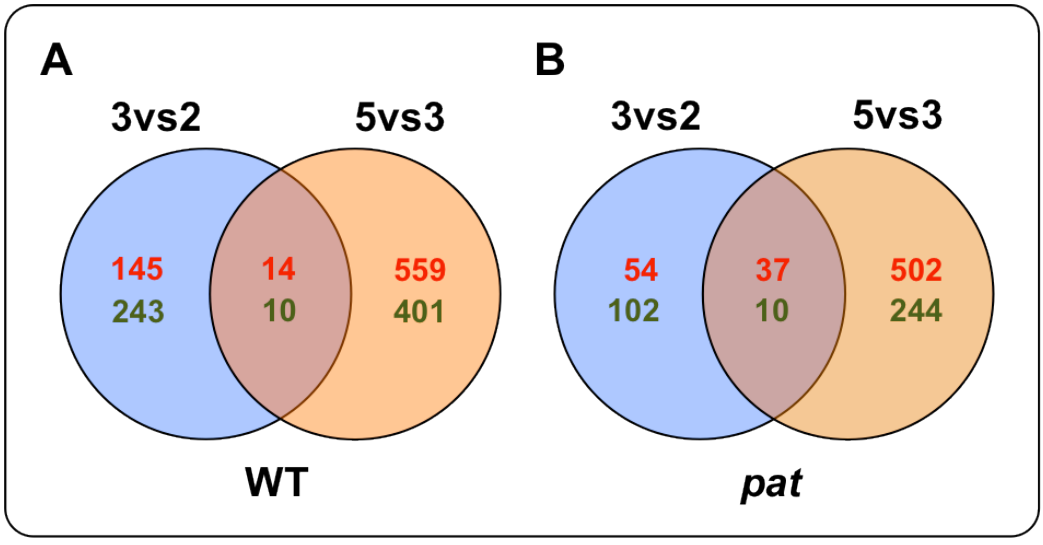

Fig. 4.2. (A and B) Venn diagram showing different up- (red) and down-regulated (green) genes comparing Stage 3 to 2 (3vs2, light blue) and 5 to 3 (5vs3, light orange) in the WT and *pat* ovary, respectively.

Comparing the number of DEGs between *pat* and WT at each developmental stage (Fig. 4.3), the smallest differences were found at Stage 2 (52 DEGs), likely reflecting only defects occurring during ovule differentiation considering that at this stage the *pat* ovary has not yet started its precocious and autonomous growth program (Fig. 4.1B).

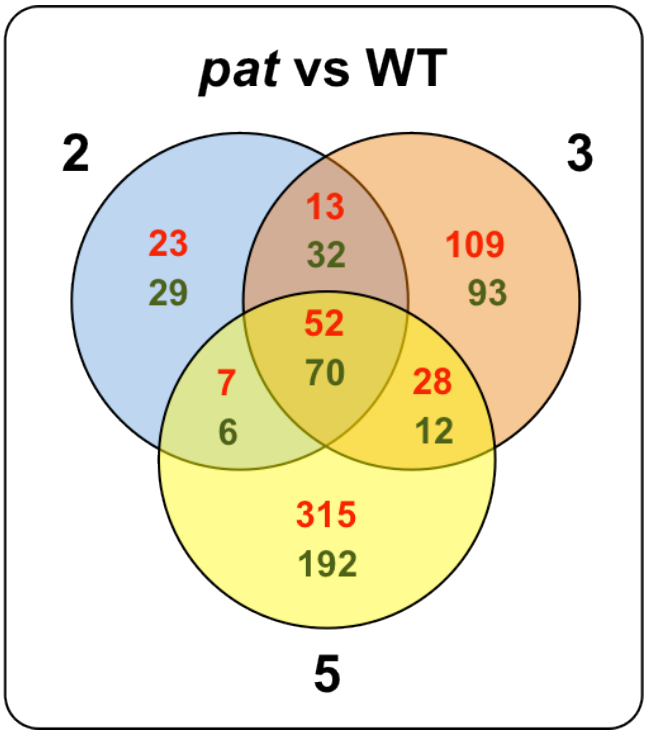

Fig. 4.3. Venn diagram showing up- (red) and down-regulated (green) genes comparing the *pat* and WT ovary at Stage 2 (light blue), 3 (light orange) and 5 (light yellow).

The 23 up- and 29 down-regulated genes at Stage 2 in the *pat* ovary compared to WT are presented in the Supplementary Table S2.

Among the 23 up-regulated DEGs, the BI205489 (LeGI v.11 code) annotated as *cytochrome P450 75B1* (*CYP75B1*), also known as *TRANSPARENT TESTA7* (*TT7*), encodes a member of the P450 monooxygenase (CYP) superfamily involved in the metabolism of flavonoids (Schoenbohm *et al.*, 2000; Nelson, 2009). This finding is in agreement with the increasing evidence that these compounds play a crucial role in the development of floral organs such as anthers in Petunia (Van der Meer *et al.*, 1992; Napoli *et al.*, 1999) and sexual reproduction in tomato plants accumulating anthocyanins in plant tissues (Mazzucato *et al.*, in press). Consistent with these findings, also tomato plants with altered flavonoid metabolism due to the silencing of the *chalcone synthase* (*CHS*) gene inhibited pollen tube growth and caused the development of parthenocarpic fruits (Schijlen *et al.*, 2007).

Among the 29 down-regulated DEGs, the AW092295 encoding for a member of the zinc finger homeobox (ZF-HD) family protein is the tomato ortholog of *HB22* in Arabidopsis. This gene was described as essential for embryo development in Arabidopsis (Pagnussaut *et al.*, 2005) and showed a flower/seed specific expression (Tan and Irish, 2006).

Another down-regulated DEG at Stage 2 in the *pat* ovary was the TC173627 annotated as *Squamosa promoter-binding protein-like 3* (*SPL3*). This gene was described in Arabidopsis as an upstream activator of *LEAFY* (*LFY*), a key regulatory gene that promotes flowering by integrating signals from the autonomous, photoperiod, age and GA pathway (Preston and Hileman, 2013). *SPL3* has been implicated in the control of heteroblasty and its higher expression related to the associated phenotype of cell size reduction (Usami *et al.*, 2009). Whereas this gene is down-regulated in *pat* before anthesis, its expression is seven-folds higher at Stage 5 and may be related with the decreased cell enlargement reported in the mutant (Mapelli *et al.*, 1978).

Other two down-regulated genes in the mutant ovary at Stage 2 were BG134081 and BI208492 annotated respectively as *Light-dependent short hypocotyls 1* (*LSH1*) and *Lateral Organ Boundaries domain protein 31* (*LOB31*). Interestingly, in Arabidopsis LSH1 (Cho and Zambryski, 2011) and LOB31 (Shuai *et al.*, 2002), as also other LOB family members (ASYMMETRIC LEAVES1, AS1 and AS2), act together with WUSCHEL, CLAVATA, CUC, KNOX, KANADI, YABBY and HD-Zip III TFs in the regulation of the meristem and lateral organs both in vegetative and reproductive tissues (Shuai *et al.*, 2002; Lin *et al.*, 2003; Cho and Zambryski, 2011). Consistent with these findings, a downregulation of *LSH1* and *LOB31* could play an important in the floral aberrant phenotype displayed by the *pat* mutant and correlates with the hypothesis that *SlHB15* is the gene underlying the *pat* mutation.

The greatest differences between WT and *pat* were detected at Stage 5, with 315 up- and 192 down-regulated DEGs, respectively (Fig. 4.3). At this Stage the mutant ovary is actively growing and the WT is just starting (Fig. 4.1B). DEGs at Stage 3 (109 up- and 93 down-regulated) represent those transcripts repressing pre-anthesis ovary growth (active in the WT but not in the mutant) or involved in early fruit growth (active in the mutant but not in the WT).

Clustering analysis and functional annotation of DEGs

The FOM analysis was used to estimate the number of clusters (K) to be generated through the KMC method. Normalized microarray expression values (NMEV) of the 1,714 DEGs were grouped into 20 clusters of co-expressed genes (Supplementary Fig. S1). Subsequently, these clusters were statistically pooled based on their centroid graph (Supplementary Fig. S2) into groups representing five different biological trends (Table 4.2).

Table 4.2. Description of the groups of clusters forming the five biological trends and named Controlling complex (CC, DEGs developmentally regulated in the WT at stages spanning anthesis, but not in the mutant), Pollination-dependent (PD, DEGs developmentally regulated in the WT at Stage 5, but not in the mutant), Fruit growth-related (FG, DEGs developmentally regulated in the mutant at Stage 5, but not in the WT, Always different (AD, DEGs different in the two genotypes at all stages) and Always similar (AS, DEGs with similar expression in the two genotypes at all stages). All WT Stage 2 expression values were indicated with 0; + or – indicated points with the centroid position higher or lower than the preceding point for a value exceeding 3σ.

Group of clusters	Cluster code[a]	Expression pattern WT / *pat*	No. of DEGs	Total no. of DEGs
CC	14	0 + 0 / 0 0 0	128	441
	6	0 – 0 / 0 0 0	46	
	15	0 + + / 0 0 0	22	
	12	0 0 – / – – –	111	
	(7, 8)	0 – – / 0 0 0	(44, 90)	
PD	(2, 3, 11, 13)	0 0 + / 0 0 0	(24, 112, 68, 165)	369
FG	(1, 4, 16)	0 0 0 / 0 0 +	(126, 97, 170)	393
AD	10	0 0 0 / + + +	71	163
	18	0 0 0 / – – –	92	
AS	(5, 10, 17, 19, 20)	variable	(49, 80, 100, 81, 38)	348

[a] See Supplementary Fig. S1 and S2.

The first group was named Controlling Complex (CC) and formed by 441 DEGs; it contained genes showing a specific developmental regulation before anthesis (Stage 3) in the WT, but not in the mutant (Fig. 4.4A and B). These transcripts are putatively involved in the control of WT ovary growth before pollination and in the expression of the parthenocarpic phenotype being deregulated in *pat*. The second group was named Pollination-dependent (PD) and contained 369 DEGs, including genes developmentally regulated in the WT at Stage 5, but not in the mutant (Fig. 4.4C). A third group was named Fruit growth-related (FG) and contained 393 DEGs up-regulated in *pat* at Stage 5, but not in the WT (Fig. 4.4D). This group represented genes involved in active processes of early fruit development that at Stage 5 are on going in the mutant, but not yet in the WT ovary. The last two groups included DEGs differentially expressed in the two genotypes at all stages (Always different, AD; Fig 4.4E) or sharing a similar expression pattern between WT and *pat* at all stages (Always similar, AS; Fig. 4.4F). The gene list of the 1714 DEGs from all the groups of clusters is reported in the Supplementary Table S3.

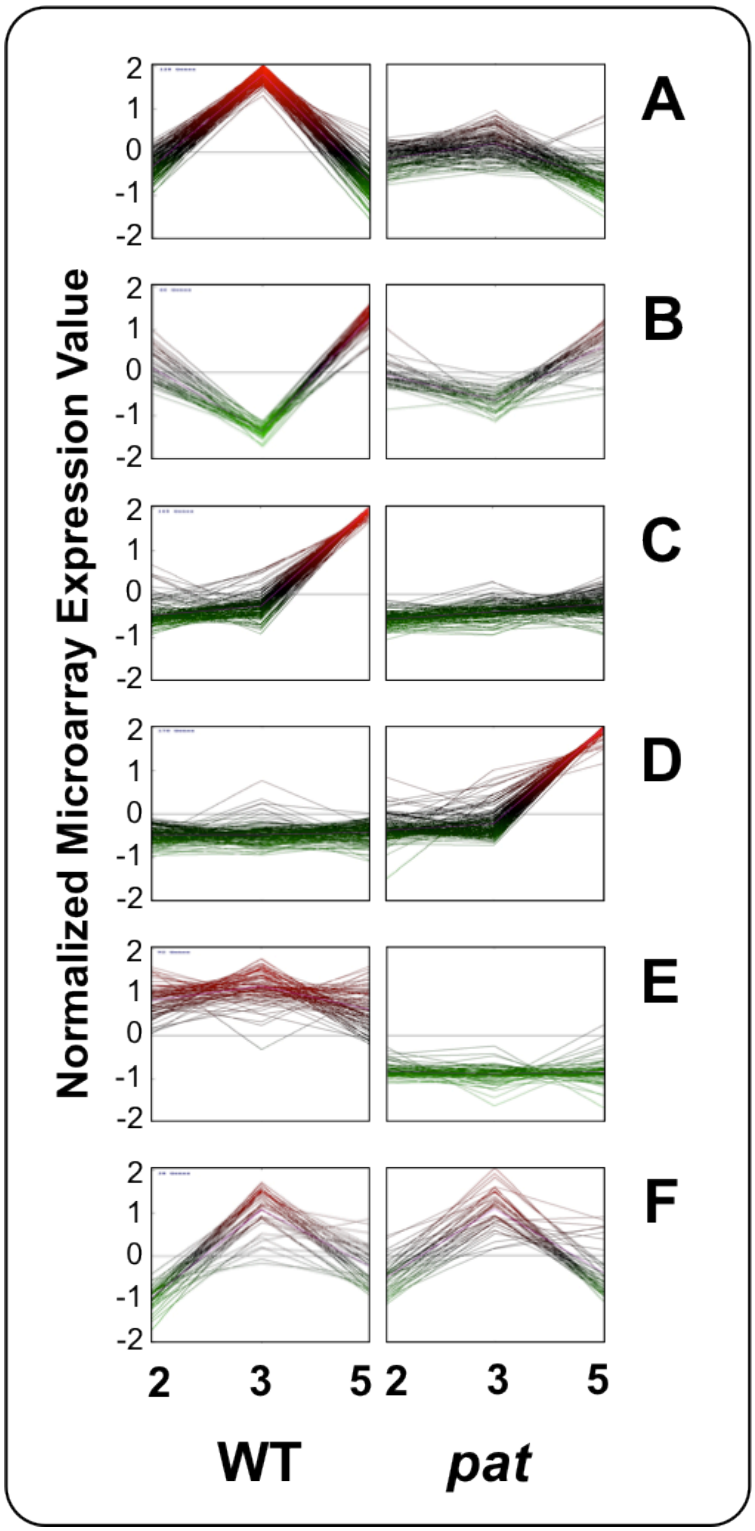

Fig. 4.4. (A and B) Representative clusters of Controlling complex, (C) Pollination-dependent, (D) Fruit growth- related, (E) Always different and (F) Always similar biological trends. On the x-axis are reported the three flower Stages (2, 3 and 5) in the WT and *pat* ovary.

Gene Ontology (GO) annotation performed with the Blast2GO software revealed that these groups of clusters were differentially composed in comparison with the total of DEGs when analyzed for functional enrichment (Table 4.3).

Table 4.3. GO functional enrichment analysis assessed by the Chi-square (χ^2) test of the groups of DEGs corresponding to the biological trends distinguishing WT and *pat* (CC, PD, FG and AD). For this analysis were considered the 25 and 20 more represented GO terms at level 3 in the Biological Process and Molecular Function GO vocabularies, respectively. Significance symbols into green and red boxes indicate respectively under- and over-represented in the considered comparison between a biological trend (CC, PD, FG and AD) and total of DEGs (TOT).

GO vocabulary	GO level	GO term	GO name	χ^2 value[a]			
				CC/ TOT	PD/ TOT	FG/ TOT	AD/ TOT
Biological Process	3	GO:0044281	small molecule metabolic process	***	-	***	-
		GO:0006950	response to stress	-	*	-	-
		GO:0055114	oxidation-reduction process	-	**	*	-
		GO:0016043	cellular component organization	-	*	-	-
		GO:0009628	response to abiotic stimulus	-	**	*	-
		GO:0009056	catabolic process	-	-	**	-
		GO:0071704	organic substance metabolic process	-	-	**	-
		GO:0022414	reproductive process	-	-	**	-
		GO:0007049	cell cycle	-	***	***	-
		GO:0032259	methylation	-	***	**	-
		GO:0051301	cell division	-	***	***	-
		GO:0019637	organophosphate metabolic process	-	*	***	-
Molecular Function	3	GO:0005515	protein binding	***	-	-	-
		GO:0016491	oxidoreductase activity	-	**	-	-
		GO:0003676	nucleic acid binding	-	-	*	*
		GO:0022857	transmembrane transporter activity	-	-	**	-
		GO:0022892	substrate-specific transporter activity	-	-	*	-
		GO:0046906	tetrapyrrole binding	-	-	***	-
		GO:0048037	cofactor binding	-	-	*	-
		GO:0061134	peptidase regulator activity	-	*	*	-
		GO:0003735	structural constituent of ribosome	-	***	*	-
		GO:0008289	lipid binding	-	-	*	-
		GO:0051540	metal cluster binding	-	-	*	-
		GO:0003682	chromatin binding	-	-	-	***

[a] Statistical significance of the X^2 test (-, not significant; *, P<0.05; **, P<0.01; ***, P<0.001).

The CC group showed enrichment for the 'small molecule metabolic process' and 'protein binding' GO terms of the Biological Process (BP) and Molecular function (MF) GO vocabularies, respectively (Table 4.3). The first GO term is related to metabolic processes involving monosaccharides. Interestingly, given the widely documented crosstalk between hormones and sugar signaling, also *IAA9*-silenced parthenorpic plants showed an upregulation of genes involved in sucrose catabolism, particularly at the post-anthesis stage and to a lesser extent at the anthesis stage, suggesting the importance of these genes in processes underlying the flower-to-fruit transition (Wang *et al.*, 2009). In the CC clusters, differences in expression between WT and *pat* were evident at Stage 3, when the mutant ovary starts its autonumous growth. Consistently, it is suggested that activation of the sugar metabolism may be an important event coupled with the initiation of pollination-independent fruit set. The second GO term over-represented in the CC biological trend is related to the formation of protein complexes functioning as activators or repressors of the gene expression. Interestingly, in this group were present orthologs of Arabidopsis TFs involved in meristem differentiation and flower organs development, such as SHOOTMERISTEMLESS (STM, in tomato LeT6/TKn2; see Chapter 5), BIG PETALp (BPEp), AINTEGUMENTA (ANT) and CRABS CLAW (CRC).

The PD group showed more GO terms significantly enriched or depleted, of which the terms 'cell cycle' and 'cell division' in BP and 'structural constituents of ribosomes' in MF represent the activation of mitosis at the onset of fruit growth after pollination (Table 4.3). In this group were present tomato members of the ARF and Aux/IAA TF families, such as SlARF9 and SlIAA14 known to actively participate in the ovary differentiation and growth during flower development and fruit set (Wang *et al.*, 2009; Wu *et al.*, 2011; Audran-Deladande *et al.*, 2012).

In the FG group GO terms significantly over-represented in PD were depleted, whereas GO categories related to cellular metabolism and growth such as 'catabolic process' and 'organic substance metabolic process' of the BP vocabulary were over-represented (Table 4.3). FG clusters included genes showing an upregulation at Stage 5 in the *pat* mutant ovary that at this stage has almost completed its cell division phase and is in the active growth phase needing energy to accomplish metabolic cellular activities.

The DEGs present in the AD group showed enriched categories only for 'nucleic acid binding' and 'chromatin binding' in the MF vocabulary (Table 4.3). These GO terms are both associated to the transcriptional regulatory machinery of the gene expression. Together with genes from CC clusters (deregulated in the *pat* ovary at Stage 3), AD

transcripts (up- or down-regulated in the *pat* ovary at all stages) could be strongly associated with the induction of the parthenocarpic phenotype showed by the mutant. Interestingly, among the up-regulated genes of this group was present *SlPBC1* encoding the beta subunit C1 of the proteasome 20S putatively involved in degradation of Aux/IAA proteins via the ubiquitin-proteasome pathway releasing free ARFs that would subsequently regulate auxin-responsive genes necessary for fruit initiation (Pandolfini *et al.*, 2007). A similar derepressing mechanism in the WT ovary after pollination is suggested for the GA-dependent degradation of DELLA proteins leading to fruit initiation (Marti *et al.*, 2007; Pandolfini *et al.*, 2007). Another interesting and strongly up-regulated gene found in this group was the *calmodulin binding transcription activator1* (*CAMTA1*). In Arabidopsis, members of the CAMTA protein family respond to IAA and stresses specifically repressing genes involved in auxin homeostasis, transport and signaling (Galon *et al.*, 2010). Among the down-regulated genes of this group was present the class A MADS-box gene *MACROCALYX* (*MC*), previously identified as a sepal size regulator (Vrebalov *et al.*, 2002). Recently, it has been shown that the MC protein interacts physically with another MADS-box protein, JOINTLESS (J), which is known as a regulator of fruit abscission (Nakano *et al.*, 2012). Interestingly, these authors, using transcriptomic analyses, showed that *MC* is also involved in phytohormone-related functions involving tomato homologs of Arabidopsis genes regulating meristem differentiation and polar auxin transport, such as *WUSCHEL* and *CUP-SHAPED COTYLEDON* (Nakano *et al.*, 2012).

Microarray validation and qRT-PCR analysis of selected genes

Microarray validation was performed by qRT-PCR studying the expression pattern in the WT and *pat* ovary of ten DEGs selected from three different groups of clusters. Seven DEGs were from the CC group (*LeT6/TKn2*, *SlBPEp*, *SlCRC*, *SlSDR*, *SlHB1*, *SlGID1L2*, *SlANT*), two from PD (*SlARF9* and *SlIAA14*) and one from AD (*SlPBC1*), respectively (Supplementary Table S1).

qRT-PCR analysis (Fig. 4.5) confirmed the expression patterns revealed with the microarray. For the ten validated DEGs correlation coefficients between the two sets of data ranged between 0.92 and 0.99 (not shown). This result strongly supported the reliability of microarray data.

In addition, qRT-PCR was adopted to study the expression patterns of six genes that were not classified as DEGs, but were considered of interest according to this thesis and literature (*SlDEF*, *SlHB15*, *SlHB15*-like, *SlARF7*, *SlARF8* and *SlIAA9*; Fig. 4.5).

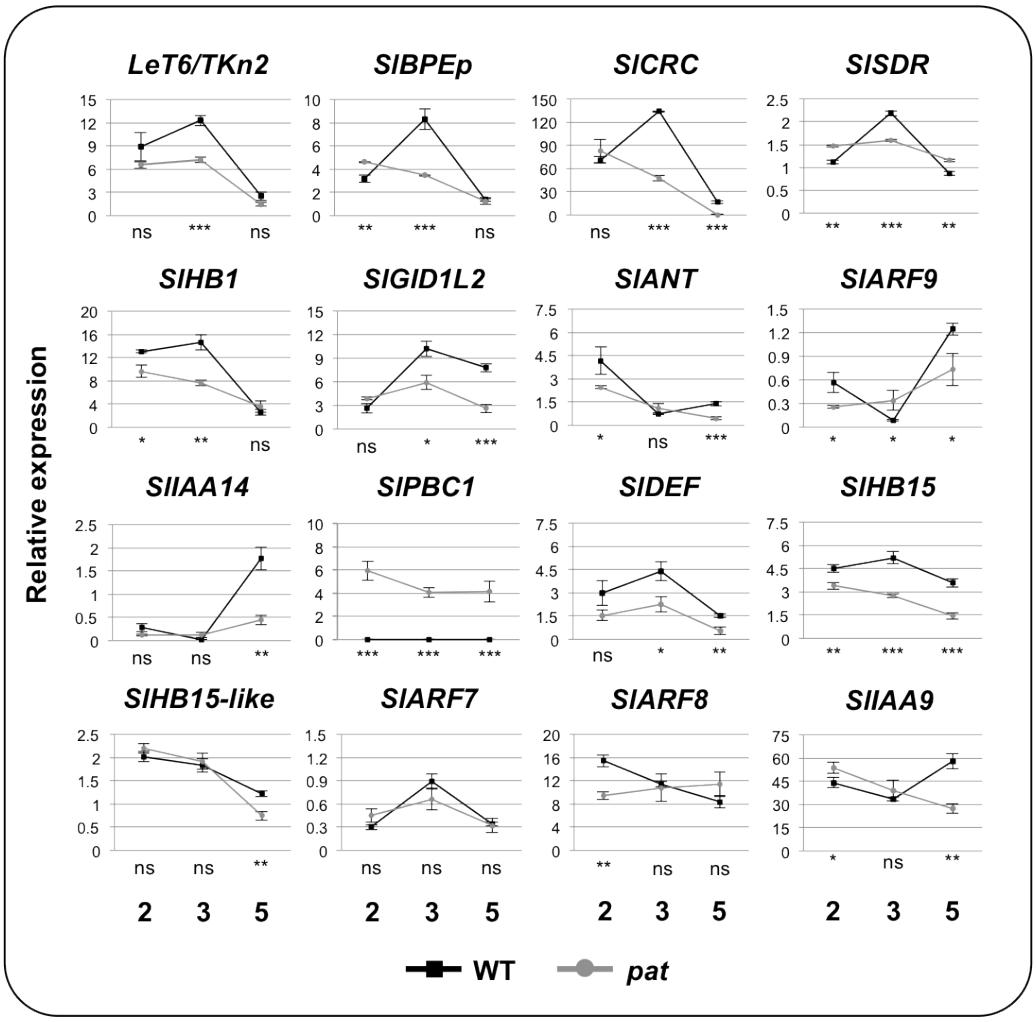

Fig. 4.5. Relative expression of the ten DEGs and other six selected genes (see text) in the WT and *pat* ovary analyzed at developmental Stages 2, 3 and 5. Data are the mean ± SEM of two indipendent biological replicates. Student's *t* test within stage (^{ns}, not significant; *, P≤0.05; **, P≤0.01; ***, P≤0.001).

Of the genes not classified as DEGs according to the microarray analysis (not significant to ANOVA or showing a lower than 3-fold difference in expression), *SlDEF* showed a pattern typical of the CC group being lower in *pat* at Stages 3 and 5 (Fig. 4.5). This is in agreement with previous reports that classified *SlDEF* as a possible repressor of ovary growth at anthesis (Mazzucato *et al.*, 2008). *SlARF7* showed a similar pattern in the WT but in *pat* was not significantly different (Fig. 4.5). *SlARF8* was down-regulated at Stage 2 in the mutant and conversely *SlIAA9* was up-regulated at Stage 5 (Fig. 4.5). *SlHB15* was consistently down-regulated in the mutant (Fig. 4.5); this gene was not significant in the microarray at the ANOVA analysis because of high variation between replicates. Finally, *SlHB15*-like was only different at Stage 5 between the two genotypes (Fig. 4.5).

qRT-PCR analysis of selected genes in parthenocarpic systems other than pat

Seven tomato selected TF genes putatively involved in the control of fruit set, *LeT6/TKn2, SlBPEp*, *SlCRC*, *SlDEF*, *SlHB15*, *SlARF8* and *SlIAA9* respectively belonging to the KNOX, bHLH, YABBY, class B MADS-box, HD-Zip III, ARF and Aux/IAA protein families (this work; Wang *et al.*, 2005; Goetz *et al.*, 2007; Olimpieri *et al.*, 2007; Mazzucato *et al.*, 2008), were found to be deregulated, not only in the *pat* mutant, but also in other parthenocarpic genotypes (Fig. 4.6).

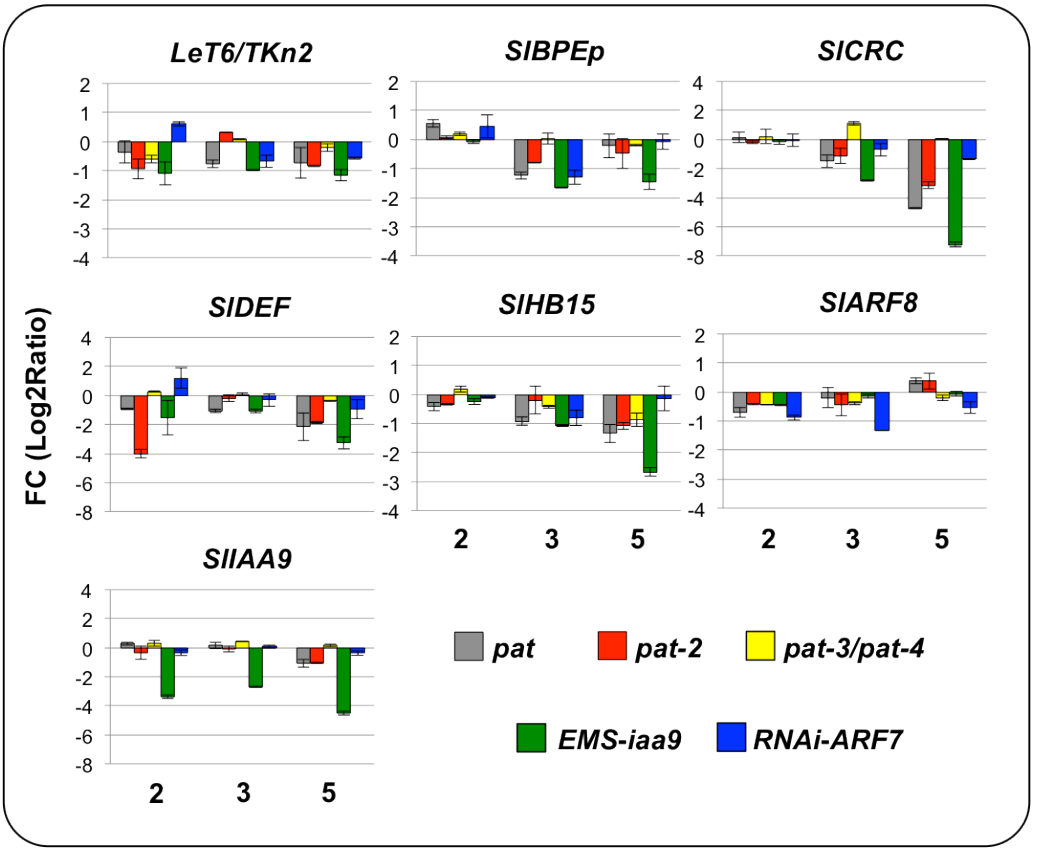

Fig. 4.6. Fold change (FC, Log2Ratio) of gene expression for the seven selected TFs (see text) in ovaries of all the parthenocarpic systems analyzed at developmental Stages 2, 3 and 5. Data are the mean ± SEM of two indipendent biological replicates.

pat-2 (bkg cv Early Mech; Philouze, 1991) is a well-studied parthenocarpic mutant in tomato; although it was described as devoid of floral defects other than parthenocarpy, in this study we found that 10% of the *pat-2* anthers showed carpelloid features (Table 4.1). This observation correlated with a downregulation of *SlDEF* in the mutant ovary at Stage 2 (Fig. 4.6). *pat-2* also presented deregulation of *LeT6/TKn2* at Stage 2 and

SlCRC at Stage 5, in parallel with *pat* (Fig. 4.6). This suggests that the *pat-2* mutation affects the ovary at early stages even if there is not clear phenotypic evidence until ovary growth.

pat-3/pat-4 (Pascual *et al.*, 2009) showed very little variation of the studied genes indicating that this mutation involves a late mechanism. Among the genes, also the role of *SlCRC* was that of a specific, late acting regulator of ovary growth, because no mutant showed variation for it at Stage 2 (Fig 4.6).

EMS-iaa9 (a TILLING loss-of-function mutant of *SlIAA9*), as expected showed a strong downregulation of *SlIAA9*, whereas for the others six studied genes displayed an expression pattern similar to *pat* (Fig. 4.6). This mutant shared with *pat* the homeotic defect of carpelloid anthers (Table 4.1) and an involvement in ovule development (F. Carriero and A. Mazzucato, unpublished), representing the stamen-ovule-ovary interaction as a driving feature of the parthenocarpic trait.

RNAi-ARF7 (de Jong *et al.*, 2009b) was confirmed for the *SlARF7* downregulation at all flower stages (not shown) and interestingly showed for *SlARF8* (Fig. 4.6), member of the same TF family, a parallel expression behavior (Fig. 4.6). At stage 3, this mutant showed a strong deregulation of *SlBPEp* (Fig. 4.6), a gene encoding a TF interacting with ARF8 in Arabidopsis petal development (Varaud *et al.*, 2011). This suggests a wider interaction of BPEp with ARF TFs and a wider range of controlled developmental processes by these protein complexes.

Chapter 5

Genetic interaction between *parthenocarpic fruit* and *Curl*, a dominant mutation affecting vegetative and floral meristem differentiation

Abstract

Knotted1-like homeobox (KNOX) transcription factors (TFs), which have been described as negative regulators of *gibberellin 20-oxidase* (*GA20ox*) genes, are highly expressed at anthesis in the ovary of wild type (WT) tomato plants and transcript levels decrease after pollination. In the *parthenocarpic fruit* (*pat*) mutant, where the ovary develops into seedless fruits independently from pollination and fertilization, the expression levels of *Tomato Knotted 2* (*LeT6/TKn2*), ortholog of the Arabidopsis *SHOOTMERISTEMLESS* (*STM*) TF, decrease prior to anthesis. These findings indicate that members of the *KNOX* gene family might act as negative regulators of fruit initiation, possibly repressing gibberellin biosynthesis in unpollinated WT ovaries. Following these observations, a phenotypic and molecular characterization of double mutant plants carrying *pat* and the dominant mutation *Curl* (*Cu*, overexpressing *LeT6/TKn2* and responsible for an abnormal development of plant vegetative structures) was performed. All phenotypes typical of the *pat* syndrome were evaluated in F_3 and F_4 individuals representing all the phenotypic combinations (*Pat cu*, *pat cu*, *Pat Cu* and *pat Cu*). For all the reproductive traits examined, including the frequency of stamen and ovule aberrations and yield traits such as fruit set, a reduction of the *pat* expressivity was observed in the *pat Cu* double mutant background. When specifically tested for parthenocarpy, emasculated not-pollinated flowers of *pat Cu* plants did not set fruits or developed fruitlets significantly smaller compared to the *pat* single mutant. Expression analysis in parthenocarpic systems other than *pat* indicated that the developmental regulation of *LeT6/Tkn2* in the ovary is conserved in different wild type backgrounds, but is not paralleled in all the parthenocarpic mutants. The GA-overdose phenotypes showed by the *pat* mutation are likely mediated by a deregulation of *LeT6/Tkn2* in the mutant ovary. This hypothesis is supported by a misexpression of *LeT6/TKn2* and key genes in GAs metabolism (*GA20ox1* and *GA2ox2*) in the *pat Cu* ovary spanning fruit set. In conclusion, the phenotypic and molecular characterization of the *pat Cu* double mutant strongly suggests an interaction between the gene underlying the *pat* mutation and *LeT6/Tkn2* in the regulation of tomato fruit set.

Introduction

Knotted1-like homeobox (KNOX) proteins are homeodomain transcription factors (TFs) involved in the maintenance of an important pluripotent cell population termed the shoot apical meristem (SAM), which generates the entire above-ground body of vascular plants (Hay and Tsiantis, 2010). KNOX members have been previously classified into two protein families, KNOX I and KNOX II (Kerstetter *et al.*, 1994). Both these two families of TFs are candidates for the control of hormone homeostasis in vegetative and floral meristematic tissues (Hay and Tsiantis, 2010).

KNOX proteins increase cytokinins (CKs) levels by activating the transcription of *ISOPENTENYL TRANSFERASE7* (*IPT7*) and reduce gibberellins (GAs) levels by directly repressing the biosynthetic gene *GA 20-oxidase1* (*GA20ox1*) and activating catabolic genes such as *GA 2-oxidase2* (*GA2ox2*) and *GA2ox4* (Hay *et al.*, 2002; Jasinski *et al.*, 2005; Yanai *et al.*, 2005).

In tomato, KNOX genes are highly expressed at anthesis in the ovary of wild type (WT) plants and decrease their expression after pollination (Olimpieri *et al.*, 2007). In the *parthenocarpic fruit* (*pat*) mutant, transcript levels of the class I KNOX gene *Tomato Knotted 2* (*TKn2,* also known as *LeT6* and hereafter referred to as *LeT6/TKn2*), the tomato ortholog of *SHOOTMERISTEMLESS* (*STM*) in Arabidopsis and *Knotted1* (*Kn1*) in maize (Hay and Tsiantis, 2010), already decrease prior to anthesis (see Fig. 4.5 in Chapter 4; Olimpieri *et al*., 2007). This result indicates that members of the *KNOX* gene family might also act as negative regulators of fruit growth, repressing GA biosynthesis in unpollinated WT ovaries (Olimpieri *et al.*, 2007).

A role for GAs in the *pat* phenotype was previously proposed by Mapelli *et al.* (1978), but the actual mechanisms responsible have been confounded by the presence of phenotypic traits that could indicate both GA deficiency and overproduction (Olimpieri *et al.*, 2007). Specifically, the *pat* mutant shows defects in organ elongation and enlargement (Mazzucato *et al.*, 1998, 1999), as do GA-deficient mutants (King, 1988; Olszewski *et al.*, 2002), yet these phenotypes could not be totally rescued by treatment with gibberellic acid (GA_3; Mazzucato *et al.*, 1999). Conversely, the levels of auxin (IAA) and GA-like substances in the ovary after anthesis were found to be higher than in the WT line (Mapelli *et al.*, 1978) and this was consistent with the occurrence of the parthenocarpic phenotype. Accordingly, expression analysis of GA-regulated genes also suggested GA saturation of the *pat* mutant ovary (Testa *et al.*, 2002). However, it has not been determined whether GA synthesis is altered before anthesis in the

mutant, nor has any investigation addressed the possibility of a GA-constitutive response, as is the case in slender mutants such as *spindly* (*spy*) in Arabidopsis that are impaired in genes encoding repressors of the GA response pathway (Jacobsen and Olszewski, 1993).

Based on these findings and to improve the understanding of the specific role of *LeT6/TKn2* in tomato fruit set, we characterized the reproductive phenotype of the *pat Cu* double mutant obtained combining *pat* with the dominant mutation *Curl* (*Cu*) responsible for the overexpression of *LeT6/TKn2* in vegetative meristems and flower tissues (Parnis *et al*., 1997).

Materials and methods

Plant material and phenotypic characterization

In summer 2010, a pilot experiment was performed with 30 F_2 plants obtained after crossing the recessive *pat* with the dominant *Cu* mutant (accession number LA3740) obtained from the Tomato Genetics Resource Center (TGRC; http://tgrc.ucdavis.edu/). The population was grown during summer in open field with standard horticultural practices at the experimental station of the Tuscia University in Viterbo, Italy. Preliminary observations of phenotypic traits related to the *pat* syndrome, such as pollen viability, stamen development, ovule morphology and fruit set were conducted on these plants segregating *pat* and *Cu*. In summer 2011, F_3 progenies segregating all the phenotypic combinations (*Pat cu*, *pat cu*, *Pat Cu* and *pat Cu*) were grown and evaluated for the same *pat* syndrome-related traits. Finally, in summer 2012, eight to twelve F_4 individuals derived from F_3 plants with a fixed genotype were grown again in open field and definitive phenotypic data were collected.

To determine the parthenocarpic behaviour, two F_4 plants of each phenotype were used for an emasculation experiment and remaining plants for the evaluation of flower organs development. Pollen, stamen and ovule morphology was examined in at least two flowers at anthesis (Stage 4; according to Mazzucato *et al*., 1998) from four different plants. Pollen viability was evaluated by light microscopy after staining the pollen with a filtered 2% (w/v) carmine acetate solution. Pollen grains were classified as viable (V) or not viable (NV) based on their staining capability and morphology. By stereomicroscopy, a quantitative estimation of stamen and ovule aberrations was scored. Stamens were classified as normal (N), short (Sh), carpelloid (Ca) or carpelloid with external ovules (Ca/EO) and ovules categorized as normal (N) or aberrant (Ab) based on their morphology. In total, 16 flowers from eight different F_4 plants were used to assess stamen and ovule morphology. Fruit set was calculated in the first four floral trusses according to the ratio between the number of flowers that set fruits and the total number of flowers per inflorescence. All the recorded data were analyzed through descriptive statistics and presented as frequency of aberrations or mean ± standard error of the mean (SEM). Based on the data, the statistical significance was assessed by Student's *t* test using Microsoft Excel 2011 or by the analysis of variance using the PROC ANOVA procedure of the SAS software (SAS Institute Inc. 2002).

Gene expression analysis and bioinformatic characterization

Expression level of *LeT6/TKn2*, *GA20ox1* and *GA2ox2* was analysed in the ovary of F_4 plants segregating *pat* and *Cu*. Total RNA from ovaries (without style) from the two flower stages spanning fruit set (Stage 3 and 5; according to Mazzucato et al., 1998) was extracted using Trizol reagent (Life Technologies, Gaithersburg, MD, USA) following the manufacturer's instructions. For reverse transcription-polymerase chain reaction (RT-PCR), first-strand cDNA was synthesized using the SuperScript II RNase-H Reverse Transcription Kit (Invitrogen, Carslbad, CA, USA) and RT-PCR experiments were performed using amounts of cDNA normalized using the house-keeping (HK) gene *CAC* (SGN-U314153; Expósito-Rodríguez *et al*., 2008). After normalization, cDNA samples were amplified with primers specific for the genes described, using a number of PCR cycles calibrated to avoid saturation. Primer sets and amplification conditions for *LeT6/TKn2*, *GA20ox1* and *GA2ox2* are reported in the Supplementary Table S4. RT-PCR products were electrophoresed through 1.5% (w/v) agarose gels and stained with ethidium bromide. RT-PCR experiments were repeated twice using two biological replications. Expression data, reported as relative expression, were derived from the ratio between the quantitative values of PCR band intensity for the target gene and the HK control measured by the Gel Analyzer procedure of the ImageJ software (http://rsb.info.nih.gov/ij/). Expression data were presented as mean ± standard error of the mean (SEM). Differences in estimated gene expression values between genotypes or stages were statistically analyzed by two-way analysis of the variance using the PROC ANOVA procedure of the SAS software (SAS Institute Inc. 2002).

The web-based application Genevestigator (Zimmermann *et al.*, 2004; https://www.genevestigator.com/) was used to investigate in tomato the temporal and spatial expression of *LeT6/TKn2.* Materials and methods used for *LeT6/TKn2* expression analysis by real-time PCR (qRT-PCR) in different parthenocarpic genotypes (*pat*, *pat-2*, *pat-3/pat-4*, *EMS-iaa9*, *RNAi-ARF7*) are described in Chapter 4 and in the Supplementary Table S1.

Results and discussion

Cu *vegetative alterations*

As previously described by Parnis *et al.* (1997), F_2 plants either homozygous or heterozygous for the *Cu* allele showed dramatic vegetative alterations. Specifically, these plants were characterized by compact foliage structures (Fig. 5.1A) that were nevertheless differentiated in the correct phyllotactic pattern (Parnis *et al.*, 1997). They consisted of compound ramified leaves with wrinkled, curled blades and an extremely corrugated leaf surface, presumably as a result of intercalary disproportionate growth and diminutive, unexpanded axillary branches (Parnis *et al.*, 1997). *Cu* inflorescences were reduced in size (Fig. 5.1B) compared to those of *cu* plants (not shown) and their flowers set fertile immature fruits with an extreme dark pigmentation (Fig. 5.1C; Parnis *et al.*, 1997).

Fig. 5.1. (A) *Cu* compact leaf structure. (B) *Cu* inflorescence showing a reduced size. (C) Dark green pigmentation observed in *Cu* immature fruits (see text).

The presence in *Cu* plants of the *pat* mutated allele in homozygous condition did not modify the altered *Cu* vegetative phenotype (not shown). Contrary, a strong interaction

between *pat* and *Cu* was mainly highlighted by the phenotypic characterization of flower organs (e.g. stamen and ovary).

Phenotypic characterization of the pat Cu *androecium and gynoecium*

All phenotypes typical of the *pat* syndrome (lower pollen viability, stamen and ovule aberrations, parthenocarpic ovary growth, increased fruit set; Mazzucato *et al*., 1998; 1999) were evaluated in F_3 and F_4 individuals with a fixed genotype representing all the phenotypic combinations *Pat cu* (hereafter referred to as WT), *pat cu* (*pat*), *Pat Cu* (*Cu*) and the double mutant *pat Cu*.

Pollen viability was reduced in *pat* compared to WT, in contrast with the double mutant *pat Cu* that showed no differences compared to its *Cu* single mutated counterpart (Fig. 5.2). In addition, the percentage of unviable pollen showed by *pat* was significantly lower than in the *pat Cu* double mutant, indicating that for this trait the *Cu* mutation is epistatic to *pat*. Overall, these observations suggest that also in tomato *KNOX* genes might be involved in pollen development and the results are in agreement with the characterization of *semaphore1* (*sem1*) mutants in maize responsible for an ectopic expression of *KNOX* genes and a reduced polar auxin transport in shoots (Scanlon *et al*., 2002). In tomato, considering these findings in maize, the hypothesis might be that the *Cu* mutation epistatic to *pat* further modify the already altered GA levels of the *pat* single mutant leading to an increment of unviable pollen formation (Fig. 5.2). Another more direct explanation could be that *Cu* overexpressing *LeT6/TKn2* in developing anther tissues repress the expression of the GA biosynthetic gene *GA20ox1* leading to unviable pollen development as observed in co-suppressed tomato plants for this gene (Olimpieri *et al*., 2011).

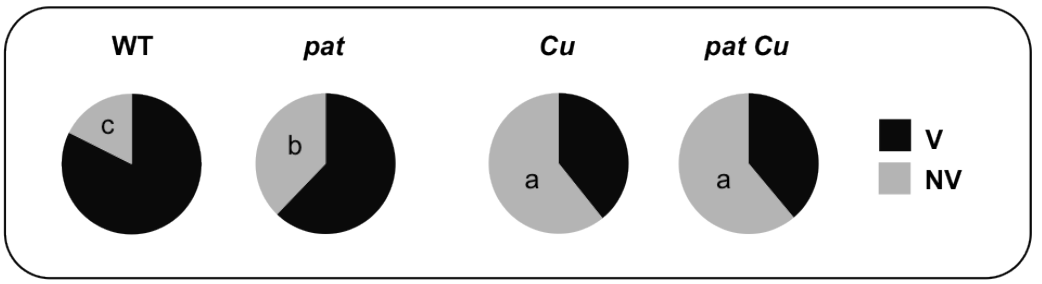

Fig. 5.2. Pollen viability in plants segregating *pat* and *Cu* (WT, *pat*, *Cu* and *pat Cu*). V and NV stand for viable and not-viable pollen, respectively. Pies show mean percentages (n = 24). Means indicated by the same lowercase letter are not significantly different for P≤0.01.

One of the most important pleiotropic effect of the *pat* mutation is represented by partial modification of stamen elements (Fig. 5.3A), which may appear as normal (N),

short (Sh), carpelloid (Ca) or carpelloid with external ovules (Ca/EO). For this trait, the *pat Cu* double mutant showed lower expressivity than the *pat* single mutant, because homeotic conversions of Ca stamens were significantly (P≤0.001) reduced in this genetic background (19.29 and 42.38% respectively in *pat Cu* and *pat*; Fig. 5.3B). Interestingly, frequency reduction of carpelloid anthers was already observed in *pat* flowers treated with GA_3 (Mazzucato *et al.*, 1999). This early report and results presented here suggest that alteration of *KNOX* genes expression in the *pat Cu* anthers could modulate the content of GAs and eventually their cross-talk with IAA required for a correct stamen development (Cecchetti *et al.*, 2004; 2008; Song *et al.*, 2013).

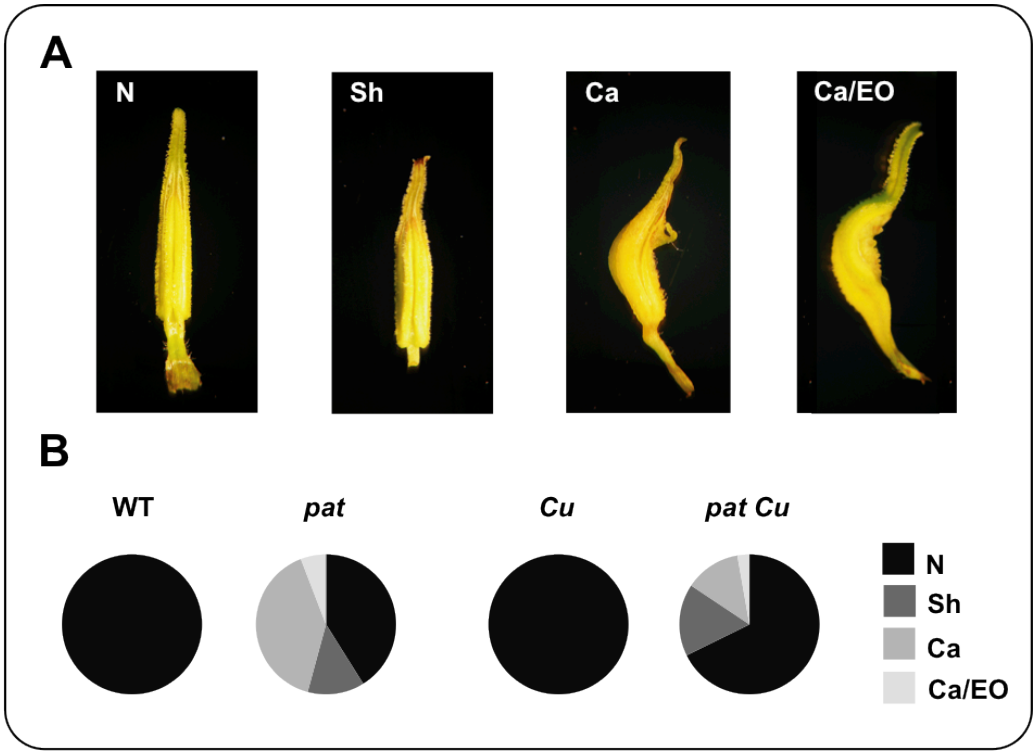

Fig. 5.3. (A) WT stamens (N, normal), lenght reduction (Sh, short) and homeotic transformations of *pat* anthers, showing stigma-like structures (Ca, carpelloid) and carpel-like structures bearing ovules (Ca/EO, carpelloid with external ovules). (B) Fequency of stamen aberrations in plants segragating *pa*t and *Cu* (WT, *pat*, *Cu* and *pat Cu*). Pies represent mean percentages (n = 16).

Parthenocarpic behaviour in *pat* is evident as the ovary already enlarges in flowers at anthesis (Fig. 5.4A; Mazzucato *et al.*, 1998). Ovary weight is thus significantly higher in *pat* than in WT and *Cu* flowers (Fig. 5.4B). In the *pat Cu* genotype, ovary weight at anthesis is similar to both WT and *Cu* single mutants, indicating a suppression of the parthenocarpic tendency (Fig. 5.4B).

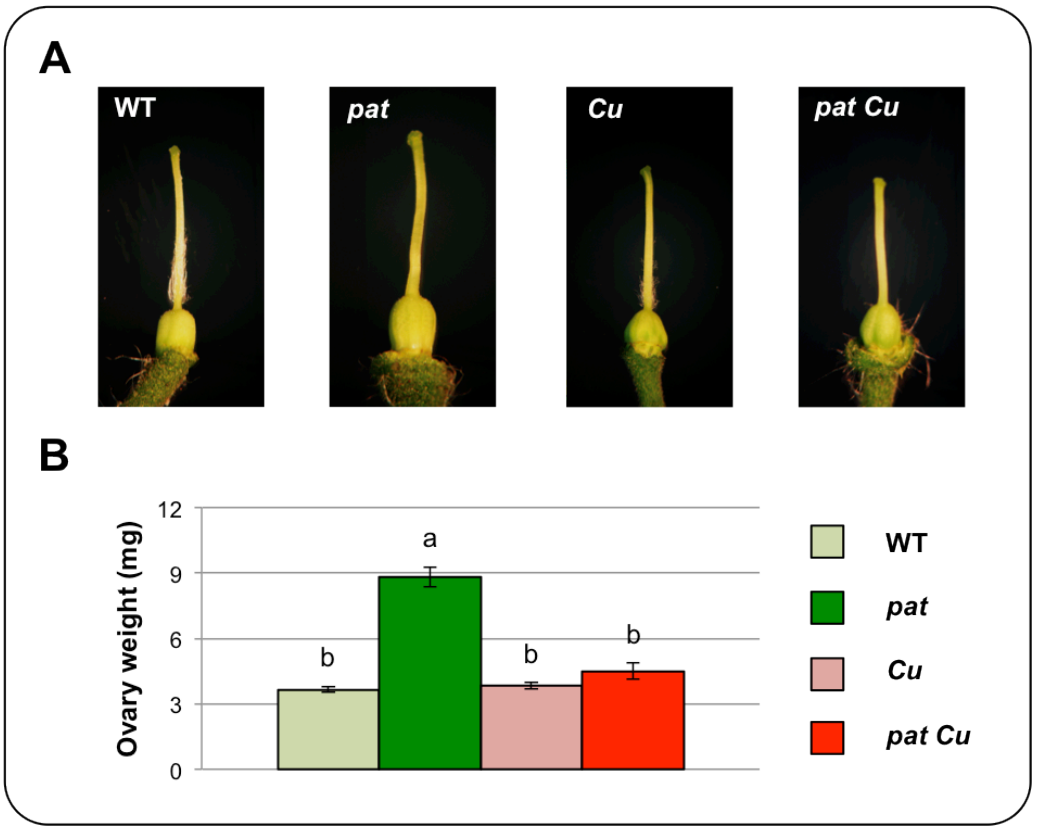

Fig. 5.4. (A) Representative ovary phenotype at anthesis in plants segragating *pa*t and *Cu* (WT, *pat*, *Cu* and *pat Cu*). (B) Ovary weight at anthesis in the same genotypes. Bars represent mean ± SEM (n = 16). Means indicated by the same lowercase letter are not significantly different for P≤0.01.

Interestingly, ovule aberrations in *pat Cu* (31.16%) were significantly (P≤0.001) reduced compared to the *pat* single mutant (44.03%), while WT and *Cu* plants showed a normal ovular phenotype (Fig. 5.5).

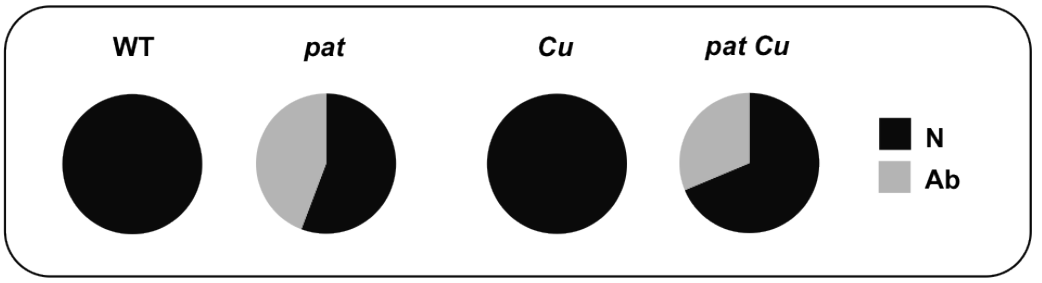

Fig. 5.5. Ovule aberrations in plants segregating *pat* and *Cu* (WT, *pat*, *Cu* and *pat Cu*). N and Ab stand for normal and aberrant ovules, respectively. Pies show mean percentages (n = 16).

This phenotypic observation may be related to the expression of *LeT6/TKn2* in WT carpels at anthesis that was found in the vascular system and in distinct regions of the ovule (Janssen *et al.*, 1998). In a more deep characterization, the expression of this

gene was found to be confined to the inner part of the ovule integument (Avivi *et al.*, 2000). Considering these findings, the reduction of ovule aberrations observed in the *pat Cu* double mutant could be addressed to a *LeT6/TKn*2 misregulation in developing ovular tissues that partially restored the ovule integument alterations showed by the *pat* single mutant (Mazzucato *et al.*, 1998) and led to a reduction of aberrant ovules. All these observations indicate that, as for androecium phenotypes (pollen and stamen development), also in the gynoecium the gene underlying the *pat* mutation and *LeT6/TKn2* are strongly interacting.

Fruit set and parthenocarpic tendency of the pat Cu *double mutant*

In the *pat Cu* double mutant the fruit set was similar to its relative *Cu* single mutant counterpart. Differently, in *pat* it was higher than in the WT as previously reported (Fig. 5.6; Mazzucato *et al.*, 1999). Both genotypes mutated for *Cu* (*Cu* and *pat Cu*) showed an elevated level of sterility and their fruit set ranged from 6 to 21% (Fig. 5.6). Again, this result indicates that *LeT6/TKn2* is involved in physiological and molecular mechanisms of tomato reproductive biology, in addition to evident vegetative alterations showed by natural mutants such as *Cu*, *Mouse-ear* (*Me*) and *clausa* (*clau*) or by transgenic lines overexpressing this gene (Parnis *et al.*, 1997; Janssen *et al.*, 1998; Avivi *et al.*, 2000). In fruit set, as for the pollen viability, the *Cu* mutation could be considered epistatic to *pat*.

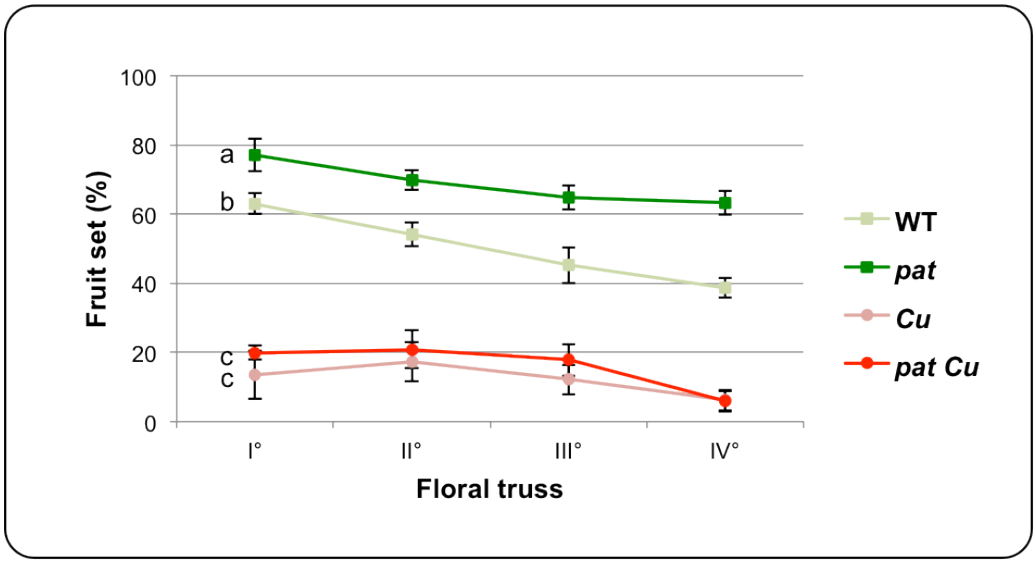

Fig. 5.6. Percentage of fruit set at the first four floral trusses in plants segregating *pat* and *Cu* (WT, *pat*, *Cu* and *pat Cu*). Points represent mean ± SEM (n=8). Statistical significance was assessed by two-way ANOVA, interaction not significant. Genotypes indicated by the same lowercase letter are mot significantly different for P≤0.001).

Further highlights of the reduction of *pat* expressivity in the *pat Cu* double mutant were obtained trough an emasculation experiment. Indeed, emasculated not-pollinated flowers of *pat Cu* plants, in 11 d, did not set fruits (not shown) or developed fruitlets significantly (P≤0.01; n = 4) smaller (82.67 ± 17.09 mg) compared to those developed in the *pat* single mutant (327.67 ± 24.40 mg). This result indicates that in the *pat Cu* double mutant the power of the autonomous ovary usually growth triggered by the *pat* mutation is strongly reduced by the overexpression of *LeT6/TKn2*.

Gene expression analysis of LeT6/TKn2*,* GA20ox1 *and* GA2ox2 *in the* pat Cu *ovary at fruit set*

Expression analysis of *LeT6/TKn2*, *GA20ox1* and *GA2ox2* during fruit set was evaluated on ovaries from flowers at opening and 2 days post anthesis stages (Stage 3 and 5, respectively; Mazzucato *et al.*, 1998). According to RT-PCR, followed by statistical analysis, the first two genes showed a significant "Genotype*Stage" interaction, whereas the latter showed no interaction.

Previous analyses showed that *LeT6/TKn2* was highly expressed in ovaries of WT plants before anthesis and down-regulated by pollination; in the *pat* mutant, the gene was deregulated at anthesis (see Fig. 4.5 in Chapter 4; Olimpieri *et al.*, 2007). Here, expression of *LeT6/TKn2* was not significantly different among genotypes at Stage 3 (Fig. 5.7).

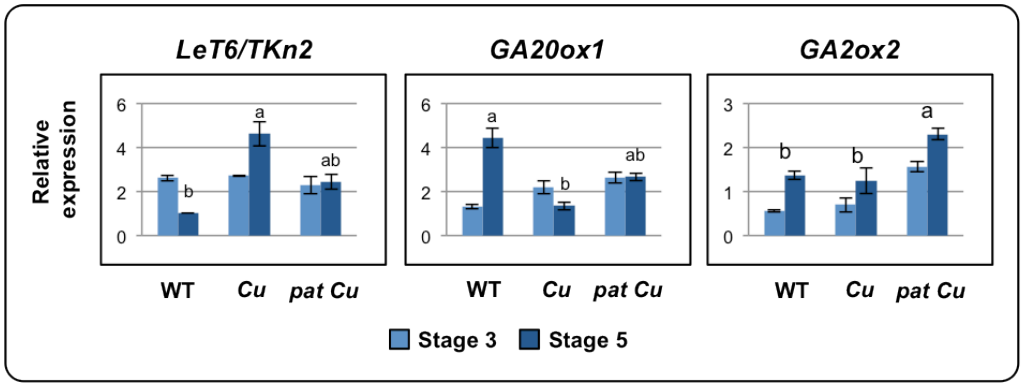

Fig. 5.7. Gene expression analysis of *LeT6/TKn2*, *GA20ox1* and *GA2ox2* in the ovary at flower stages spanning fruit set (Stage 3 and Stage 5; Mazzucato *et al.*, 1998) of WT (*Pat cu*), *Cu* (*Pat Cu*) and *pat Cu* F_4 plants. Bars represent mean ± SEM of two biological replicates. For *LeT6/TKn2* and *GA20ox1*, means indicated by the same lowercase letter within Stage 5 are not significantly different for P≤0.01; for *GA2ox2*, genotypes indicated by the same lowercase letter are not significantly different for P≤0.01.

At Stage 5, *LeT6/TKn2* was overexpressed in the *Cu* ovary, whereas in *pat Cu* genotype assumed an intermediate value (Fig. 5.7). The *GA20ox1* was also not

differently expressed at Stage 3, but showed significant differences at Stage 5, which were opposite to those observed for *LeT6/TKn2*. Notably, also in this case the double mutant assumed an intermediate value (Fig. 5.7). For *GA2ox2*, where no interaction was found, a significantly higher expression was found in the double mutant compared to WT and *Cu* (Fig. 5.7).

Overall, this analysis indicated that the lower *pat* expressivity in the *pat Cu* genotype is mediated by the overexpression of *LeT6/TKn2* in the mutant ovary during flower-to-fruit transition, which counteracts the GA-overdose phenotypes showed by the *pat* mutation.

Bioinformatic characterization of LeT6/TKn2 *and gene expression cues from other parthenocarpic genotypes*

In silico analysis using the web-based application Genevestigator (Zimmermann *et al.*, 2004) showed that highest *LeT6/TKn2* expression levels are found in carpels, despite the demonstrated role of this gene in vegetative meristem differentiation and leaf development (Fig. 5.8A). Considering the overall plant development, this TF peaks during flowering, when fruit set takes place (Fig. 5.8B).

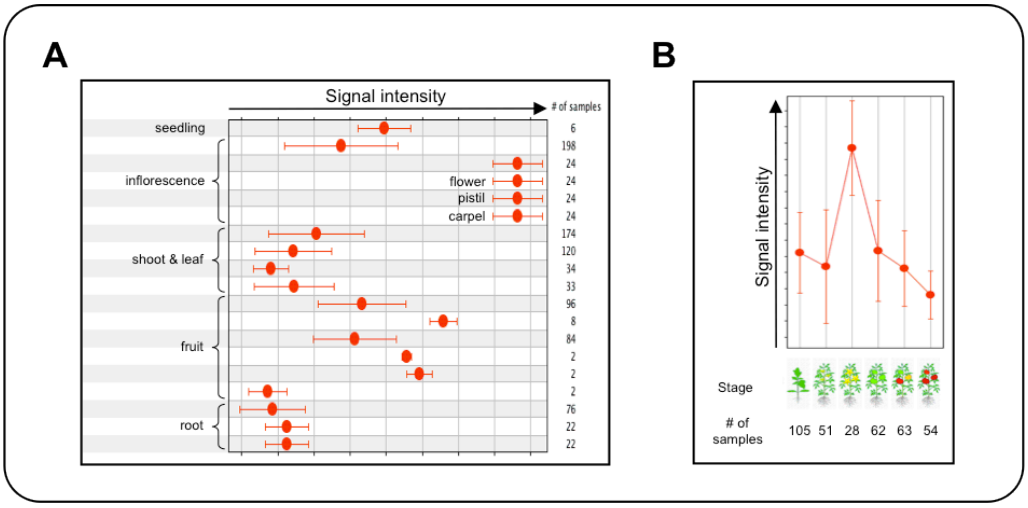

Fig. 5.8. (A) *LeT6/TKn2* expression level in different tomato plant tissues and (B) during different plant developmental stages. Signal intensity measures the absolute *LeT6/TKn2* expression assayed in a number of transcriptomic experiments (# of samples) deposited in Genevestigator.

Expression analysis of *LeT6/TKn2* in the ovaries of parthenocarpic systems other than *pat* indicated that the developmental regulation of the gene at fruit set is generally conserved in different wild type backgrounds, but its deregulation is not paralleled in all the parthenocarpic tomato mutants analysed (Fig. 5.9). The mutations *pat-2* and *pat-*

3/pat-4 showed no deregulation of the gene, indicating that their genetic control is likely downstream of or in a different pathway than *LeT6/TKn2*. Differently, tomato plants silenced for *SlIAA9* or *SlARF7* (see chapter 4) showed deregulation of this gene in the ovary (Fig. 5.9) indicating that the auxin response, which is under their negative control, is an effector of *LeT6/TKn2* down-regulation at fruit set.

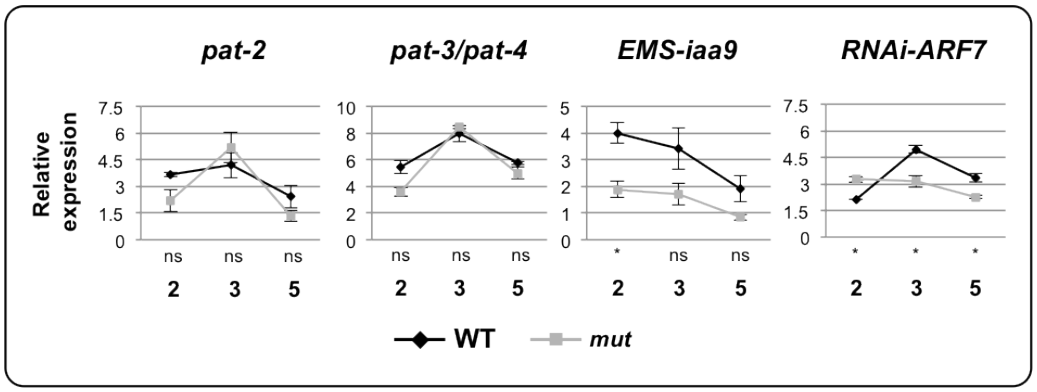

Fig. 5.9. Relative expression of *LeT6/TKn2* in the WT and mutant (*mut*) ovary of the different parthenocarpic systems analyzed at flower bud (2), opening (3) and 2 days post anthesis (5) developmental stages. Data are the mean ± SEM of two indipendent biological replicates. Student's *t* test between wild type (WT) and mutant (*mut*) genotype of the same parthenocarpic system within stage. ^{ns}, not significant; *, P≤0.05.

Overall, a reduction of the *pat* expressivity was observed in the *pat Cu* double mutant for all the reproductive traits examined. Taken together, the data obtained trough the phenotypic and molecular characterization of *pat Cu* indicated *LeT6/TKn2* as an important negative regulator of ovary growth during flower-to-fruit transition and suggested a role in mediating the IAA-GA cross-talk during tomato reproductive phases.

Chapter 6

General discussion

General discussion

The biological function of the fruit is the protection of embryos and seeds during their development and the facilitation of seed dispersal after maturation. Normally, the onset of fruit development from the ovary (i.e. fruit set) occurs after flower pollination and ovule fertilization, and is coordinated by signals produced in developing embryos (Gillaspy *et al.*, 1993).

Fruit set and development can be uncoupled from fertilization and seed development as indicated by the existence of seedless mutant plants (e.g. tomato *pat* mutants; reviewed by Lukyanenko, 1991; reviewed by Gorguet *et al.,* 2005) and seedless crops obtained by traditional breeding methods (i.e. seedless grape, citrus, cucumber and watermelon; Varoquaux *et al.*, 2000).

A plant is considered to be seedless if it is able to produce a fruit with no seed, traces of aborted seeds or a much-reduced number of seeds. Two main mechanisms are responsible for the formation of seedless fruits: (i) parthenocarpy, where the fruit develops in the absence od pollination and/or fertilization; and (ii) stenospermocarpy, where pollination and fertilization are required, but embryos either do not form or they abort before completion of seed formation (Varoquaux et al., 2000).

The importance of parthenocarpic mutations is due to their possible use in breeding programs, as well as in studies aimed to the comprehension of mechanisms underlying the fruit set. In fact, an understanding of the molecular events associated to parthenocarpy would provide information on factors regulating fruit and seed formation, and thus open new perspectives for yield improvements by conventional breeding and/or biotechnological means.

Among the different sources of natural parthenocarpy described in tomato the *pat* mutation (Bianchi and Soressi, 1969), object of the thesis, is of particular interest because of its strong expressivity (Fig. 1.1A-D), high fruit set and enhanced fruit quality (Fig. 1.1E and F; Falavigna *et al.*, 1978; Mazzucato et *al.*, 1999; F. Ruiu and A Mazzucato, unpusblished).

As a pleiotropic effect, *pat* flowers show homeotic transformation of the anthers and aberrancy of ovules (Mazzucato *et al.,* 1998). Moreover, *pat* plants display also vegetative alterations such as defects in cotyledon number and morphology (Olimpieri *et al.*, 2007). All these phenotypes showed by the *pat* mutant could be addressed to a hormonal imbalance mainly of IAA and GAs (Mapelli *et al.*, 1978; Olimpieri *et al.*, 2007).

The locus of the *pat* mutation, through a positional cloning approach, was mapped on the long arm of chromosome 3 between the two COS markers T0796 and T1143 of the tomato genetic map EXPEN 2000 (Fulton *et al.*, 2002; www.solgenomics.net/), defining a genetic window of 1.2 cM (Beraldi *et al.,* 2004). Recently, by pursuing the microsynteny between tomato and Arabidopsis, the target region containing the *Pat* locus was narrowed to less than 0.2 cM between two markers named T17 and T20 corresponding respectively to the SGN loci *Solyc03g120880* and *Solyc03g120980* (Selleri, 2010; see Chapter 2). The small size of the new target region and the recent publication of the tomato genome sequence allowed us to pursue a candidate gene approach. Following this method, the *Solyc03g120910* was indicated as the candidate gene underlying the *pat* mutation (Selleri, 2010; see Chapter 2). This gene encodes for the tomato HD-Zip III TF ortholog of ATHB15/CNA/ICU4 in Arabidopsis. In tomato, according to this finding, we named the gene *SlHB15*.

Starting from this background, the following discussion will reflect the experimental chapters of this thesis. Using different methodological approaches, the hypothesis that *SlHB15* represents the gene underlying the *pat* mutation was reinforced and information regarding the molecular basis of the complex phenotype exhibited by the *pat* mutant was increased.

The G583R lesion in the SlHB15 protein encoded by the pat *allele*

As described in Chapter 2, the point mutation G1747A found in the CDS of the *pat* allele (Fig. 2.3A; Selleri, 2010) is responsible for the G583R amino acid change in the SlHB15^{pat} protein (Fig. 2.3B; Selleri, 2010) located in a highly conserved region between the two characterized HD-Zip III domains SAD and MEKHLA (Fig. 2.3C). The G583R amino acid substitution carried by the SlHB15^{pat} protein was predicted as not tolerated for the protein function. A modification of its functionality was highlighted by the prediction of its 3D model. Indeed, the SlHB15^{pat} mutated protein showed a destructurated folding when compared to the SlHB15^{WT} protein (Fig. 2.4).

Following these findings and considering that HD-Zip III proteins form homo- and heterodimers to accomplish their regulatory role of TF (Ariel *et al.*, 2007; Elhiti and Stasolla, 2011), it can be proposed that the *pat* mutant phenotype is caused by an alteration of the SlHB15^{pat} protein structure leading to a modification of protein functionalities, such as interaction with the DNA of target gene promoters and/or homo-heterodimerization. To support this data, the ATHB15/CNA/ICU4 protein encoded by

the Arabidopsis *hoc* mutant presents a single amino acid change in the MEKHLA domain responsible for an hypothetical modification of the protein fuction (Duclercq *et al.*, 2010). The *hoc* mutant shows a bushy phenotype due to extra rosette leaves developing from early axillary meristems. As *pat* in tomato, the *hoc* phenotype in Arabidopsis could be addressed to a modulation in homo- and/or heterodimerization activity, in contrast to *ATHB15/CNA/ICU4* knockout lines that, being balanced by a combinatory and/or antagonistic action of other HD-Zip III proteins, result in a nearly-normal WT phenotype (Prigge *et al.*, 2005; Duclercq *et al.*, 2011). A similar hypothesis on the activities of HD-Zip III homo- or heterodimers was reported by Ochando *et al.* (2008) to explain the phenotype of the *ATHB15/CNA/ICU4* loss- or gain-of-function mutants.

The implication of SlHB15 *in fruit set and IAA homeostasis*

In Arabidopsis, the HD-Zip III subfamily protein includes five members (*ATHB8*, *ATHB9/PHV*, *ATHB14/PHB*, *ATHB15/CNA/ICU4* and *IFL1*/*REV*), whereas in tomato six members are present because *SlHB15* presents a paralogous gene (*SlHB15*-like) located on chromosome 12 (Table 2.1 and Fig. 2.5).

As reported in Table 2.2, among the HD-Zip III genes in tomato, *SlHB15* is highly expressed during tomato flower and early fruit development, whereas *SlHB15*-like peaks in the mature fruit, indicating a putative role in the regulation of ripening-associated metabolic processes. Consistent with this analysis, a functional modification of the SlHB15 protein, as hypothesized in the *pat* mutant by bioinformatic means, could lead to parthenocarpy.

In Arabidopsis, the *ATHB15/CNA/ICU4* gene is co-localized and co-expressed with many IAA-related genes, as showed by the functional association network generated (Fig. 2.6), thus suggesting its active partecipation in the regulation of the IAA homeostasis in plant organs. In addition, it has been determined that the expression of the HD-Zip III genes mirrors the predicted flow of IAA in both vascular and nonvascular plants (Floyd and Bowman, 2006; Floyd *et al.*, 2006; Izhaki and Bowman, 2007).

Starting from the observation that *ATHB15/CNA/ICU4* and *SlHB15* share 83.7% of identity at the amino acid level (Table 2.1), it can be hypothesized that most of genes interacting with *ATHB15/CNA/ICU4* and highlighted in the functional association network (Fig. 2.6) represent putatively those interacting with *SlHB15* in tomato. Interestingly, among these genes, members of the ARF, Aux/IAA, PIN and Aux/LAX TF families, such as *MP*/*ARF5*, *BDL/IAA12*, *PIN1*, *LAX2* and *LAX3* involved in the IAA

signaling and transport were present (Fig. 2.6). All these TF families are involved in the regulation of the IAA homeostasis and polar auxin transport in several plant tissues and during different developmetal processes (e.g. flower development and fruit set). In tomato, the alteration of specific members of such gene families led to parthenocarpy as observed in plants expressing an aberrant form of the *ARF8* gene or in *ARF7-, IAA9-* and *PIN4*-silenced plants (Wang *et al.*, 2005; Goetz *et al.*, 2007; de Jong *et al.*, 2009b; Mounet *et al.*, 2012).

Consistent with these findings, in the *pat* mutant some pleiotropic effects such as an altered number of cotyledons, aberrations of stamens and ovules, and parthenocarpy could be strongly associated with an altered polar auxin transport (Mazzucato *et al.*, 1998; Olimpieri *et al.*, 2007).

SlHB15 *RNAi and complementation*

In order to confirm that *SlHB15* is the gene underlying the *pat* mutation, RNAi and complementation approaches were performed. So far, these experiments were not exhaustive due to different reasons, such as difficulty of genetic transformation (Fig. 3.2) and gene structure complexity (Fig. 2.3A) for making constructs, associated to the complex biological scenario in which the gene is involved (see Chapter 2 and Chapter 3). However, phenotypic observations of putatively RNAi-*SlHB15* silenced plants reinforced the hypothesis that *SlHB15* is the candidate gene underlying the *pat* mutation. Indeed, these putative transformants showed features phenocopying those presented by *pat* (Fig.3.5E-H; Mazzucato *et al.*, 1998) and by other parthenocarpic mutants in tomato impaired in the function of the *IAA9* gene (Fig. 3.3A-C; Wang *et al.*, 2005; Zhang *et al.*, 2007; A. Mazzucato and F. Carriero, unpublished).

Also, a preliminary complementation experiment could not proof that *SlHB15* represents the *Pat* gene. So far, to exclude technical problems, other experiments using both the developed RNAi (Fig. 3.1; pARTSAS-*SlHB15*) and complementation (Fig. 3.6; pBI121-*SlHB15*) constructs have to be performed. However, considering that both constructs are driven by the constitutive *CaMV* 35S promoter, it could be useful to follow other transgenic approaches (e.g. use of tissue-specific or inducible promoters) for the gene confirmation. Finally, different approaches (e.g. TILLING) could provide the definitive proof that *SlHB15* represent the *Pat* gene and eventually give interesting insights about the function of this gene for plant development in tomato.

Comparison between pat *and single* ATHB15/CNA/ICU4 *mutants in Arabidopsis*

In order to evaluate if single mutants for *ATHB15/CNA/ICU4* display phenotypes reminding those showed by *pat* in tomato, we performed a phenotypic characterization of the *cna-1* (Green *et al.*, 2005) and *icu4-1* (Ochando *et al.*, 2006) mutants in Arabidopsis.

Notably, both mutants phenocopied *pat* for many vegetative and reproductive traits. Specifically, tricotyledon seedlings showed by *pat* (Fig. 3.8A) were presented also by the *icu4-1* gain-of-function mutant (Fig. 3.9B) and a reduction of the time to flowering similar to *pat* (Fig. 3.10A) was observed in the *cna-1* loss-of-function mutant (Fig. 3.10B). Interestingly, deviations of cotyledons were often associated to a deregulation of the polar auxin transport, as observed in Arabidopsis mutants, such as *cuc1* and *cuc2* (Takada *et al.*, 2001). The *cuc1 cuc2* double mutant also displays aberrant ovules lacking the growth of the outer ovule integument (Ishida *et al.*, 2000), as *pat* do in tomato (Fig. 3.7A; Mazzucato *et al.*, 1998).

Consistent with these results, recently Berger *et al.* (2009) showed that *goblet* (*gob*) mutants impaired in a tomato ortholog of *CUC* genes in Arabidopsis presented cotyledonary alterations reminding those displayed by *pat* (Olimpieri *et al.*, 2007). Similar cotyledonary deviations were also observed in the recently developed MicroTom line carrying the *pat* mutation (MT-*pat*; F. Ruiu and A. Mazzucato, unpublished). Moreover, *gob* mutants showed also a capacity to set parthenocarpic fruits showing ectopic carpels inside the gynoecium (Berger *et al.*, 2009) as observed in the MT-*pat* line (not shown; F. Ruiu and A. Mazzucato, unpublished).

Again, in the light of these results, it can be proposed a strong relationship between cotyledonary alterations, ovular defects and parthenocarpy probably due to a modification of the polar auxin transport.

Surprisingly, as *pat* in tomato (Fig. 3.13B), also *cna-1* (Fig. 3.13D) and *icu4-1* (Fig. 3.13F) presented ovular defects associated to a parthenocarpic behaviour (Table 3.1). These results represent novel insights, because in none of the single mutants characterized for *ATHB15/CNA/ICU4* in Arabidopsis were previously described similar phenotypes. So far, ovular defects reminding those presented by *pat* were described only in other HD-Zip III mutants, such as the single gain-of-function *phb-1d* (McConnel and Barton, 1998) and *phv-1d* (Fig. 3.7B; Kelley *et al.*, 2009) or in the triple loss-of-function *cna phb phv* (Fig. 3.7C; Kelley *et al.*, 2009).

All these findings pose the question of why loss- and gain-of-function mutations in HD-

Zip III genes produce similar phenotypes. Based on the ability proposed for HD-Zip III TFs to dimerize, it can be suggested that the production of homo- and/or heterodimers, with different activities depending on the protein(s) involved in the dimers, might account for the complex interactions shown by HD-Zip III genes. In this context, the phenotype of specific mutants should result from the types of dimers formed in the different tissues, which would depend ultimately on the relative level of each HD-Zip III product. This hypothesis would imply that HD-Zip III TFs are not fully equivalent in function, as has already been suggested (Prigge *et al.*, 2005).

Finally, the *pat* mutant showed also a disorganization in the arrangement of vascular bundles in both hypocotyl (Fig. 3.15B) and epicotyl (Fig. 3.15D) similar to those displayed by different single, double and triple HD-Zip III mutants in Arabidopsis (Fig. 3.15E; Prigge *et al.*, 2005). A disorganization of the plant vasculature has also been observed in other parthenocarpic tomato mutants impaired in the *IAA9* gene function (Wang *et al.*, 2005).

Consistent with these observations, it could be proposed that a disorganization of the vasculature may enhance the sink strength and the sugar supply to the fruit and hence directly links the effects of IAA and photoassimilates on the initiation of fruit set and early development. Interestingly, a disorganized vasculature in the *pat* mutant could be directly linked to the formation of aberrant ovules, as observed in parthenocarpic pepper lines lacking a correct development of vascular strands connecting placenta and ovules showing carpel-like structures (Tiwari *et al.*, 2011; 2013).

Insights from the transcriptomic analysis comparing the WT and pat *ovary during fruit set*

In order to dissect the complex floral phenotype and to detect genes involved in the pollination-independent fruit set showed by the *pat* mutant, a microarray approach was used (see Chapter 4).

In this experiment, two pre- (Stage 2 and 3) and one (Stage 5) post-anthesis stage were selected to study and compare molecular events during flower-to-fruit transition in WT and *pat* ovaries (Fig. 4.1A). Based on this flower stadiation, at Stage 4 pollination occurs (Mazzucato *et al.*, 1998).

Ovary size is not significantly different in WT and *pat* flowers until Stage 2, but it begins to be consistently higher in *pat* from Stage 3 onwards (Fig. 4.1B). Stage 5 marks the beginning of ovary growth in the WT. Transcriptomic pair-wise comparisons analyzed among different stages within genotype and between genotypes within the same stage

(Fig. 4.1B) highlighted interesting DEGs putatively related to both floral aberrations and parthenocarpy displayed by the *pat* mutant.

Interestingly, among the DEGs down-regulated at Stage 2 in the *pat* ovary and likely involved in floral aberrations (Supplementary Table S2), tomato ortholog of *LSH1* and *LOB31* genes are strongly related to *SlHB15,* the *pat* candidate gene. Indeed, in Arabidopsis both genes have been described to participate together with HD-Zip III and other important TF families (KNOX, CUC, KANADI, YABBY) in the regulation of the meristem and formation of lateral organs both in vegetative and reproductive tissues (Shuai *et al.*, 2002; Lin *et al.*, 2003; Cho and Zambryski, 2011). A downregulation of the tomato orthologs of these two genes could be linked to the floral aberrations exhibited by *pat* flowers.

Following a clustering analysis, the 1,714 DEGs (Supplementary Table S3) were pooled into five groups of clusters representing different biological trends (Table 4.2 and Fig. 4.4). Four of these five groups (CC, PD, FG, AD), distinguishing WT from *pat* (Fig. 4.4), were subjected to a GO functional enrichment analysis that highlighted interesting cues regarding their composition (Table 4.3).

For example, the CC group of clusters, containing genes up- or down-regulated in the WT ovary at Stage 3 and deregulated in *pat* (Fig. 4.4A and B), was enriched of sequences related to the GO terms ‘small molecule metabolic process’ and ‘protein binding’. The first GO term, involving metabolic processes of monosaccharides, suggested that the activation of the sugar metabolism, as observed in *IAA9*-silenced parthenocarpic plants (Wang *et al.*, 2009), may be an important event coupled with the initiation of pollination-independent fruit set. The second GO term was related to the formation of protein complexes involved in the regulation of the gene expression. Indeed, in this group were present tomato orthologs of Arabidopsis TFs involved in meristem differentiation and flower organs development, such as STM (LeT6/TKn2 in tomato; see Chapter 5), BPEp, ANT and CRC belonging respectively to the KNOX, bHLH, AP2/ERF and YABBY protein families.

In particular, BPEp physically interacting with ARF8, a negative regulator of fruit set (Wang *et al.*, 2005; 2009), determines the final size of the petal in Arabidopsis by controlling cell division and expansion (Varaud *et al.*, 2011). Similarly to BPEp, ANT regulates in Arabidopsis the growth of plant organs by affecting cell proliferation and/or cell expansion in an organ-specific manner (Anastasiou and Lenhard, 2007; Krikek, 2009). Interestingly, *ant* mutants display, as *pat* in tomato, aberrant ovules lacking the growth of the integuments (Elliott *et al.*, 1996). Finally, CRC is the member of the YABBY family required for nectary and carpel development in Arabidopsis (Bowman

and Smyth, 1999; Lee *et al.*, 2004).

Notably, tomato orthologs of all the above described TFs were down-regulated in the *pat* mutant ovary at Stage 3 (Fig. 4.5), except *SlANT* that showed no significant difference in expression at this stage, but was up-regulated at Stage 2 and 5 in the WT ovary compared to *pat* (Fig. 4.5). These results suggest that these TFs play an important role in the control of fruit set and their deregulation in the *pat* ovary during flower-to-fruit transition could play an important role in the expression of its parthenocarpic phenotype. This result represents a novelty, because so far these genes have never been directly associated to parthenocarpy.

Microarray validation was performed by qRT-PCR studying the expression pattern in the WT and *pat* ovary of ten DEGs (Fig. 4.5; see Chapter 4) selected from three different groups of clusters (CC, PD and AD). For the ten validated DEGs correlation coefficients between the two estimations ranged between 0.92 and 0.99 (not shown). Notably, this result strongly supported the reliability of microarray data.

Expression of selected genes in parthenocarpic systems other than pat

By qRT-PCR, selected genes showing a deregulated expression pattern in *pat* compared to the WT (Fig. 4.5), such as *LeT6/TKn2*, *SlBPEp*, *SlCRC*, *SlDEF*, *SlHB15*, *SlARF8* and *SlIAA9* were found to be deregulated also in other parthenocarpic genotypes (*pat-2*, *pat-3/pat-4*, *EMS-iaa9* and *RNAi-ARF7*; Fig. 4.6). Interestingly, studies conducted in both Arabidopsis and tomato showed that the majority of these genes are particularly expressed in ovules (Wang *et al.*, 2005; Goetz *et al.*, 2007; Skinner and Gasser, 2009). This observation is consistent with the concept that cross-talk between ovules and ovary is a key regulator of fruit set, thus potentially its deregulation could lead to parthenocarpy.

This comparative approach allowed us to propose a simplified model for the control of the ovary growth and fruit set in tomato. In the model are reported ‘Controlling complex’ genes highlighted in this work and/or known from the literature. Also the putative time in which the differerent parthenocarpic genotypes, studied in this work, trigger parthenocarpy has been included in the model (Fig. 6.1).

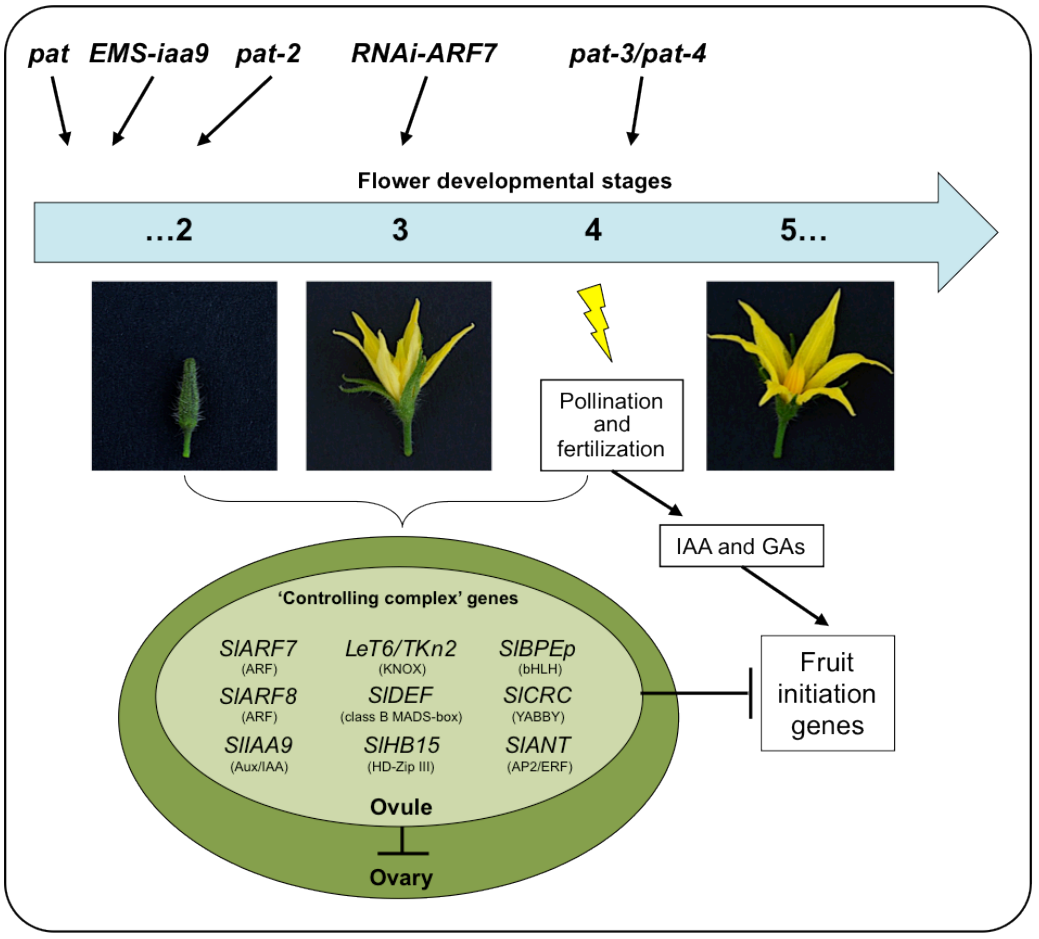

Fig. 6.1. Simplified model for the control of the ovary growth and fruit set in tomato. Based on the transcriptomic analysis conducted in Chapter 4, parthenocarpy induction by *pat* and *EMS-iaa9* mutants begin at early stages during flower development. Before anthesis, *pat* and *EMS-iaa9* are followed by *pat-2* and *RNAi-ARF7* respectively at Stage 2 and 3, whereas *pat-3/pat-4* acts later, concomitantly to anthesis (Stage 4). In the WT ovary, fruit initiation genes are activated by pollination and fertilization through IAA- and GA-signals. In the ovule, the 'Controlling complex' genes are involved in the control of the ovary and fruit initation genes at pre-anthesis, mainly at Stage 3. Into brachets, below the gene name of these repressors, is reported the respective TF family.

Role of LeT6/TKn2 *in the differentiation of tomato floral organs and fruit set*

As reported in Chapter 5, KNOX TFs which have been described as negative regulators of the *GA20ox* genes (Hay *et al.*, 2002), are highly expressed at anthesis in the WT ovary of tomato plants and transcript levels decrease only after pollination. In the *pat* mutant, the expression levels of the KNOX gene *LeT6/TKn2* decrease prior to anthesis (Fig. 4.5; Olimpieri *et al.*, 2007). These results indicate that this gene acts as a negative regulator of fruit initiation, possibly repressing GA biosynthesis in unpollinated WT ovaries.

Following these findings, we performed a phenotypic and molecular characterization of

the double mutant *pat Cu* (see Chapter 5), obtained crossing *pat* and the dominant *Cu* mutant, overexpressing *LeT6/TKn2* and showing an abnormal development of plant vegetative (Fig. 5.1A) and reproductive (Fig. 5.1B) structures (Parnis *et al.*, 1997). The *pat Cu* background was used as biological system to confirm findings described above and to obtain new information about the role of *LeT6/TKn2* in the differentiation of floral organs and fruit set.

Notably, the typical percentages of carpelloid stamens (Fig. 5.3B) and aberrant ovules (Fig. 5.5) showed by *pat* in this study and described in earlier reports (Mazzucato *et al.*, 1998; 1999) were significantly reduced in the *pat Cu* genotype. This observation is in agreement with a deregulation of GA levels in *pat* due to the action of *LeT6/TKn2* in these floral organs. Consistently, it has been determined that the GA promotion of the development of floral organs is partly mediated by KNOX genes (Mutasa-Göttens and Hedden, 2009).

When specifically tested for parthenocarpy, emasculated not-pollinated flowers of *pat Cu* plants did not set fruits or developed fruitlets significantly smaller compared to the *pat* single mutant (see Chapter 5). Again, this result indicated an involvement of *LeT6/TKn2* in the regulation of fruit set. In the *pat Cu* double mutant, the capacity of the autonomous ovary growth usually triggered by the *pat* mutation is reduced by an upregulation of *LeT6/TKn2* responsible for a downregulation of the GA biosynthetic gene *GA20ox1* and an upregulation of the GA catabolic gene *GA2ox2* (Fig. 5.7).

Consistently, this KNOX-GA module operates also in tomato leaves where the expression of the *GA20ox1* is repressed in response to *LeT6/TKn2* overexpression, and the effects of *LeT6/TKn2* overexpression are suppressed by a constitutive GA signaling (Hay *et al.*, 2002; Jasinski *et al.*, 2008). Thus, antagonism between KNOX and GA activities in tomato regulates the correct pattern of both leaflet (Hay and Tsiantis, 2010) and floral organs formation.

Finally, as presented in Chapter 5, the study of reproductive processes in the *pat Cu* double mutant suggested that *SlHB15* (the HD-Zip III gene indicated as underlying the *pat* mutation) and the KNOX gene *LeT6/TKn2* interact at the genetic level. Consistently, it has been shown that Arabidopsis HD-Zip III gain-of-function mutants had reduced *GA20ox1* expression, thus mimicking the effects of KNOX overexpression (Grigg *et al.*, 2005). These findings are in agreement with both the *GA20ox1* upregulation in the *pat* ovary (Olimpieri *et al.*, 2007) and its downregulation in the *pat Cu* genotype overexpressing *LeT6/TKn2*.

Concluding remarks

The different methodological approaches used in this thesis increased the knowledge about the genetic and molecular mechanisms underlying the *pat* mutation. Concomitantly, the functional characterization of this particular mutant showing a strong competence for parthenocarpy and floral defects add new information regarding the molecular network regulating fruit set in tomato. Moreover, the transcriptomic analysis conducted studying and comparing the WT and *pat* ovary during flower-to-fruit transition allowed the identification of new putative regulators of fruit set in tomato. These genes could represent good targets to obtain parthenocarpy through reverse genetic approaches.

Supplementary Tables and Figures

Supplementary Table S1. Gene description and primer sets used for qRT-PCR analyses of DEGs and other relevant genes involved in fruit set (see text in Chapter 4).

LeGI v.11 code or (SGN Solyc ID)	Gene name[a]	Gene description[b]	Primer sequence (5'-3')
NP000147 (Solyc02g081120)	*LeT6/TKn2*	knotted 2 protein (LeT6/TKn2)/ Homeobox protein SHOOTMERISTEMLESS (STM)	Fw_CCATCGTCTCTTGACTGCTTATCT Rv_AGGATCTTCTCCAATGATTCCACC
TC181791 (Solyc03g113550)	*SlBPEp*	basic helix-loop-helix (bHLH) family protein/ BIGPETALp (BPEp)	Fw_CAAAGTAGTAAACCTGAGCCACCT Rv_TTGCAGAATTTTCATCCTCTCGCT
TC177922 (Solyc05g012150)	*SlCRC*	transcription factor CRABS CLAW (CRC)	Fw_GCACCTTTTGTTGTAAAACCTCCT Rv_AGCTTCTCTATGTGGTATCTCTGG
AI484773 (Solyc10g080890)	*SlSDR*	short-chain dehydrogenase/ reductase (SDR) family protein	Fw_ATTTGTCAGAGGAGGAATGGGAGA Rv_CGATTAAGACCAGCGGTAGAAGAG
TC176065 (Solyc05g006980)	*SlHB1*	HD-Zip I family protein (HB1)	Fw_AGGCTCAAAAAGCAACAACTCCAA Rv_CCATCAGTGTAATGTGGGCTATCT
TC184962 (Solyc09g074270)	*SlGID1L2*	gibberellin receptor (GID1L2)	Fw_TACAAACCTGCCCCGAAAAATGAG Rv_ACCGTGGAAGAAGATAATGACAGG
BI927245 (Solyc04g077490)	*SlANT*	aintegumenta-like protein/ AP2/ERF family protein AINTEGUMENTA (ANT)	Fw_GTGTTGGTGGTCAAAAGAATGAGG Rv_ATGGAGAATGATGTAGGGTTACGA
BI927929 (Solyc08g082630)	*SlARF9*	auxin response factor ARF family protein (ARF9)	Fw_CAACCTCGGAGACATTTACTTACC Rv_CTGTCCATTATTACCCCTCAAGAA
TC174743 (Solyc09g083290)	*SlIAA14*	auxin-responsive AUX/IAA family protein (IAA14)/ indole acetic acid-induced protein 7 (IAA7)	Fw_TAACAAAGATCCAATCAAGCCACC Rv_ATGCAGCAGTAGTCTTCTCACTTT
BG134100 (Solyc03g033740)	*SlPBC1*	20S proteasome beta subunit C1 (PBC1)	Fw_AAAACCCTAGCTATCTCTCT Rv_TTACACAGTAATCAGCATCT
(Solyc04g081000)	*SlDEF*	floral homeotic protein APETALA3 (AP3)/ DEFICIENS (DEF)	Fw_TAAGTCCCTCTATCACGACCAAAC Rv_TCCTATTCACATCCTTTAGCTTCC
(Solyc03g120910)	*SlHB15*	HD-Zip III family protein (HB15)/ lipid-binding START domain-containing protein	Fw_GGAATGGATGAAAATGCTGTTGGA Rv_GAGTGAAATAATGCGAAACCCAGA
(Solyc12g044410)	*SlHB15*-like	HD-Zip III family protein (HB15-like)/ lipid-binding START domain-containing protein	Fw_GAAAATGCAAGACTCAAAGAAGAG Rv_GAAGAACTCCAAAATCAACAGGAG
(Solyc07g042260)	*SlARF7*	auxin response factor ARF family protein (ARF7)	Fw_CCAAGTTATCCTAATCTTCCTTCC Rv_GTAAAGCCTCCTGGTCATATTTG
(Solyc02g037530)	*SlARF8*	auxin response factor ARF family protein (ARF8)	Fw_CTGCTCAAACCCAAATGCTGTC Rv_GGTAAGTGTGTTGGTGAGCCTG
(Solyc04g076850)	*SlIAA9*	auxin-responsive AUX/IAA family protein (IAA9)	Fw_TAGATGCTTTACCTGATTACGACA Rv_TGCAGACAAACTCCAATATCAAAC
(Solyc08g006960)	*CAC**	clathrin adaptor complexes subunit family protein (CAC)	Fw_GATGTCCTTATCAACCGTCTCTAC Rv_ACAAGAAAGAACAGCCTCCAATCT

[a] Tomato gene name adopted in this study (see text in Chapter 4). * *CAC* (SGN-U314153 or Solyc08g006960) represents the house-keeping gene used for qRT-PCR data normalization (Expósito-Rodríguez *et al*., 2008). [b] Gene description obtained combining information from Blast2GO (http://www.blast2go.com/), SGN (http://solgenomics.net/) and TAIR (http://www.arabidopsis.org/).

Supplementary Table S2. DEGs up- or down-regulated at Stage 2 in the *pat* mutant ovary, putatively involved in the expression of stamen and ovule aberrations (see text in Chapter 4). NA stands for not annotated.

LeGI v.11 code	Gene description[a]	Fold change pat2 vs wt2 (Log2Ratio)
AI776847	L-lactate dehydrogenase	4.52
BI205489	Cytochrome P450 75B1 (CYP75B1)/ transparent testa 7 protein (TT7)	2.88
AI488598	Proline dehydrogenase	2.72
BP891117	Zinc finger CCCH domain-containing protein 2	2.68
TC171684	Germin-like protein (GER3)/auxin-binding protein ABP19a	2.24
BG735152	Unknown protein	2.20
TC186514	Oxidoreductase 2OG-Fe(II) oxygenase family protein	2.08
BE353780	Unknown protein	2.07
BI933170	Cupin family protein	2.02
TC174721	Unknown protein	2.01
TC179040	Unknown protein	1.98
AW031677	Polygalacturonase (pectin lyase fold)	1.95
TC172139	Proton-dependent oligopeptide transport (POT) family protein	1.87
BI206797	Dehydration-responsive family protein	1.86
TC187251	Peroxidase 3 (PER3)/rare cold-inducible protein (RCI3A) (PRC)	1.86
TC189788	Serine/threonine protein kinase	1.74
AJ784677	Serine carboxypeptidase S10 family protein	1.73
TC188243	Zinc finger (C3HC4-type RING finger) family protein	1.69
TC185991	Glycoside hydrolase family 2 protein	1.62
BE462550	Phenylcoumaran benzylic ether reductase	1.62
TC170144	Eukaryotic translation initiation factor 5A-1 (eIF-5A-1)	1.62
TC175860	DNA-damage-repair/toleration protein, chloroplast (DRT111)	1.61
TC173817	Caffeoyl-CoA 3-O-methyltransferase	1.60
AW036485	Phospholipid diacylglycerol acyltransferase	-2.26
TC173443	RNA recognition motif-containing protein	-2.93
TC179877	Acylaminoacyl-peptidase like protein	-2.83
BI927749	NA	-2.83
TC173349	WD-40 repeat-containing protein	-2.71
TC184573	Internal rotenone-insensitive NADH dehydrogenase	-2.47
TC189983	NA	-2.47
BG134081	Light-dependent short hypocotyls 1 (LSH1)	-2.14
TC170535	NA	-2.14
BE436484	Ubiquitin	-2.09
TC174093	Stress responsive A/B barrel domain family protein	-1.93
TC179013	Chlorophyll A-B binding protein / LHCII type I (LHB1B1)	-1.91
AW092295	Zinc finger homeobox (ZF-HD) family protein (HB22)	-1.91
TC173627	Squamosa promoter-binding protein-like 3 (SPL3)	-1.80
BG138536	Phosphatidylinositol-specific phospholipase c	-1.80
BP896019	Serine-glyoxylate aminotransferase	-1.79
TC181545	UDP-glucosyltransferase	-1.78
TC172605	Phosphatidylinositol-specific phospholipase c	-1.77
TC178723	Kinase interacting family protein	-1.75
TC170112	L-galactose-1-phosphate phosphatase 2	-1.73
BI208492	Lateral Organ Boundaries domain protein 31 (LOB31)	-1.72
TC178505	Unknown Protein	-1.72
TC169888	Polyphenol oxidase	-1.71
BE463153	Ferrodoxin-related protein	-1.70
TC178310	Beta-amylase (CT-BMY)/1,4-alpha-D-glucan maltohydrolase	-1.65
AW441578	Unknown protein	-1.65
AW932559	Dihydroflavonol 4-reductase family	-1.62
TC186433	Glutathione S-transferase	-1.60
TC173156	Phenylalanine ammonia-lyase	-1.59

[a] Gene description obtained combining information from Blast2GO (http://www.blast2go.com/), SGN (http://solgenomics.net/) and TAIR (http://www.arabidopsis.org/).

Supplementary Table S3. Gene list of the 1714 DEGs showing a greater than 3-fold change in at least one of the pair-wise comparisons analyzed between genotypes and stages (see text in Chapter 4). No. from 1 to 441, from 442 to 810, from 811 to 1203, from 1204 to 1366 and from 1367 to 1714 are respectively the genes from CC, PD, FG, AD and AS groups of clusters (see text in Chapter 4).

No.	LeGI v.11 code	No.	LeGI v.11 code	No.	LeGI v.11 code	No.	LeGI v.11 code
1	TC172228	51	AW618471	101	BI933466	151	AW928600
2	AW979587	52	AW648686	102	BP887956	152	AW944805
3	BP877410	53	AW944984	103	BP903297	153	BI203968
4	BP884182	54	BG130653	104	BW685678	154	BP881826
5	NP1427430	55	BP896019	105	NP209477	155	DV105440
6	TC173932	56	BP900602	106	TC169857	156	DV105811
7	TC174950	57	BP907953	107	TC169888	157	TC170464
8	TC176522	58	TC171234	108	TC169934	158	TC230504
9	TC177661	59	TC172281	109	TC170716	159	TC181135
10	TC178217	60	TC223104	110	TC171426	160	TC182362
11	TC219600	61	TC172857	111	TC220926	161	TC182693
12	TC183168	62	TC173575	112	TC172605	162	TC186285
13	TC184879	63	TC173812	113	TC173215	163	TC187104
14	TC185241	64	TC174952	114	TC173443	164	TC189513
15	TC185473	65	TC176135	115	TC226504	165	AI772759
16	TC186109	66	TC176479	116	TC174484	166	AI778224
17	TC187249	67	TC178310	117	TC174807	167	AW036395
18	TC187833	68	TC178689	118	TC176875	168	AW617074
19	TC242830	69	TC179013	119	TC229018	169	BE354508
20	TC189354	70	TC179508	120	TC177975	170	BE460145
21	CN385197	71	TC179883	121	TC178723	171	BG131411
22	AI488684	72	TC235602	122	TC179877	172	TC189263
23	AI490821	73	TC183615	123	TC243692	173	CN385703
24	AW617602	74	TC183715	124	TC181545	174	TC174334
25	AW624132	75	TC185163	125	TC229339	175	TC228668
26	AW929604	76	TC224545	126	TC183457	176	TC180805
27	AW934641	77	TC185612	127	TC184143	177	TC186351
28	BG123938	78	TC186910	128	TC184573	178	AW650573
29	BG125893	79	TC186947	129	TC185821	179	BI208805
30	BG126340	80	TC189608	130	TC187256	180	TC174416
31	BG127218	81	TC190232	131	TC188288	181	TC192342
32	BG127709	82	AF096256	132	TC189167	182	TC224513
33	BG129759	83	AI895312	133	TC190010	183	TC188117
34	BG133058	84	BE354754	134	TC190277	184	TC188758
35	BG133150	85	DY523444	135	AW036352	185	TC191081
36	BI208544	86	TC217859	136	BE354656	186	AI484754
37	BI210028	87	TC177988	137	BF113627	187	AI490546
38	BI926149	88	AW930927	138	BG138085	188	AI782046
39	BP881986	89	BE460535	139	BI208492	189	AI894746
40	NP589727	90	TC225688	140	BP911320	190	AW031282
41	TC175435	91	TC170535	141	BW691934	191	AW034219
42	TC177878	92	TC189983	142	DV105326	192	AW222294
43	TC182219	93	AW034237	143	TC169931	193	AW443554
44	TC186445	94	AW036485	144	TC172503	194	AW625489
45	BF098582	95	AW092295	145	TC218407	195	BE436484
46	TC185289	96	BG138536	146	TC173627	196	BE462748
47	TC227389	97	BI925306	147	TC180803	197	BF097550
48	TC187272	98	BI927245	148	TC186329	198	BG127142
49	AI489859	99	BI927749	149	TC189047	199	BG134212
50	AI778137	100	BI932000	150	AI778687	200	BG642873

Supplementary Table S3. *Continued*

No.	LeGI v.11 code	No.	LeGI v.11 code	No.	LeGI v.11 code	No.	LeGI v.11 code
201	BG643283	251	TC183570	301	BP887770	351	BE461668
202	BG735015	252	TC244839	302	BP891843	352	BG129702
203	BI206878	253	TC228684	303	CD003492	353	BI935045
204	BI924044	254	TC183839	304	TC171011	354	BW690274
205	BP880052	255	TC237380	305	TC171684	355	TC223531
206	BP883766	256	TC219856	306	TC174419	356	TC241557
207	BP889312	257	TC184398	307	TC176616	357	TC227286
208	BW688542	258	TC236731	308	TC181023	358	TC178948
209	BW689803	259	TC184942	309	TC186818	359	TC180545
210	BW690011	260	TC185049	310	TC188260	360	TC182601
211	BW690039	261	TC185188	311	TC188548	361	CN384800
212	CD002128	262	TC186122	312	TC189392	362	AW621265
213	DV105082	263	TC188064	313	CN384529	363	TC222346
214	TC217856	264	TC190215	314	AI489699	364	TC174238
215	TC170146	265	TC190888	315	AI489709	365	TC176942
216	TC217159	266	TC191104	316	AW621986	366	TC187397
217	TC170336	267	TC171233	317	AW931964	367	TC242148
218	TC170388	268	AI771135	318	BI933829	368	BF112926
219	TC170677	269	AW649767	319	TC172469	369	BW685635
220	TC225948	270	BG128276	320	TC173004	370	TC181791
221	TC171232	271	BG128465	321	TC173142	371	TC218148
222	TC171252	272	BP879489	322	TC183817	372	TC174975
223	TC171394	273	BW689433	323	TC186801	373	TC180807
224	TC172186	274	CK574993	324	DN170172	374	TC184272
225	TC217468	275	TC226727	325	AB204909	375	TC184963
226	TC172501	276	TC224533	326	AI484773	376	TC237552
227	TC223186	277	TC175412	327	AI773591	377	AW621645
228	TC172592	278	TC175496	328	AI781315	378	TC221091
229	TC172832	279	TC177154	329	AW737342	379	TC171511
230	TC233801	280	TC223054	330	BE354244	380	TC171672
231	TC225716	281	TC225005	331	BG135346	381	TC174407
232	TC173916	282	TC184181	332	BP889896	382	TC177351
233	TC175429	283	TC184814	333	CD003341	383	TC185261
234	TC176065	284	TC189569	334	TC230719	384	TC189348
235	TC220515	285	TC190937	335	TC173676	385	TC189829
236	TC176922	286	BP905322	336	TC175268	386	AI490621
237	TC176927	287	CK720539	337	TC178623	387	BP893456
238	TC177350	288	TC172627	338	TC179892	388	BP903368
239	TC177948	289	TC180876	339	TC180780	389	TC170591
240	TC178505	290	TC181971	340	TC219333	390	TC171479
241	TC179290	291	TC177922	341	TC182291	391	TC177089
242	TC179520	292	TC233252	342	AI490307	392	TC235376
243	TC179638	293	TC188741	343	BP910437	393	TC182699
244	TC227877	294	CN385412	344	TC171486	394	TC182732
245	TC181042	295	AI484821	345	TC174725	395	TC182990
246	TC181174	296	AI897928	346	TC175766	396	TC188280
247	TC181383	297	AW221979	347	TC177188	397	BG123512
248	TC231498	298	AW626218	348	TC218289	398	BG643895
249	TC182081	299	BG133126	349	TC180319	399	NP000147
250	TC183567	300	BG643749	350	TC181386	400	TC226699

Supplementary Table S3. *Continued*

No.	LeGI v.11 code	No.	LeGI v.11 code	No.	LeGI v.11 code	No.	LeGI v.11 code
401	TC180375	451	TC173469	501	BG125874	551	TC182007
402	TC182759	452	TC174889	502	BG133346	552	TC182567
403	TC173072	453	TC175527	503	BG134419	553	TC182783
404	TC227277	454	TC176531	504	BG135328	554	TC183517
405	TC242958	455	TC186656	505	BG135888	555	TC185376
406	TC235611	456	TC186701	506	BG136972	556	TC185518
407	TC191259	457	TC186868	507	BG643644	557	TC185692
408	AW032450	458	TC188473	508	BG643671	558	TC185749
409	BG125347	459	TC191254	509	BI206366	559	TC186514
410	BI930807	460	BF050163	510	BI208315	560	TC186562
411	TC219032	461	TC172642	511	BI926081	561	TC186747
412	TC221703	462	TC173383	512	BI926524	562	TC190154
413	TC177453	463	TC187678	513	BI926828	563	TC190451
414	TC178134	464	BG630102	514	BI927163	564	TC190538
415	TC182502	465	TC173693	515	BI927929	565	AJ785497
416	TC187158	466	AI483378	516	BP880156	566	TC176381
417	AW623189	467	BG128239	517	BP885521	567	AI487516
418	BP899564	468	BI925601	518	BW692199	568	BI931185
419	TC177158	469	TC173352	519	NP183617	569	TC171117
420	TC184755	470	TC177461	520	TC169909	570	TC171344
421	AW624867	471	NP964619	521	TC217533	571	TC182840
422	BF113654	472	AI483159	522	TC217816	572	BE462708
423	BI922387	473	AI485203	523	TC170912	573	BI921915
424	BM411546	474	AI487697	524	TC243550	574	AW219357
425	TC178015	475	AI773730	525	TC172002	575	BI206305
426	TC234918	476	AI775983	526	TC172231	576	TC227199
427	TC184525	477	AI896328	527	TC172443	577	AI483110
428	TC185368	478	AW031182	528	TC173126	578	TC191828
429	TC188595	479	AW031458	529	TC173263	579	TC206166
430	TC184962	480	AW041173	530	TC217447	580	AI771343
431	TC191046	481	AW220357	531	TC174029	581	AI771483
432	BP888316	482	AW220360	532	TC174093	582	AW040580
433	TC190055	483	AW398317	533	TC174131	583	BG132798
434	TC191071	484	AW398443	534	TC174506	584	BP885031
435	AW737462	485	AW623501	535	TC175091	585	BP901139
436	TC225704	486	AW650948	536	TC175241	586	TC217747
437	TC217531	487	AW735872	537	TC175368	587	TC217682
438	TC187683	488	AW737400	538	TC175529	588	TC170625
439	DV105192	489	AW929554	539	TC175653	589	TC227491
440	TC170495	490	AW929651	540	TC175729	590	TC223581
441	TC189218	491	AW934666	541	TC177532	591	TC173858
442	TC190309	492	BE450444	542	TC177569	592	TC227631
443	AI486732	493	BE463261	543	TC178113	593	TC227441
444	AI488578	494	BE463351	544	TC179281	594	TC225959
445	AI776142	495	BF050386	545	TC221629	595	TC176525
446	BG138068	496	BF051260	546	TC180608	596	TC225273
447	BI926787	497	BF097728	547	TC180761	597	TC177558
448	BP884071	498	BF113945	548	TC180911	598	TC223057
449	TC172142	499	BG123774	549	TC181534	599	TC182719
450	TC172568	500	BG124885	550	TC181831	600	TC182904

Supplementary Table S3. *Continued*

No.	LeGI v.11 code	No.	LeGI v.11 code	No.	LeGI v.11 code	No.	LeGI v.11 code
601	TC184419	651	TC186128	701	BI933688	751	TC177577
602	TC188196	652	TC186384	702	BI934200	752	TC177734
603	TC188243	653	TC186573	703	BM536049	753	TC178195
604	TC189745	654	TC186917	704	BP894571	754	TC179569
605	BG141046	655	TC240841	705	BP906184	755	TC237541
606	BI921679	656	TC187566	706	BW689458	756	TC180027
607	BM412783	657	TC228150	707	CD002813	757	TC226252
608	BP894292	658	TC219272	708	DV105534	758	TC181043
609	TC224317	659	TC189500	709	TC169877	759	TC181904
610	TC222917	660	TC189601	710	TC217656	760	TC238027
611	TC187100	661	TC190156	711	TC219066	761	TC182476
612	TC241816	662	TC190364	712	TC170245	762	TC183400
613	AW929662	663	TC190952	713	TC170371	763	TC183401
614	TC218577	664	DN168562	714	TC170739	764	TC236978
615	TC173041	665	AI777620	715	TC170974	765	TC183863
616	TC230693	666	AI896047	716	TC171896	766	TC184291
617	TC232176	667	AI897637	717	TC171996	767	TC184353
618	AI780666	668	AW032557	718	TC172088	768	TC184721
619	BE461162	669	AW034854	719	TC236504	769	TC184843
620	BI204242	670	AW036108	720	TC172442	770	TC184895
621	TC228938	671	AW618214	721	TC172617	771	TC185480
622	TC178543	672	AW618586	722	TC172679	772	TC185579
623	TC223138	673	AW622830	723	TC172690	773	TC185774
624	TC183053	674	AW624539	724	TC172950	774	TC185855
625	TC184873	675	AW737363	725	TC172985	775	TC191300
626	TC185524	676	AW737686	726	TC173167	776	AI772843
627	TC239281	677	AW737713	727	TC173482	777	AW032627
628	TC186020	678	AW737843	728	TC173524	778	BE353928
629	TC189160	679	BE354322	729	TC231677	779	BE461079
630	AI488274	680	BE450508	730	TC173640	780	BG125453
631	AI772965	681	BE463142	731	TC228441	781	BG136349
632	AI781845	682	BG123511	732	TC234500	782	BG136891
633	TC175439	683	BG124052	733	TC174270	783	BI932692
634	TC183300	684	BG136274	734	TC174691	784	TC223430
635	TC191002	685	BG137464	735	TC174740	785	TC224409
636	TC170806	686	BG137777	736	TC174833	786	TC171761
637	TC174805	687	BG138689	737	TC175028	787	TC173171
638	TC221604	688	BG138904	738	TC228525	788	TC174743
639	BG140208	689	BG139757	739	TC176013	789	TC175078
640	BI206349	690	BG140023	740	TC176156	790	TC175543
641	BP879985	691	BG140261	741	TC176223	791	TC234278
642	TC221193	692	BG140348	742	TC176326	792	TC179951
643	BE451417	693	BG140551	743	TC176333	793	TC228476
644	TC218369	694	BG140693	744	TC176518	794	TC181324
645	TC244761	695	BG140753	745	TC176792	795	TC182283
646	TC186223	696	BG140790	746	TC176907	796	TC190599
647	TC240838	697	BG140878	747	TC176936	797	DN171941
648	TC189483	698	BG627057	748	TC177255	798	BE450268
649	TC189785	699	BG642542	749	TC177448	799	BG124035
650	TC189925	700	BI922697	750	TC177468	800	BP887151

Supplementary Table S3. *Continued*

No.	LeGI v.11 code	No.	LeGI v.11 code	No.	LeGI v.11 code	No.	LeGI v.11 code
801	TC170112	851	TC222093	901	BI422530	951	AW648982
802	TC175232	852	TC218788	902	BI924636	952	AW929708
803	TC177742	853	TC183518	903	BI925070	953	AW930429
804	TC220737	854	TC184076	904	BI927479	954	AW932559
805	TC184867	855	TC184452	905	BI928287	955	BE458287
806	AJ784594	856	TC184882	906	BM413043	956	BG125710
807	BG139978	857	TC185125	907	BP876985	957	BG125851
808	BW689985	858	TC238730	908	BP881110	958	BG133566
809	TC171894	859	TC186665	909	BP881656	959	BG628365
810	TC190389	860	TC186678	910	BP889499	960	BP878398
811	TC224931	861	TC186745	911	BP897144	961	BP880579
812	TC176962	862	TC186914	912	BP897235	962	BP883491
813	TC180238	863	TC187071	913	BP899248	963	BP900034
814	TC231617	864	TC227037	914	BP899250	964	BW689691
815	TC190968	865	TC226900	915	BP900299	965	CK725215
816	TC191240	866	TC189267	916	BP902678	966	TC169946
817	TC169886	867	TC189977	917	BP903085	967	TC170519
818	TC217490	868	TC190554	918	BP907496	968	TC171329
819	TC228098	869	TC190725	919	BP907731	969	TC219221
820	TC223804	870	CO751446	920	BP907834	970	TC172539
821	TC233612	871	DN168570	921	TC217605	971	TC230885
822	TC229756	872	AI482630	922	TC170686	972	TC173085
823	TC173488	873	AI773231	923	TC170815	973	TC173170
824	TC227264	874	AI773800	924	TC240021	974	TC219509
825	TC174413	875	AI773960	925	TC171350	975	TC173734
826	TC220900	876	AI773965	926	TC220200	976	TC223927
827	TC174940	877	AI774005	927	TC236705	977	TC173982
828	TC239405	878	AI774648	928	TC173548	978	TC174045
829	TC227959	879	AI775116	929	TC173587	979	TC174254
830	TC175602	880	AI776458	930	TC174798	980	TC174939
831	TC237091	881	AI777438	931	TC182785	981	TC227514
832	TC177002	882	AI780155	932	TC185661	982	TC175660
833	TC227884	883	AI780287	933	DN167860	983	TC176145
834	TC177669	884	AW038604	934	AW094263	984	TC176225
835	TC179133	885	AW039478	935	BE353181	985	TC223330
836	TC232512	886	AW092663	936	BF096921	986	TC177194
837	TC179524	887	AW160300	937	AW399349	987	TC177205
838	TC179722	888	AW442770	938	TC170657	988	TC177738
839	TC179744	889	AW443766	939	TC172349	989	TC177944
840	TC179916	890	AW617387	940	TC225723	990	TC178352
841	TC180105	891	AW617986	941	TC183516	991	TC178469
842	TC180115	892	AW618492	942	AI489033	992	TC178855
843	TC180161	893	AW649237	943	AI490595	993	TC179080
844	TC230167	894	AW929179	944	AI774976	994	TC218145
845	TC180348	895	AW929538	945	AW033582	995	TC180466
846	TC180479	896	BE461623	946	AW037577	996	TC181039
847	TC180633	897	BG124012	947	AW218598	997	TC181836
848	TC229029	898	BG124383	948	AW221189	998	TC182073
849	TC181847	899	BG135910	949	AW624998	999	TC182987
850	TC235566	900	BG644080	950	AW625306	1000	TC183080

Supplementary Table S3. *Continued*

No.	LeGI v.11 code	No.	LeGI v.11 code	No.	LeGI v.11 code	No.	LeGI v.11 code
1001	TC183343	1051	AI779076	1101	TC176285	1151	AW033986
1002	TC183446	1052	AW030425	1102	TC176567	1152	AW039847
1003	TC184151	1053	AW160197	1103	TC176772	1153	AW221294
1004	TC184267	1054	AW217174	1104	TC176806	1154	AW398971
1005	TC184345	1055	AW398321	1105	TC177735	1155	AW441578
1006	TC185267	1056	AW618546	1106	TC178887	1156	AW617144
1007	TC185684	1057	AW625197	1107	TC180085	1157	AW621208
1008	TC186102	1058	AW648389	1108	TC180086	1158	AW623139
1009	TC187160	1059	AW737661	1109	TC180162	1159	AW624263
1010	TC187767	1060	AW929983	1110	TC181167	1160	AW932642
1011	TC188222	1061	AW931358	1111	TC181449	1161	BE433403
1012	TC221935	1062	AW945125	1112	TC227101	1162	BF113928
1013	TC221135	1063	AW979569	1113	TC232435	1163	BG136126
1014	TC232655	1064	BE354126	1114	TC235429	1164	BI926180
1015	TC238140	1065	BE458511	1115	TC182471	1165	BP880374
1016	DN168016	1066	BF097030	1116	TC182866	1166	BP890923
1017	NP964556	1067	BF097061	1117	TC233440	1167	BP896153
1018	AW622542	1068	BF114420	1118	TC182954	1168	DV104879
1019	BG643825	1069	BG129285	1119	TC183083	1169	TC169848
1020	TC172354	1070	BG131073	1120	TC183178	1170	TC171322
1021	TC171567	1071	BG626575	1121	TC183236	1171	TC220657
1022	TC174589	1072	BG629531	1122	TC183601	1172	TC172038
1023	TC225800	1073	BG735051	1123	TC184588	1173	TC217730
1024	TC240803	1074	BI931482	1124	TC185618	1174	TC175690
1025	BG131536	1075	BI934701	1125	TC185817	1175	TC176045
1026	TC176147	1076	BP886754	1126	TC185852	1176	TC176547
1027	TC182406	1077	BP888333	1127	TC186064	1177	TC224755
1028	TC187075	1078	BP889466	1128	TC227081	1178	TC218159
1029	TC174393	1079	BP892717	1129	TC186322	1179	TC218157
1030	TC227689	1080	CD003298	1130	TC186423	1180	TC180930
1031	TC182530	1081	DV104551	1131	TC186580	1181	TC181985
1032	BG125659	1082	DV105204	1132	TC186655	1182	TC219202
1033	TC179173	1083	TC217132	1133	TC186740	1183	TC183887
1034	TC182821	1084	TC222542	1134	TC187244	1184	TC183904
1035	TC185995	1085	TC171195	1135	TC187273	1185	TC237298
1036	TC186205	1086	TC217499	1136	TC188679	1186	TC186433
1037	TC187490	1087	TC171402	1137	TC189200	1187	AJ785224
1038	TC188028	1088	TC171494	1138	TC229061	1188	TC190565
1039	TC229939	1089	TC171803	1139	TC226628	1189	AI772225
1040	TC189284	1090	TC171913	1140	TC190275	1190	AW399066
1041	TC189620	1091	TC220103	1141	CN385118	1191	BE460594
1042	TC243865	1092	TC227888	1142	DN171578	1192	BE463153
1043	AJ784745	1093	TC218181	1143	DN172321	1193	TC231746
1044	DV104153	1094	TC223469	1144	TC170217	1194	TC224075
1045	TC170219	1095	TC221651	1145	TC174764	1195	TC226940
1046	TC170596	1096	TC174126	1146	TC183410	1196	TC180126
1047	TC189818	1097	TC227534	1147	TC186159	1197	AW615964
1048	AA824781	1098	TC175681	1148	AI487581	1198	AW617854
1049	AI484452	1099	TC175755	1149	AI777124	1199	TC181447
1050	AI490441	1100	TC175982	1150	AI895685	1200	TC239864

Supplementary Table S3. *Continued*

No.	LeGI v.11 code	No.	LeGI v.11 code	No.	LeGI v.11 code	No.	LeGI v.11 code
1201	TC180193	1251	TC179463	1301	TC191044	1351	BE431497
1202	TC183689	1252	TC181760	1302	CN384685	1352	BI934543
1203	TC177820	1253	TC182013	1303	CN384999	1353	TC172087
1204	DN169113	1254	TC183266	1304	AI483872	1354	TC175546
1205	TC169933	1255	TC239375	1305	AI778562	1355	TC176889
1206	AI776342	1256	TC185818	1306	AI782078	1356	TC238092
1207	AI894926	1257	TC185991	1307	AW036520	1357	AI897583
1208	AW033935	1258	TC186750	1308	AW091778	1358	BF098216
1209	AW096366	1259	TC187077	1309	AW441807	1359	BI925095
1210	AW934628	1260	TC187251	1310	AW442574	1360	BP889238
1211	BE431886	1261	TC187739	1311	AW622053	1361	TC186646
1212	BE434816	1262	TC189414	1312	AW622338	1362	AA824873
1213	BE463238	1263	TC189637	1313	AW929160	1363	BI207682
1214	BG124196	1264	TC190125	1314	AW944935	1364	TC230145
1215	BG134027	1265	AJ784677	1315	BE433684	1365	AW650258
1216	BG134100	1266	CN385767	1316	BE450167	1366	AW219012
1217	BG134398	1267	TC196774	1317	BE461779	1367	AW621583
1218	BG735152	1268	AW031677	1318	BF050933	1368	TC223619
1219	BI206581	1269	BP891117	1319	BF096394	1369	AW399145
1220	BI206797	1270	TC180374	1320	BG135351	1370	AW616444
1221	BI923390	1271	AI488598	1321	BG630682	1371	AW626181
1222	BI926418	1272	AW218332	1322	BI921125	1372	BG133176
1223	BI934163	1273	AW929452	1323	BI926967	1373	BI204529
1224	BI934304	1274	BE449967	1324	BI928061	1374	BI931564
1225	BM410803	1275	TC188276	1325	BM409024	1375	BM413524
1226	BP882001	1276	TC190648	1326	BP876239	1376	BP889104
1227	BP883502	1277	TC173525	1327	BP887469	1377	DV105044
1228	BP902543	1278	TC178410	1328	BP889607	1378	DY523540
1229	CK715469	1279	TC179165	1329	CD002512	1379	TC170453
1230	TC217610	1280	TC179286	1330	CD003322	1380	TC217971
1231	TC170794	1281	TC179289	1331	CK715039	1381	TC223336
1232	TC171053	1282	TC180874	1332	TC220829	1382	TC172787
1233	TC171978	1283	TC181045	1333	TC235405	1383	TC173925
1234	TC217648	1284	TC181618	1334	TC172360	1384	TC174711
1235	TC225966	1285	TC182240	1335	TC172692	1385	TC174810
1236	TC174085	1286	TC182623	1336	TC172721	1386	TC175744
1237	TC174165	1287	TC242971	1337	TC174769	1387	TC176763
1238	TC175860	1288	TC183966	1338	TC175693	1388	TC177541
1239	TC219269	1289	TC184078	1339	TC175833	1389	TC236360
1240	TC176023	1290	TC185057	1340	TC175874	1390	TC179007
1241	TC176185	1291	TC185151	1341	TC180732	1391	TC179486
1242	TC176197	1292	TC226600	1342	TC181093	1392	TC180233
1243	TC227616	1293	TC185581	1343	TC189702	1393	TC180250
1244	TC176754	1294	TC185770	1344	TC227018	1394	TC180415
1245	TC229160	1295	TC186073	1345	AI486825	1395	TC181329
1246	TC177231	1296	TC186095	1346	AI772856	1396	TC181477
1247	TC177475	1297	TC188291	1347	AI899036	1397	TC181901
1248	TC178550	1298	TC189078	1348	AW031909	1398	TC181967
1249	TC233630	1299	TC189079	1349	AW929265	1399	TC183613
1250	TC178954	1300	TC190481	1350	BE353825	1400	TC184086

Supplementary Table S3. *Continued*

No.	LeGI v.11 code	No.	LeGI v.11 code	No.	LeGI v.11 code	No.	LeGI v.11 code
1401	TC184931	1451	TC217343	1501	TC177254	1551	CN641317
1402	TC233402	1452	TC171154	1502	TC187674	1552	NP597560
1403	TC188721	1453	TC224121	1503	TC190408	1553	TC169840
1404	TC188757	1454	TC217981	1504	AA824943	1554	TC217974
1405	TC189000	1455	TC173605	1505	AI485622	1555	TC228572
1406	TC189510	1456	TC175609	1506	AI486244	1556	TC170629
1407	BI926754	1457	TC225281	1507	AI488671	1557	TC171311
1408	TC174818	1458	TC225178	1508	AI488762	1558	TC171731
1409	TC235535	1459	TC176302	1509	AI489057	1559	TC171806
1410	DN171377	1460	TC179054	1510	AI489893	1560	TC172210
1411	AI484516	1461	TC179580	1511	AI775168	1561	TC172352
1412	TC177149	1462	TC180655	1512	AI776847	1562	TC224315
1413	BG134237	1463	TC181676	1513	AI778865	1563	TC174123
1414	BI205489	1464	TC183436	1514	AI895869	1564	TC175380
1415	TC238934	1465	TC222035	1515	AI896120	1565	TC175465
1416	BI207755	1466	TC184651	1516	AW035766	1566	TC175639
1417	BF096480	1467	TC185090	1517	AW094424	1567	TC176434
1418	BG134081	1468	CO751053	1518	AW217786	1568	TC178264
1419	BG135269	1469	BG130115	1519	AW221739	1569	TC179040
1420	BG631811	1470	BG139862	1520	AW618261	1570	TC232380
1421	TC229990	1471	BP902924	1521	AW621482	1571	TC179523
1422	TC220615	1472	TC176081	1522	AW622193	1572	TC179576
1423	TC233388	1473	TC176972	1523	AW622253	1573	TC182267
1424	TC180225	1474	TC179193	1524	AW623550	1574	TC182592
1425	TC184134	1475	BG643903	1525	AW931531	1575	TC183092
1426	TC187227	1476	TC220217	1526	AW945034	1576	TC184127
1427	TC190123	1477	TC188847	1527	BE354280	1577	TC184844
1428	TC190825	1478	AW650894	1528	BE354727	1578	TC185793
1429	CN385562	1479	TC177096	1529	BE433157	1579	TC185798
1430	TC173833	1480	TC178912	1530	BE449245	1580	TC185937
1431	TC215133	1481	TC182126	1531	BE461515	1581	TC185955
1432	AI774599	1482	TC186680	1532	BE463367	1582	TC186119
1433	AI778155	1483	BG124425	1533	BF050158	1583	TC186164
1434	AW092686	1484	TC187777	1534	BG124486	1584	TC187010
1435	AW443417	1485	TC190416	1535	BG126128	1585	TC225585
1436	AW616728	1486	DN168508	1536	BG139631	1586	TC187910
1437	BG124520	1487	AI896655	1537	BG140399	1587	TC243721
1438	BG127797	1488	DV104733	1538	BG642916	1588	TC188665
1439	BG133169	1489	TC179000	1539	BG791258	1589	TC189611
1440	BG134870	1490	TC185822	1540	BI203547	1590	TC190331
1441	BG135198	1491	TC244691	1541	BI206593	1591	TC190641
1442	BG625962	1492	BI209710	1542	BI927000	1592	DN171595
1443	BI207366	1493	BW687235	1543	BI932597	1593	NP1427113
1444	BI927801	1494	TC178112	1544	BP878709	1594	TC174637
1445	BI929870	1495	TC179278	1545	BP884965	1595	NP000648
1446	BI933324	1496	AI771790	1546	BP886125	1596	TC189788
1447	BI934009	1497	AW039058	1547	BP887839	1597	DV104760
1448	BP884127	1498	BF114093	1548	BP889041	1598	TC169884
1449	BP889445	1499	BI207671	1549	BW686055	1599	TC235200
1450	TC217559	1500	TC175614	1550	CD003481	1600	TC221209

Supplementary Table S3. *Continued*

No.	LeGI v.11 code	No.	LeGI v.11 code	No.	LeGI v.11 code
1601	TC174009	1651	TC182927	1701	BP908484
1602	TC226080	1652	TC183184	1702	TC172139
1603	TC228805	1653	TC183502	1703	TC172677
1604	TC227956	1654	TC187028	1704	TC174556
1605	TC176516	1655	TC240689	1705	TC188618
1606	TC177093	1656	TC190719	1706	TC170126
1607	TC177668	1657	AI771318	1707	AW032992
1608	TC235998	1658	AW928957	1708	AW041301
1609	TC178789	1659	BE353801	1709	BF096362
1610	TC180646	1660	BI930921	1710	BG132120
1611	TC181270	1661	TC241069	1711	DV105517
1612	TC181927	1662	TC182197	1712	TC217994
1613	TC235377	1663	TC183329	1713	TC176969
1614	TC182853	1664	DV105174	1714	TC174198
1615	TC183598	1665	TC175188		
1616	TC184085	1666	BP906879		
1617	TC242102	1667	TC181720		
1618	TC185015	1668	TC172925		
1619	TC185502	1669	TC178583		
1620	TC187267	1670	BP901371		
1621	TC187745	1671	TC223347		
1622	TC187887	1672	TC175775		
1623	TC189230	1673	TC177613		
1624	CN385189	1674	TC182968		
1625	DN170679	1675	TC184331		
1626	AI776620	1676	BP903433		
1627	AI777959	1677	TC172678		
1628	AW219351	1678	TC181121		
1629	AW626136	1679	AJ784567		
1630	AW737808	1680	TC171331		
1631	AW738477	1681	TC171863		
1632	AW931691	1682	TC175048		
1633	BE462550	1683	TC223935		
1634	BG131458	1684	TC182915		
1635	BG630026	1685	BG132553		
1636	BI204903	1686	BF114097		
1637	BI210154	1687	TC173572		
1638	BI422499	1688	BF113744		
1639	BI932571	1689	TC218548		
1640	BI933170	1690	TC175105		
1641	BP879277	1691	TC179200		
1642	BP885455	1692	TC182999		
1643	BW688183	1693	TC235332		
1644	TC172127	1694	TC187074		
1645	TC172183	1695	TC188964		
1646	TC172346	1696	AI488195		
1647	TC175036	1697	AI899157		
1648	TC176586	1698	BE353780		
1649	TC182365	1699	BI210041		
1650	TC182528	1700	BI922113		

Supplementary Table S4. Sets of RT-PCR primers and PCR conditions used to amplify *LeT6/TKn2*, *GA20ox1* and *GA2ox2* genes (see text in Chapter 5).

Gene name[a]	SGN Solyc ID	Primer sequence (5'-3')	Ta (°C)	No. of PCR cycles
LeT6/TKn2	Solyc02g081120	Fw_CCATCGTCTCTTGACTGCTTATCT Rv_AGGATCTTCTCCAATGATTCCACC	58	24
GA20ox1	Solyc03g006880	Fw_CATTGTGGTTATGCTAGTAG Rv_GTAGTAGTGTTGTGTTGATC	58	32
GA2ox2	Solyc03g120970	Fw_TGAGGAATTTCACGGAGAGG Rv_TCGACGATCTTAGGAGGAGAA	58	28
*CAC**	Solyc08g006960	Fw_GATGTCCTTATCAACCGTCTCTAC Rv_ACAAGAAAGAACAGCCTCCAATCT	58	24

[a] Tomato gene name adopted in this study (see text in Chapter 5). * *CAC* (SGN-U314153 or Solyc08g006960) represents the house-keeping gene used for RT-PCR data normalization (Expósito-Rodríguez *et al.*, 2008).

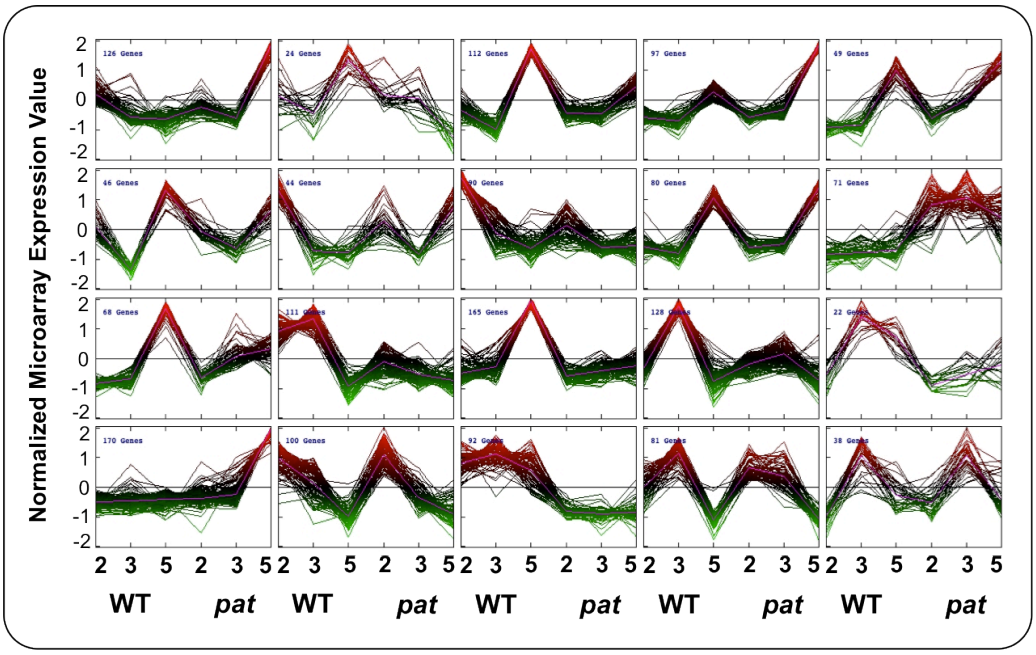

Supplementary Fig. S1. Expression graphs of the 20 clusters generated using the KMC method. In each cluster, on the x-axis are consecutively reported the three flower Stages (2, 3 and 5) in the WT and *pat* ovary (from left to right). The 1st line identifies clusters from 1 to 5 (from left to right respectively), 2nd line from 6 to 10, 3rd line from 11 to 15 and 4th line from 16 to 20.

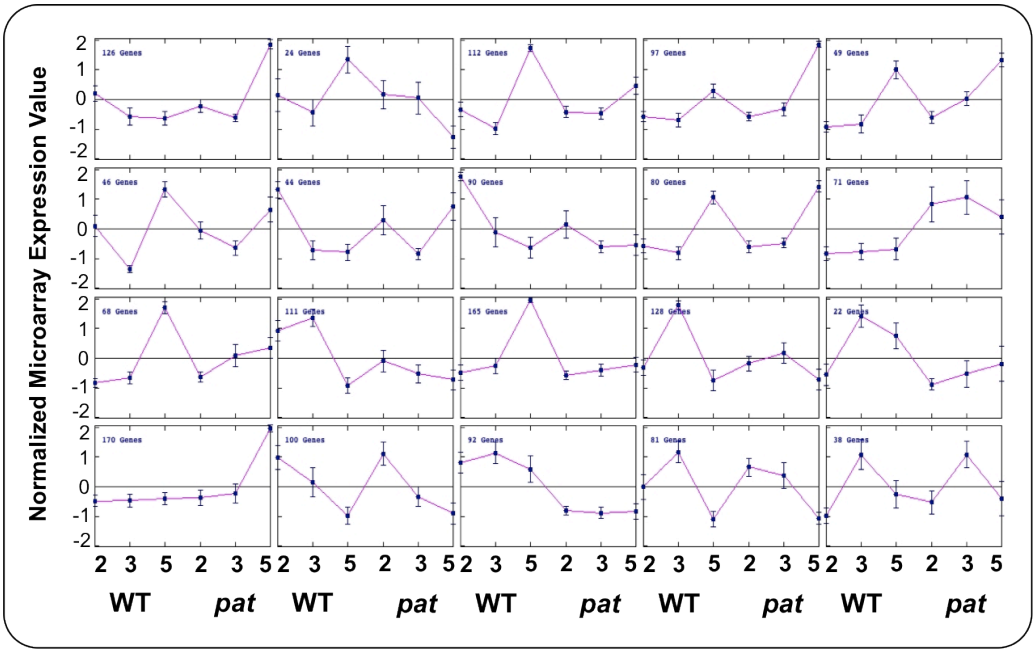

Supplementary Fig. S2. Centroid graphs of the 20 clusters generated using the KMC method and presented in the above Supplementary Fig. S1. In each cluster, on the x-axis are consecutively reported the three flower Stages (2, 3 and 5) in the WT and *pat* ovary (from left to right). The 1st line identifies clusters from 1 to 5 (from left to right respectively), 2nd line from 6 to 10, 3rd line from 11 to 15 and 4th line from 16 to 20. These centroid graphs were used to statistically categorize clusters into groups representing the five different biological trends (CC, PD, FG, AD and AS; see text in Chapter 4).

References

Allen KD, Sussex IM. 1996. Falsiflora and anantha control early stages of floral meristem development in tomato (Lycopersicon esculentum Mill.). *Planta* **200,** 254-264.

Ampomah-Dwamena C, Morris BA, Sutherland P, Veit B, Yao JL. 2002. Down-regulation of TM29, a tomato SEPALLATA homolog, causes parthenocarpic fruit development and floral reversion. *Plant Physiology* **130,** 605-617.

Anastasiou E, Lenhard M. 2007. Growing up to one's standard. *Current Opinion in Plant Biology* **10,** 63-69.

Angenent GC, Franken J, Busscher M, Van Dijken A, van Went J, Dons HJ, van Tunen AJ. 1995. A novel class of MADS box genes is involved in ovule development in petunia. *The Plant Cell* **7,** 1569-1582.

Anthony RG et al. 2004. A protein kinase target of a PDK1 signalling pathway is involved in root hair growth in *Arabidopsis*. *The EMBO Journal* **23,** 572-581.

Antognoni F, Ghetti F, Mazzucato A, Franceschetti M, Bagni N. 2002. Polyamine pattern during flower development in the parthenocarpic fruit (pat) mutant of tomato. *Physiologia Plantarum* **116,** 539-547.

Ariel FD, Manavella P, Dezar C, Chan RL. 2007. The true story of the HD-Zip family. *Trends in Plant Science* **12,** 419-426.

Arumuganathan K, Earle ED. 1991. Nuclear DNA content of some important plant species. *Plant Molecular Biology Report* **9,** 208-218.

Atanassova B. 1999. Functional male sterility (ps-2) in tomato (Lycopesicon esculentum Mill.) and its application in breeding and hybrid seed production. *Euphytica* **107,** 13-21.

Atherton JG, Harris GP. 1986. Flowering. In: Atherton JG, Rudich J, eds. The tomato crop – A scientific basis for improvement. Chapman and Hall, London, pp. 167-200.

Audran-Delalande C, Bassa C, Mila I, Regad F, Zouine M, Bouzayen M. 2012. Genome-wide identification, functional analysis and expression profiling of the Aux/IAA gene family in tomato. *Plant and Cell Physiology* **53,** 659-672.

Avivi Y, Lev-Yadun S, Morozova N, Libs L, Williams L, Zhao J, Varghese G, Grafi G. 2000. Clausa, a tomato mutant with a wide range of phenotypic perturbations, displays a cell type-dependent expression of the homeobox gene LeT6/TKn2. *Plant physiology* **124,** 541-552.

Baker SC, Robinson-Beers K, Villanueva JM, Gaiser JC, Gasser CS. 1997. Interactions among genes regulating ovule development in Arabidopsis thaliana. *Genetics* **145,** 1109-1124.

Balbi V, Lomax TL. 2003. Regulation of early tomato fruit development by the diageotropica gene. *Plant Physiology* **131,** 186-197.

Bao N, Lye K-W, Barton MK. 2004. MicroRNA binding sites in Arabidopsis class III HD-ZIP mRNAs are required for methylation of the template chromosome. *Developmental Cell* **7,** 653-662.

Barone A, Chiusano ML, Ercolano MR, Giuliano G, Grandillo S, Frusciante L. 2008. Structural and functional genomics of tomato. *International Journal of Plant Genomics*, doi: 10.1155/2008/820274.

Barone A, Di Matteo A, Carputo D, Frusciante L. 2009. High-throughput genomics enhances tomato breeding efficiency. *Current Genomics* **10,** 1-9.

Beraldi D, Picarella ME, Soressi GP, Mazzucato A. 2004. Fine mapping of the parthenocarpic fruit (pat) mutation in tomato. *Theoretical and Applied Genetics* **108,** 209-216.

Berger Y, Harpaz-Saad S, Brand A, Melnik H, Sirding N, Alvarez JP, Zinder M, Samach A, Eshed Y, Ori N. 2009. The NAC-domain transcription factor GOBLET specifies leaflet boundaries in compound tomato leaves. *Development* **136,** 823-832.

Bianchi A, Soressi GP. 1969. Mutanti di pomodoro artificialmente indotti suscettibili di utilizzazione nel miglioramento genetico. *Sementi Elette* **XV,** 2-6.

Bombarely A, Menda N, Tecle IY, Buels RM, Strickler S, Fischer-York T, Pujar A, Leto J, Gosselin J, Mueller LA. 2011. The Sol Genomics Network (solgenomics.net): growing tomatoes using Perl. *Nucleic Acids Research* **39,** 1149-1155.

Bowman JL, Floyd SK. 2008. Patterning and polarity in seed plant shoots. *Annual Review of Plant Biology* **59,** 67-88.

Bowman JL, Smyth DR. 1999. CRABS CLAW, a gene that regulates carpel and nectary development in Arabidopsis, encodes a novel protein with zinc finger and helix-loop-helix domains. *Development* **126,** 2387-2396.

Byrne ME. 2006. Shoot meristem function and leaf polarity: the role of class III HD–ZIP genes. *PLoS Genetics* **2,** e89.

Carmi N, Salts Y, Dedicova B, Shabtai S, Barg R. 2003. Induction of parthenocarpy in tomato via specific expression of the rolB gene in the ovary. *Planta* **5,** 725-735.

Cecchetti V, Pomponi M, Altamura MM, Pezzotti M, Marsilio S, D'Angeli S, Tornielli GB, Costantino P, Cardarelli M. 2004. Expression of *rolB* in tabacco flowers affects the coordinated processes of anther dehiscence and style elongation. *The Plant Journal* **38,** 512-525.

Cecchetti V, Altamura MM, Falasca G, Costantino P, Cardarelli M. 2008. Auxin regulates *Arabidopsis* anther dehiscence, pollen maturation, and filament elongation. *The Plant Cell* **20,** 1760-1774.

Chaabouni S, Jones B, Delalande C, Wang H, Li Z, Mila I, Frasse P, Latché A, Pech JC, Bouzayen M. 2009. Sl-IAA3, a tomato Aux/IAA at the crossroads of auxin and ethylene signalling involved in differential growth. *Journal of Experimental Botany* **4,** 1349-1362.

Chen PY, Wang CK, Soong SC, To KY. 2003. Complete sequence of the binary vector pBI121 and its application in cloning T-DNA insertion from transgenic plants. *Molecular Breeding* **11,** 287-293.

Cho E, Zambryski PC. 2011. Organ boundary1 defines a gene expressed at the junction between the shoot apical meristem and lateral organs. *Proceedings of the National Academy of Sciences* **108,** 2154-2159.

Clark SE, Williams RW, Meyerowitz EM. 1997. The CLAVATA1 gene encodes a putative receptor kinase that controls shoot and floral meristem size in Arabidopsis. *Cell* **89,** 575-585.

Coen ES, Meyerowitz EM. 1991. The war of the whorls: genetic interactions controlling flower development. *Nature* **353,** 31-37.

Colombo L, Franken J, Koetje E, van Went J, Dons HJ, Angenent GC, van Tunen AJ. 1995. The petunia MADS box gene FBP11 determines ovule identity. *The Plant Cell* **7,** 1859-1868.

Colombo L, Battaglia R, Kater MM. 2008. Arabidopsis ovule development and its evulotionary conservation. *Trends in Plant Science* **13,** 444-450.

Crooks GE, Hon G, Chandonia JM, Brenner SE. 2004. WebLOGO: a sequence logo generator. *Genome Research* **14,** 1188-1190.

de Jong M, Mariani C, Vriezen WH. 2009a. The role of auxin and gibberellin in tomato fruit set. *Journal of Experimental Botany* **60,** 1523-1532.

de Jong M, Wolters-Arts M, Feron R, Mariani C, Vriezen WH. 2009b. The Solanum lycopersicum auxin response factor 7 (SlARF7) regulates auxin signaling during tomato fruit set and development. *The Plant Journal* **57,** 160-170.

Deng W, Yang Y, Ren Z, Audran-Delalande C, Mila I, Wang X, Song H, Hu Y, Bouzayen M, Li Z. 2012. The tomato SlIAA15 is involved in trichome formation and axillary shoot development. *New Phytologist* **194,** 379-390.

Dengler NG. 1984. Comparison of leaf development in normal (+/+), entire (e/e), and lanceolate (La/+) plants of tomato, Lycopersicon esculentum 'Ailsa Craig'. *Botanical Gazelle* **145,** 66-77.

Dharmasiri N, Estelle M. 2004. Auxin signaling and regulated protein degradation. *Trends in Plant Science* **9,** 302-308.

Di Matteo A, Rigano MM, Sacco A, Frusciante L, Barone A. 2011. Genetic transformation in tomato: novel tools to improve fruit quality and pharmaceutical production. In: Alvarez M, eds. Biochemistry, genetics and molecular biology in "*Genetic transformation*", doi: 10.5772/2452.

Dinkel H et al. 2012. ELM-the database of eukaryotic linear motifs. Nucleic Acids Research **40,** doi: 10.1093/nar/gkr1064.

Dorcey E, Urbez C, Blázquez M. 2009. Fertilization-dependent auxin response in ovules triggers fruit development through the modulation of gibberellin metabolism in Arabidopsis. *The Plant Journal* **58,** 318-332.

Duclercq J, Assoumou Ndong YP, Guerineau F, Sangwan RS, Catterou M. 2011. Arabidopsis shoot organogenesis is enhanced by an amino acid change in the ATHB15 transcription factor. *Plant Biology* **13**, 317-324.

Elhiti M, Stasolla C. 2009. Structure and function of homodomain-leucine zipper (HD-Zip) proteins. *Plant Signaling & Behavior* **4,** 86-88.

Elliott R, Betzner A, Huttner E. 1996. AINTEGUMENTA, an APETALA2-like gene of Arabidopsis with pleiotropic roles in ovule development and floral organ growth. *The Plant Cell* **8,** 155-168.

Emery JF, Floyd SK, Alvarez J, Eshed Y, Hawker NP, Izhaki A, Baum SF, Bowman JL. 2003. Radial patterning of Arabidopsis shoots by class III HD-ZIP and KANADI genes. *Current Biology* **13,** 1768-1774.

Eshed Y, Baum SF, Perea JV, Bowman JL. 2001. Establishment of polarity in lateral organs of plants. *Current Biology* **11,** 1251-1260.

Estevez JM, Kieliszewski MJ, Khitrov N, Somerville C. 2006. Characterization of synthetic hydroxyproline-rich proteoglycans with arabinogalactan protein and extensin motifs in Arabidopsis. *Plant Physiology* **142,** 458-470.

Expósito-Rodríguez M, Borges AA, Borges-Pérez A, Pérez JA. 2008. Selection of internal control genes for quantitative real-time RT-PCR studies during tomato development process. *BMC Plant Biology* **8,** 131.

Falavigna A, Badino M, Soressi GP. 1978. Potential of the monomendelian factor pat in the tomato breeding for industry. *Genetica Agraria* **32**, 159-160.

Ferrando C, Cuartero J, Costa J, Catalá MS, Nuez F. 1987. Relationship between the system pat-2 and pat-3/pat-4 which determine parthenocarpy in tomato. In: Synopses 10th meeting EUCARPIA TOMATO WORKING GROUP. "Modern Trends in Tomato Genetics and Breeding", pp. 8-13.

FitzGerald J, Luo M, Chaudhury A, Berger F. 2008. DNA methylation causes predominant maternal controls of plant embryo growth. *PLoS One* **28,** e2298.

Fleet CM, Sun T. 2005. A DELLAcate balance: the role of gibberellin in plant morphogenesis. *Current Opinion in Plant Biology* **8,** 77-85.

Floyd SK, Bowman JL. 2006. Distinct developmental mechanisms reflect the independent origins of leaves in vascular plants. *Current Biology* **16,** 1911-1917.

Floyd SK, Zalewski CS, Bowman JL. 2006. Evolution of class III homeodomain-leucine zipper genes in streptophytes. *Genetics* **173,** 373-388.

Fos M, Nuez F, García-Martínez JL. 2000. The gene pat-2, which induces natural parthenocarpy, alters the gibberellin content in unpollinated tomato ovaries. *Plant Physiology* **122,** 471-480.

Fos M, Proaño K, Nuez F, García-Martínez JL. 2001. Role of gibberellins in parthenocarpic fruit development induced by the genetic system pat-3/pat-4 in tomato. *Physiologia Plantarum* **111,** 545-550.

Fos M, Proaño K, Alabadi D, Nuez F, Carbonell J. 2003. Polyamine metabolism is altered in unpollinated parthenocarpic pat-2 tomato ovaries. *Plant Physiology* **31,** 359-366.

Fu X, Harberd NP. 2003. Auxin promotes Arabidopsis root growth by modulating gibberellin response. *Nature* **421,** 740-743.

Fulton TM, Hoeven R Van Der, Eannetta NT, Tanksley SD. 2002. Identification , analysis , and utilization of conserved ortholog set markers for comparative genomics in higher plants. *The Plant Cell* **14,** 1457-1467.

Gallavotti A, Barazesh S, Malcomber S, Hall D, Jackson D, Schmidt RJ, McSteen P. 2008. sparse inflorescence1 encodes a monocot-specific YUCCA-like gene required for vegetative and reproductive development in maize. *Proceedings of the National Academy of Sciences* **105,** 15196-15201.

Galon Y, Snir O, Fromm H. 2010. How calmodulin binding transcription activators (CAMTAs) mediate auxin responses. *Plant Signaling & Behavior* **5,** 1311-1314.

García-Martínez J, Carbonell J. 1980. Fruit-set of unpollinated ovaries of Pisum sativum L. *Planta* **147,** 451-456.

George W, Scott J, Spilttstoesser W. 1984. Parthenocarpy in tomato. *Horticola Review* **6,** 65-84.

Gillaspy G, Ben-David H, Gruissem W. 1993. Fruits: a developmental perspective. *The Plant Cell* **5,** 1439-1451.

Giovannoni JJ. 2004. Genetic regulation of fruit development and ripening. *The Plant Cell* **16,** 170-180.

Gleave AP. 1992. A versatile binary vector system with a T-DNA organizational structure conducive to efficient integration of cloned DNA into the plant genome. *Plant Molecular Biology* **20,** 1203-1207.

Goetz M, Vivian-smith A, Johnson SD, Koltunow AM. 2006. AUXIN RESPONSE FACTOR8 is a negative regulator of fruit initiation in Arabidopsis. *The Plant Cell* **18,** 1873-1886.

Goetz M, Hooper LC, Johnson SD, Rodrigues JCM, Vivian-Smith A, Koltunow AM. 2007. Expression of aberrant forms of AUXIN RESPONSE FACTOR8 stimulates parthenocarpy in Arabidopsis and tomato. *Plant Physiology* **145,** 351-366.

Goldman MH, Goldberg RB, Mariani C. 1994. Female sterile tobacco plants are produced by stigma-specific cell ablation. *The EMBO Journal* **13,** 2976-2984.

Gómez P, Jamilena M, Capel J, Zurita S. 1999. Stamenless, a tomato mutant with homeotic conversions in petals and stamens. *Planta* **209,** 172-179.

Gorguet B, Van Heusden a W, Lindhout P. 2005. Parthenocarpic fruit development in tomato. *Plant Biology* **7,** 131-139.

Gorguet B, Eggink PM, Ocaña J, Tiwari A, Schipper D, Finkers R, Visser RGF, Van Heusden AW. 2008. Mapping and characterization of novel parthenocarpy QTLs in tomato. *Theoretical and Applied Genetics* **116,** 755-767.

Goto K, Meyerowitz EM. 1994. Function and regulation of the Arabidopsis floral homeotic gene PISTILLATA. *Genes and Development* **8,** 1548-1560.

Green KA, Prigge MJ, Katzman RB, Clark SE. 2005. CORONA , a member of the class III homeodomain leucine zipper gene family in Arabidopsis, regulates stem cell specification and organogenesis. *The Plant Cell* **17,** 691-704.

Grigg SP, Canales C, Hay A, Tsiantis M. 2005. SERRATE coordinates shoot meristem function and leaf axial patterning in Arabidopsis. *Nature* **437,** 1022-1026.

Guilfoyle TJ, Hagen G. 2007. Auxin response factors. *Current Opinion in Plant Biology* **10,** 453-460.

Gustafson FG. 1936. Inducement of fruit development by growth-promoting chemicals. *Proceedings of the National Academy of Sciences* **22,** 628-636.

Gustafson FG. 1937. Parthenocarpy induced by pollen extracts. *American Journal of Botany* **24,** 102-107.

Gustafson FG. 1939. The cause of natural parthenocarpy. *American Journal of Botany* **26,**135-138.

Gustafson FG. 1942. Parthenocarpy: natural and artificial. *Botanical Review* **8,** 599-654.

Hamann T, Benkova E, Bäurle I, Kientz M, Jürgens G. 2002. The Arabidopsis BODENLOS gene encodes an auxin response protein inhibiting MONOPTEROS-mediated embryo patterning. *Genes and Development* **16,** 1610-1615.

Hamann T, Mayer U, Jürgens G. 1999. The auxin-insensitive bodenlos mutation affects primary root formation and apical-basal patterning in the Arabidopsis embryo. *Development* **126,** 1387-1395**.**

Hardtke CS, Berleth T. 1998. The Arabidopsis gene MONOPTEROS encodes a transcription factor mediating embryo axis formation and vascular development. *The EMBO Journal* **17,** 1405-1411.

Hay A, Kaur H, Phillips A, Hedden P, Hake S, Tsiantis M. 2002. The gibberellin pathway mediates KNOTTED1-type homeobox function in plants with different body plans. *Current Biology* **12,** 1557-1565.

Hay A, Tsiantis M. 2010. KNOX genes: versatile regulators of plant development and diversity. *Development* **137,** 3153-3165.

Hazra P, Dutta AK, Chatterjee P. 2010. Altered gibberellin and auxin levels in the ovaries in the manifestation of genetic parthenocarpy in tomato (Solanum lycopersicum). *Current Science* **99,** 1439-1443.

Hileman LC, Sundstrom JF, Litt A, Chen M, Shumba T, Irish VF. 2006. Molecular and phylogenetic analyses of the MADS-box gene family in tomato. *Molecular Biology and Evolution* **23,** 2245-2258.

Hirt H, Garcia AV, Oelmüller R. 2011. AGC kinases in plant development and defense. *Plant Signaling & Behavior* **6**, 1030-1033.

Honma T, Goto K. 2001. Complexes of MADS-box proteins are sufficient to convert leaves into floral organs. *Nature* **409,** 525-529.

Hu J et al. 2008. Potential sites of bioactive gibberellin production during reproductive growth in Arabidopsis. *The Plant Cell* **20**, 320-336.

Ishida T, Aida M, Takada S, Tasaka M. 2000. Involvement of CUP-SHAPED COTYLEDON genes in gynoecium and ovule development in Arabidopsis thaliana. *Plant & Cell Physiology* **41**, 60-67.

Izhaki A, Bowman JL. 2007. KANADI and class III HD-Zip gene families regulate embryo patterning and modulate auxin flow during embryogenesis in Arabidopsis. *The Plant Cell* **19,** 495-508.

Jacobsen SE, Olszewski NE. 1993. Mutations at the SPINDLY locus of Arabidopsis alter gibberellin signal transduction. *The Plant Cell* **5,** 887-896.

Janssen B, Lund L, Sinha N. 1998. Overexpression of a homeobox gene, LeT6, reveals indeterminate features in the tomato compound leaf. *Plant Physiology* **117,** 771-786.

Jasinski S, Piazza P, Craft J, Hay A, Woolley L, Rieu I, Phillips A, Hedden P, Tsiantis M. 2005. KNOX action in Arabidopsis is mediated by coordinate regulation of cytokinin and gibberellin activities. *Current Biology* **15,** 1560-1565.

Jasinski S, Tattersall A, Piazza P, Hay A, Martinez-Garcia JF, Schmitz G, Theres K, McCormick S, Tsiantis M. 2008. PROCERA encodes a DELLA protein that mediates control of dissected leaf form in tomato. *The Plant Journal* **56,** 603-612.

Jensen WA. 1962. Botanical Histochemistry - Principles and practice. University of California, Berkeley. W. H. Freeman and Company.

Kahle KT, Ring AM, Lifton RP. 2008. Molecular physiology of the WNK kinases. *Annu Rev Physiol* **70**, 329-355.

Kelley DR, Gasser CS. 2009. Ovule development: genetic trends and evolutionary considerations. *Sexual Plant Reproduction* **22,** 229-234.

Kelley DR, Skinner DJ, Gasser CS. 2009. Roles of polarity determinants in ovule development. *The Plant Journal* **57,** 1054-1064.

Kerstetter R, Vollbrecht E, Lowe B, Veit B, Yamaguchi J, Hake S. 1994. Sequence analysis and expression patterns divide the maize knotted1-like homeobox genes into two classes. *The Plant Cell* **6**, 1877-1887.

Kim J et al. 2005. microRNA-directed cleavage of ATHB15 mRNA regulates vascular development in Arabidopsis inflorescence stems. *The Plant Journal* **42,** 84-94.

King PJ. 1988. Plant hormone mutants. *Trends in Genetics* **4,** 157-162.

Koltunow AM, Grossniklaus U. 2003. Apomixis: A developmental perspective. *Annual Review of Plant Biology* **54,** 547-574.

Krizek BA. 2009. Making bigger plants: Key regulators of final organ size. *Current Opinion in Plant Biology* **12,** 17-22.

Kumar P, Henikoff S, Ng PC. 2009. Predicting the effects of coding non-synonymous variants on protein function using the SIFT algorithm. *Nature Protocols* **4,** 1073-1081.

Lam BC-H, Blumwald E. 2002. Domains as functional building blocks of plant proteins. *Trends in Plant Science* **7**, 544-5499.

Lang JD, Ray S, Ray A. 1994. Sin1, a mutation affecting female fertility in Arabidopsis, interacts with mod1, its recessive modifier. *Genetics* **137,** 1101-1110.

Lee J, Baum SF, Alvarez J, Patel A, Chitwood DH, Bowman JL. 2005. Activation of CRABS CLAW in the nectaries and carpels of Arabidopsis. *The Plant Cell* **17,** 25-36.
Lee S-J, Cobb MH, Goldsmith EJ. 2009. Crystal structure of domain–swapped STE20 OSR1 kinase domain. *Protein Science* **18,** 304-313.

Lemaire-chamley M, Petit J, Garcia V, Just D, Baldet P, Fagard M, Mouassite M, Cheniclet C, Rothan C. 2005. Changes in transcriptional profiles are associated with early fruit tissue specialization in tomato. *Plant Physiology* **139,** 750-769..

Liang P, Pardee AB. 1992. Differential display of eukaryotic messenger RNA by means of the polymerase chain reaction. *Science* **257,** 967-971.

Lifschitz E, Brodai L, Hareven D, Hurwitz C, Prihadash A, Pnueli L, Samach A, Zamir D. 1993. Molecular mapping of flower development in tomato. In: Yoder J, ed. Molecular Biology of Tomato. Technomic Publishing Co. Inc., Lancaster PA, USA, pp. 175-184.

Lifschitz E, Eviatar T, Rozman A, Shalit A, Goldshmidt A, Amsellem Z, Alvarez JP, Eshed Y. 2006. The tomato FT ortholog triggers systemic signals that regulate growth and flowering and substitute for diverse environmental stimuli. *Proceedings of the National Academy of Sciences* **103,** 6398-6403.

Lin WC, Shuai B, Springer PS. 2003. The Arabidopsis LATERAL ORGAN BOUNDARIES-Domain gene ASYMMETRIC LEAVES2 functions in the repression of KNOX gene expression and in adaxial-abaxial patterning. *The Plant Cell* **15,** 2241-2252.

Lippman ZB, Cohen O, Alvarez JP, Abu-Abied M, Pekker I, Paran I, Eshed Y, Zamir D. 2008. The making of a compound inflorescence in tomato and related nightshades. *PLoS Biology* **6,** doi: 10.1371/journal.pbio.0060288, e288.

Lora J, Hormaza JI, Herrero M, Gasser CS. 2011. Seedless fruits and the disruption of a conserved genetic pathway in angiosperm ovule development. *Proceedings of the National Academy of Sciences* **108,** 5461-5465.

Lozano R, Giménez E, Cara B, Capel J, Trinidad A. 2009. Genetic analysis of reproductive development in tomato. *The International Journal of Developmental Biology* **53,** 1635-1648.

Lukyanenko AN. 1991. Parthenocarpy in tomato. In: Kalloo G, ed. Genetic Improvement of Tomato. Monographs on Theoretical and Applied Genetics. Springer-Verlag, Berlin, pp. 167-178.

Magnani E, Barton MK. 2011. A per-ARNT-sim-like sensor domain uniquely regulates the activity of the homeodomain leucine zipper transcription factor REVOLUTA in Arabidopsis. *The Plant Cell* **23,** 567-582.

Mallory AC, Vaucheret H. 2006. Functions of microRNAs and related small RNAs in plants. *Nature Genetics* **38,** S31-S36.

Mapelli S, Frova C, Torti G, Soressi, GP. 1978. Relationship between set, development and activities of growth regulators in tomato fruits. *Plant Cell Physiology* **19,** 1281-1288.

Martí C, Orzáez D, Ellul P, Moreno V, Carbonell J, Granell A. 2007. Silencing of DELLA induces facultative parthenocarpy in tomato fruits. *The Plant Journal* **52,** 865-876.

Martinelli F, Uratsu SL, Reagan RL, Chen Y, Tricoli D, Fiehn O, Rocke DM, Gasser CS, Dandekar AM. 2009. Gene regulation in parthenocarpic tomato fruit. *Journal of Experimental Botany* **60,** 3873-3890.

Mazzucato A, Taddei AR, Soressi GP. 1998. The parthenocarpic fruit (pat) mutant of tomato (Lycopersicon esculentum Mill.) sets seedless fruits and has aberrant anther and ovule development. *Development* **125**, 107-114.

Mazzucato A, Testa G, Biancari T, Soressi GP. 1999. Effect of gibberellic acid treatments, environmental conditions, and genetic background on the expression of the parthenocarpic fruit mutation in tomato. *Protoplasma* **1,** 18-25.

Mazzucato A, Olimpieri I, Ciampolini F, Cresti M, Soressi GP. 2003. A defective pollen-pistil interaction contributes to hamper seed set in the parthenocarpic fruit tomato mutant. *Sexual Plant Reproduction* **16,** 157-164.

Mazzucato A, Olimpieri I, Siligato F, Picarella ME, Soressi GP. 2008. Characterization of genes controlling stamen identity and development in a parthenocarpic tomato mutant indicates a role for the DEFICIENS ortholog in the control of fruit set. *Physiologia Plantarum* **132**, 526-537.

Mcabee JM, Hill TA, Skinner DJ, Izhaki A, Hauser BA, Meister RJ, Reddy GV, Meyerowitz EM, Bowman JL, Gasser CS. 2006. ABERRANT TESTA SHAPE encodes a KANADI family member, linking polarity determination to separation and growth of Arabidopsis ovule integuments. *The Plant Journal* **46,** 522-531.

McConnell JR, Barton K. 1998. Leaf polarity and meristem formation in Arabidopsis. *Development* 125, 2935-2942.

McConnell JR, Emery J, Eshed Y, Bao N, Bowman J, Barton MK. 2001. Role of PHABULOSA and PHAVOLUTA in determining radial patterning in shoots. *Nature* **411**, 709-713.

Meyerowitz EM, Bowman JL, Brockman LL, Drews GN, Jack T, Sieburth LE, Weigel D. 1991. A genetic and molecular model for flower development in Arabidopsis thaliana. *Development* **S1,** 157-167.

Modrusan Z, Reiser L, Feldmann KA, Fischer RL, Haughn GW. 1994. Homeotic transformation of ovules into carpel-like structures in Arabidopsis. *The Plant Cell* **6,** 333-349.

Molesini B, Pandolfini T, Rotino GL, Dani V, Spena A. 2009. Aucsia gene silencing causes parthenocarpic fruit development in tomato. *Plant Physiology* **149,** 534-548.

Molinero-Rosales N, Jamilena M, Zurita S, Gomez S, Capel J, Lozano R. 1999. FALSIFLORA, the tomato orthologue of FLORICAULA and LEAFY, controls flowering time and floral meristem identity. *The Plant Journal* **20,** 685-693.

Molinero-Rosales N, Latorre A, Jamilena M, Lozano R. 2004. SINGLE FLOWER TRUSS regulates the transition and maintenance of flowering in tomato. *Planta* **218**, 427-434.

Mounet F, Moing A, Kowalczyk M, Rohrmann J, Petit J, Garcia V, Maucourt M, Yano K, Deborde C, Aoki K, Bergès H, Granell A, Fernie AR, Bellini C, Rothan C, Lemaire-Chamley M. 2012. Down-regulation of a single auxin efflux transport protein in tomato induces precocious fruit development. *Journal of Experimental Botany* **63,** 4901-4917**.**

Moussian B, Schoof H, Haecker A, Jürgens G, Laux T. 1998. Role of the ZWILLE gene in the regulation of central shoot meristem cell fate during Arabidopsis embryogenesis. *The EMBO Journal* **17,** 1799-1809.

Mukherjee K, Bürglin TR. 2006. MEKHLA, a novel domain with similarity to PAS domains, is fused to plant homeodomain-leucine zipper III proteins. *Plant Physiology* **140,** 1142-1150.

Mukherjee K, Brocchieri L, Bürglin TR. 2009. A comprehensive classification and evolutionary analysis of plant homeobox genes. *Molecular biology and Evolution* **26**, 2775-2794.

Mutasa-Göttgens E, Hedden P. 2009. Gibberellin as a factor in floral regulatory networks. *Journal of Experimental Botany* **60,** 1979-1989.

Nakano T, Kimbara J, Fujisawa M, Kitagawa M, Ihashi N, Maeda H, Kasumi T, Ito Y. 2012. MACROCALYX and JOINTLESS interact in the transcriptional regulation of tomato fruit abscission zone development. *Plant Physiology* **158,** 439-450.

Napoli CA, Fahy D, Wang HY, Taylor LP. 1999. White anther: A petunia mutant that abolishes pollen flavonol accumulation, induces male sterility, and is complemented by a chalcone synthase transgene. *Plant Physiology* **120,** 615-622.

Nash AF, Gardner RG, Henderson WR. 1985. Evaluation of allelism and seed set of eight stamenless tomato mutants. *Horticultural Science* **20,** 440-442.

Nelson DR. 2009. The cytochrome P450 homepage. *Human Genomics* **4,** 59-65.

Nitsch JP. 1950. Growth and morphogenesis of the strawberry as related to auxin. *American Journal of Botany* **37,** 211-215.

Nitsch JP. 1952. Plant hormones in the development of fruits. *The Quarterly Review of Biology* **27,** 33-57.

Nitsch JP. 1970. Hormonal factors in growth and development. In: Hulme AC, ed. Food Science and Technology. Academic Press, London, pp. 427-472.

Nitsch LMC, Oplaat C, Feron R, Ma Q, Wolters-Arts M, Hedden P, Mariani C, Vriezen WH. 2009. Abscisic acid levels in tomato ovaries are regulated by LeNCED1 and SlCYP707A1. *Planta* **229,** 1335-1346.

Nogler GA. 1984. Gametophytic apomixis. In: Johri BM, ed. Embryology of angiosperms. Springer-Verlag, Berlin, pp. 475-518.

Nothnagel EA. 1997. Proteoglycans and related components in the plant cells. *International Review of Cytology* **174,** 195-291.

Nuez F, Costa J, Cuartero J. 1986. Genetics of the parthenocarpy for tomato varieties “Sub-Artic Plenty”, “75/59” and “Severianin”. *Zeitschrift Pflanzenzuchtung-Journal of Plant Breeding* **96,** 200-206.

Ochando I, Jover-Gil S, Ripoll JJ, Candela H, Vera A, Ponce MR, Martínez-Laborda A, Micol JL. 2006. Mutations in the MicroRNA complementarity site of the INCURVATA4 gene perturb meristem function and adaxialize lateral organs in Arabidopsis. *Plant Physiology* **141,** 607-619.

Ochando I, González-Reig S, Ripoll J-J, Vera A, Martínez-Laborda A. 2008. Alteration of the shoot radial pattern in Arabidopsis thaliana by a gain-of-function allele of the class III HD-Zip gene INCURVATA4. *The International Journal of Developmental Biology* **52**, 953-961.

Olimpieri I, Siligato F, Caccia R, Mariotti L, Ceccarelli N, Soressi GP, Mazzucato A. 2007. Tomato fruit set driven by pollination or by the parthenocarpic fruit allele are mediated by transcriptionally regulated gibberellin biosynthesis. *Planta* **226**, 877-888.

Olimpieri I, Mazzucato A. 2008. Phenotypic and genetic characterization of the pistillate mutation in tomato. *Theoretical and Applied Genetics* **118,** 151-163.

Olimpieri I, Caccia R, Picarella ME, Pucci A, Santangelo E, Soressi GP, Mazzucato A. 2011. Constitutive co-suppression of the GA 20-oxidase1 gene in tomato leads to severe defects in vegetative and reproductive development. *Plant Science* **180,** 496-503.

Olszewski N, Sun T, Gubler F. 2002. Gibberellin signaling : biosynthesis, catabolism, and response pathways. *The Plant Cell* **14,** S61-80.

Ortiz R, Vuylsteke D. 1995. Factors influencing seed set in triploid Musa spp. L. and production of euploid hybrids. *Annals of Botany* **75,** 151-155.

Ozga J, Huizen R Van, Reinecke D. 2002. Hormone and seed-specific regulation of pea fruit growth. *Plant Physiology* **128,** 1379-1389.

Ozga JA, Reinecke DM. 2003. Hormonal Interactions in Fruit Development. *Journal of Plant Growth Regulation* **22,** 73-81.

Pagnussat GC, Yu HJ, Ngo QA, Rajani S, Mayalagu S, Johnson CS, Capron A, Xie LF, Ye D, Sundaresan V. 2005. Genetic and molecular identification of genes required for female gametophyte development and function in Arabidopsis. *Development* **132,** 603-614.

Pandolfini T, Molesini B, Spena A. 2007. Molecular dissection of the role of auxin in fruit initiation. *Trends in Plant Science* **12,** 327-329.

Parnis A, Cohen O, Gutfinger T, Hareven D, Zamir D, Lifschitz E. 1997. The dominant developmental mutants of tomato, Mouse-ear and Curl, are associated with distinct modes of abnormal transcriptional regulation of a Knotted gene. *The Plant Cell* **9**, 2143-2158.

Pascual L, Blanca JM, Cañizares J, Nuez F. 2009. Transcriptomic analysis of tomato carpel development reveals alterations in ethylene and gibberellin synthesis during pat3/pat4 parthenocarpic fruit set. *BMC Plant Biology* **9,** 67.

Pattison RJ, Catalá C. 2012. Evaluating auxin distribution in tomato (Solanum lycopersicum) through an analysis of the PIN and AUX/LAX gene families. *The Plant Journal* **70**, 585-598.

Pecaut P, Philouze J. 1978. A sha pat line obtained by natural mutation. *Report of the Tomato Genetics Cooperative* **28,** 12.

Pelaz S, Ditta GS, Yanofsky MF. 2000. B and C floral organ identity functions require SEPALLATTA MADS-box genes. *Nature* **405**, 200-203.

Péret B et al. 2012. AUX/LAX genes encode a family of auxin influx transporters that perform distinct functions during Arabidopsis development. *The Plant Cell* **24**, 2874-2885.

Perrimon N, Bernfield M. 2001. Cellular functions of proteoglycans-an overview. *Seminars in Cell & Developmental Biology* **12,** 65-67.

Philouze J. 1983. Parthenocarpie naturelle chez la tomate. I. Revue bibliographique. *Agronomie* **3,** 611-620.

Philouze J. 1991. Description of isogenic lines, except for one, or two, monogenically controlled morphological traits in tomato, Lycopersicon esculentum Mill. *Euphytica* **56,** 121-131.

Philouze J, Maisonneuve B. 1978. Heredity of the natural ability to set parthenocarpic fruits in a German line. *Report of the Tomato Genetics Cooperative* **28,** 12.

Philouze J, Pecaut P. 1986. Parthénocarpie naturelle chez la tomate. III. Etude de la parthénocarpie due au gène pat (parthenocarpic fruit) de la lignée 'Montfavet 191'. *Agronomie* **6**, 243-248.

Picken AJF. 1984. Quantitative morphology of the developing cucumber leaf. *Annals of Botany* **53,** 527-539.

Pike LM, Peterson CE. 1969. Inheritance of parthenocarpy in the cucumber (Cucumis sativus L.). *Euphytica* **18,** 101-105.

Pinyopich A, Ditta GS, Savidge B, Liljegren SJ, Baumann E, Wisman E, Yanofsky MF. 2003. Assessing the redundancy of MADS-box genes during carpel and ovule development. *Nature* **424,** 85-88.

Pnueli L, Hareven D, Rounsley SD, Yanofsky MF, Lifschitz E. 1994a. Isolation of the tomato AGAMOUS gene TAG1 and analysis of its homeotic role in transgenic plants. *The Plant Cell* **6,** 163-173.

Pnueli L, Hareven D, Broday L, Hurwitz C, Lifschitz E. 1994b. The TM5 MADS box gene mediates organ differentiation in the three inner whorls of tomato flowers. *The Plant Cell* **6,** 175-186.

Pnueli L, Carmel-Goren L, Hareven D, Gutfinger T, Alvarez J, Ganal M, Zamir D, Lifschitz E. 1998. The SELF-PRUNING gene of tomato regulates vegetative to reproductive switching of sympodial meristems and is the ortholog of CEN and TFL1. *Development* **125,** 1979-1989.

Preston JC, Hileman LC. 2013. Functional evolution in the plant SQUAMOSA-PROMOTER BINDING PROTEIN-LIKE (SPL) gene family. *Frontiers in Plant Science* **4,** 80.

Prigge MJ, Clark SE. 2006. Evolution of the class III HD-Zip gene family in land plants. *Evolution & development* **8,** 350-361.

Prigge MJ, Otsuga D, Alonso JM, Ecker JR, Drews GN, Clark SE. 2005. Class III homeodomain-leucine zipper gene family members have overlapping, antagonistic, and distinct roles in Arabidopsis development. *The Plant Cell* **17,** 61-76.

Pysh LD, Wysocka-Diller JW, Camilleri C, Bouchez D, Benfey PN. 1999. The GRAS gene family in Arabidopsis: sequence characterization and basic expression analysis of the SCARECROW-LIKE genes. *The Plant Journal* **18,** 111-119.

Quinet M, Kinet JM. 2007. Transition to flowering and morphogenesis of reproductive structures in tomato. *The International Journal of Developmental Biology* **1,** 64-74.

Ray A, Robinson-Beers K, Ray S, Baker SC, Lang JD, Preuss D, Milligan SB, Gasser CS. 1994. Arabidopsis floral homeotic gene BELL (BEL1) controls ovule development through negative regulation of AGAMOUS gene (AG). *Proceedings of the National Academy of Sciences* **91,** 5761-5765.

Ren Z, Li Z, Miao Q, Yang Y, Deng W, Hao Y. 2011. The auxin receptor homologue in Solanum lycopersicum stimulates tomato fruit set and leaf morphogenesis. *Journal of Experimental Botany* **62**, 2815-2826.

Rick CM 1978. The tomato. *Scientific American* **239,** 76-87.

Rick CM, Butler L. 1956. Cytogenetics of tomato. *Advances Genetics* **8,** 847-857.

Rieu I, Ruiz-Rivero O, Fernandez-Garcia N, Griffiths J, Powers SJ, Gong F, Linhartova T, Eriksson S, Nilsson O, Thomas SG, Phillips AL, Hedden P. 2008b. The gibberellin biosynthetic genes AtGA20ox1 and AtGA20ox2 act, partially redundantly, to promote growth and development throughout the Arabidopsis life cycle. *The Plant Journal* **53**, 488-504.

Rieu I, Eriksson S, Powers SJ, Gong F, Griffiths J, Woolley L, Benlloch R, Nilsson O, Thomas SG, Hedden P, Phillips AL. 2008a. Genetic analysis reveals that C19-GA 2-oxidation is a major gibberellin inactivation pathway in Arabidopsis. *The Plant Cell* **20,** 2420-2436.

Robles P, Pelaz S. 2005. Flower and fruit development in Arabidopsis thaliana. *The International Journal of Developmental biology* **49**, 633-643.

Ross J, O'Neill D. 2001. New interactions between classical plant hormones. *Trends in Plant Science* **6,** 2-4.

Rotino GL, Perri E, Zottini M, Sommer H, Spena A. 1997. Genetic engineering of parthenocarpic plants. *Nature Biotechnology* **15,** 1398-1401.

Rowland O, Ludwig AA, Merrick CJ, Baillieul F, Tracy FE, Durrant WE, Fritz-Laylin L, Nekrasov V, Sjölander K, Yoshioka H, Jones JDG. 2005. Functional analysis of Avr9/Cf-9 rapidly elicited genes identifies a protein kinase, ACIK1, that is essential for full Cf-9–dependent disease resistance in tomato. *The Plant Cell* **17,** 295–310.

Roy A, Kucukural A, Zhang Y. 2010. I-TASSER: a unified platform for automated protein structure and function prediction. *Nature Protocols* **5,** 725-738.

Ru P, Xu L, Ma H, Huang H. 2006. Plant fertility defects induced by the enhanced expression of microRNA167. *Cell Research* **16,** 457-465.

Ruan Y-L, Patrick JW, Bouzayen M, Osorio S, Fernie AR. 2012. Molecular regulation of seed and fruit set. *Trends in Plant Science* **17,** 656-665.

Rubatzky VE, Yamaguchi M. 1997. Tomatoes, peppers, eggplants, and other solanaceous vegetables. In: Rubatzky VE, Yamaguchi M., eds. World vegetables: principles, production, and nutritive values. Springer-Verlag, London, pp. 532-576.

Ruiu F. 2006. Integrazione della mutazione positional sterile-2 (ps-2) nella mappa molecolare di pomodoro. Graduation thesis. University of Tuscia, Viterbo, Italy.

Saeed AI et al. 2003. TM4: A free, open-source system for microarray data management and analysis. *BioTechniques* **34,** 374-378.

Sawhney VK. 1992. Floral mutants in tomato: development, physiology and evolutionary implications. *Canadian Journal of Botany* **70,** 701-707.

Sawhney VK. 1994. Genic male sterility in tomato and its manipulation in breeding. In: Vasil IK, ed. Genetic control of self-incompatibility and reproductive development in flowering plants. Kluwer Academic Publishers, The Netherlands, pp. 443-458.

Scanlon MJ, Henderson DC, Bernstein B. 2002. SEMAPHORE1 functions during the regulation of ancestrally duplicated knox genes and polar auxin transport in maize. *Development* **129,** 2663-2673.

Scarpella E, Marcos D, Friml J, Berleth T. 2006. Control of leaf vascular patterning by polar auxin transport. *Genes and Development* **20,** 1015-1027.

Schena M, Davis RW. 1992. HD-Zip proteins: members of an Arabidopsis homeodomain protein superfamily. *Proceedings of the National Academy of Sciences* **89,** 3894-3898.

Schijlen EGWM, De Vos CHR, Martens S, Jonker HH, Rosin FM, Molthoff JW, Tikunov YM, Angenent GC, Van Tunen AJ, Bovy AG. 2007. RNA interference silencing of chalcone synthase, the first step in the flavonoid biosynthesis pathway, leads to parthenocarpic tomato fruits. *Plant Physiology* **144,** 1520-1530.

Schoenbohm C, Martens S, Eder C, Forkmann G, Weisshaar B. 2000. Identification of the arabidopsis thaliana flavonoid 3'-hydroxylase gene and functional expression of the encoded P450 enzyme. *Biological Chemistry* **381,** 749-753.

Schrick K, Nguyen D, Karlowski WM, Mayer KF. 2004. START lipid/sterol-binding domains are amplified in plants and are predominantly associated with homeodomain transcription factors. *Genome Biology* **5,** R41.

Selleri L. 2010. Positional cloning of the parthenocarpic fruit (pat) mutant gene and identification of new parthenocarpic sources in tomato (Solanum lycopersicum L.). PhD thesis. University of Tuscia, Viterbo, Italy.

Serrani JC, Carrera E, Ruiz-Rivero O, Gallego-Giraldo L, Peres LEP, García-Martínez JL. 2010. Inhibition of auxin transport from the ovary or from the apical shoot induces parthenocarpic fruit-set in tomato mediated by gibberellins. *Plant Physiology* **153,** 851-862.

Serrani JC, Sanjuán R, Ruiz-Rivero O, Fos M, García-Martínez JL. 2007. Gibberellin regulation of fruit set and growth in tomato. *Plant Physiology* **145,** 246-257.

Serrani JC, Ruiz-Rivero O, Fos M, García-Martínez JL. 2008. Auxin-induced fruit-set in tomato is mediated in part by gibberellins. *The Plant Journal* **56**, 922-934.

Shuai B, Reynaga-Peña C, Springer P. 2002. The lateral organ boundaries gene defines a novel, plant-specific gene family. *Plant Physiology* **129,** 747-761.

Skinner DJ, Gasser CS. 2009. Expression-based discovery of candidate ovule development regulators through transcriptional profiling of ovule mutants. *BMC Plant Biology* **9**, 29.

Song S, Qi T, Huang H, Xie D. 2013. Regulation of stamen development by coordinated actions of jasmonate, auxin and gibberellin in Arabidopsis. *Molecular Plant* **6,** doi: 10.1093/mp/sst054.

Soressi GP, Salamini F. 1975. A monomendelian gene inducing parthenocarpic fruits. *Report of the Tomato Genetics Cooperative* **25,** 22.

Soukas A, Cohen P, Socci ND, Friedman JM. 2000. Leptin-specific patterns of gene expression in white adipose tissue. *Genes and Development* **14,** 963-980.

Srivastava A, Handa AK. 2005. Hormonal Regulation of Tomato Fruit Development: A Molecular Perspective. *Journal of Plant Growth Regulation* **24,** 67-82.

Stevens MA and Rick CM. 1986. Genetics and breeding. In: Atherton JG, Rudich J, eds. The tomato crop: a scientific basis for improvement. Chapman and Hall, London, pp. 35-109.

Sun H, Uchii S, Watanabe S, Ezura H. 2006. A highly efficient transformation protocol for Micro-Tom, a model cultivar for tomato functional genomics. *Plant & Cell Physiology* **47,** 426-431.

Swarup K et al. 2008. The auxin influx carrier LAX3 promotes lateral root emergence. *Nature Cell Biology* **10,** 946-954.

Takada S, Hibara K, Ishida T, Tasaka M. 2001. The CUP-SHAPED COTYLEDON1 gene of Arabidopsis regulates shoot apical meristem formation. *Development* **128,** 1127-1135.

Tan QK, Irish VF. 2006. The Arabidopsis zinc finger-homeodomain genes encode proteins with unique biochemical properties that are coordinately expressed during floral development. *Plant Physiology* **140,** 1095-1108.

Tang W, Kelley D, Ezcurra I, Cotter R, McCormick S. 2004. LeSTIG1, an extracellular binding partner for pollen receptor kinase LePRK1 and LePRK2, promotes pollen tube growth in vitro. *The Plant Journal* **39,** 343-353.

Testa G, Caccia R, Tilesi F, Soressi G, Mazzucato A. 2002. Sequencing and characterization of tomato genes putatively involved in fruit set and early development. *Sexual Plant Reproduction* **14,** 269-277.

The Tomato Genome Consortium 2012. The tomato genome sequence provides insights into fleshy fruit evolution. *Nature* **485,** 635-641.

Thomas S, Sun T. 2004. Update on gibberellin signaling. A tale of the tall and the short. *Plant Physiology* **135,** 668-676.

Tiwari A, Vivian-Smith A, Voorrips RE, Habets MEJ, Xue LB, Offringa R, Heuvelink EP. 2011. Parthenocarpic potential in Capsicum annuum L. is enhanced by carpelloid structures and controlled by a single recessive gene. *BMC Plant Biology* **11,** 143.

Tiwari A, Vivian-Smith A, Ljung K, Offringa R, Euvelink E. 2013. Physiological and morphological changes during early and later stages of fruit growth in Capsicum annuum. *Physiologia Plantarum* **147,** 396-406.

Tobutt K. 1994. Combining apetalous parthenocarpy with columnar growth habit in apple. *Euphytica* **77**, 51-54.

Tucker MR, Hinze A, Tucker EJ, Takada S, Jürgens G, Laux T. 2008. Vascular signalling mediated by ZWILLE potentiates WUSCHEL function during shoot meristem stem cell development in the Arabidopsis embryo. *Development* **135,** 2839-2843.

Usami T, Horiguchi G, Yano S, Tsukaya H. 2009. The more and smaller cells mutants of Arabidopsis thaliana identify novel roles for SQUAMOSA PROMOTER BINDING PROTEIN-LIKE genes in the control of heteroblasty. *Development* **136,** 955-964.

Van der Hoorn RAL, Wulff BB, Rivas S, Durrant MC, van der Ploeg A, de Wit PJ, Jones JD. 2005. Structure-function analysis of Cf-9, a receptor-like protein with extracytoplasmic leucine-rich repeats. *The Plant Cell* **17,** 1000-1015.

Van Der Meer IM, Stam ME, Van Tunen AJ, Mol JNM, Stuitje AR. 1992. Antisense inhibition of flavonoid biosynthesis in petunia anthers results in male sterility. *The Plant Cell* **4,** 253-262.

Vanneste S, Friml J. 2009. Auxin: a trigger for change in plant development. *Cell* **136**, 1005-1016.

Varaud E, Brioudes F, Szécsi J, Leroux J, Brown S, Perrot-Rechenmann C, Bendahmane M. 2011. AUXIN RESPONSE FACTOR8 regulates Arabidopsis petal growth by interacting with the bHLH transcription factor BIGPETALp. *The Plant Cell* **23,** 973-983.

Varoquaux F, Blanvillain R, Delseny M, Gallois P. 2000. Less is better: new approaches for seedless fruit production. *Trends in Biotechnology* **18,** 233-242.

Vernoux T, Kronenberger J, Grandjean O, Laufs P, Traas J. 2000. PIN-FORMED 1 regulates cell fate at the periphery of the shoot apical meristem. *Development* **127,** 5157-5165.

Villanueva JM, Broadhvest J, Hauser BA, Meister RJ, Schneitz K, Gasser CS. 1999. INNER NO OUTER regulates abaxial-adaxial patterning in Arabidopsis ovules. *Genes and Development* **13,** 3160-3169.

Vivian-Smith A. 2001. The molecular basis for the initiation of fruit development and parthenocarpy. PhD thesis. University of Adelaide, Adelaide, Australia.

Vivian-Smith A, Koltunow AM. 1999. Genetic analysis of growth-regulator-induced parthenocarpy in Arabidopsis. *Plant Physiology* **121,** 437-451.

Vivian-Smith A, Luo M, Chaudhury A, Koltunow A. 2001. Fruit development is actively restricted in the absence of fertilization in Arabidopsis. *Development* **128,** 2321–2331.

Vrebalov J, Ruezinsky D, Padmanabhan V, White R, Medrano D, Drake R, Schuch W, Giovannoni J. 2002. A MADS-Box gene necessary for fruit ripening at the tomato ripening-inhibitor (Rin) locus. *Science* **296,** 343-346.

Vriezen WH, Feron R, Maretto F, Keijman J, Mariani C. 2008. Changes in tomato ovary transcriptome demonstrate complex hormonal regulation of fruit set. *New Phytologist* **177,** 60-76.

Wang H, Jones B, Li Z, Frasse P, Deladande C, Regad F, Chaabouni S, Latché A, Pech J-C, Bouzayen M. 2005. The tomato Aux/IAA transcription factor IAA9 is involved in fruit development and leaf morphogenesis. *The Plant Cell* **17,** 2676-2692.

Wang H, Schauer N, Usadel B, Frasse P, Zouine M, Hernould M, Latché A, Pech J-C, Fernie AR, Bouzayen M. 2009. Regulatory features underlying pollination-dependent and -independent tomato fruit set revealed by transcript and primary metabolite profiling. *The Plant Cell* **21,** 1428-1452.

Wang Y, Liu K, Liao H, Zhuang C, Ma H, Yan X. 2008. The plant WNK gene family and regulation of

flowering time in Arabidopsis. *Plant Biology* **10,** 548-562.

Warde-Farley D et al. 2010. The GeneMANIA prediction server: biological network integration for gene prioritization and predicting gene function. *Nucleic Acids Research* **38**, 214-220.

Weiss D, Ori N. 2007. Mechanisms of cross talk between gibberellin and other hormones. *Plant Physiology* **144,** 1240-1246.
Wesley SV et al. 2001. Construct design for efficient, effective and high throughput gene silencing in plants. *The Plant Journal* **27,** 581-590.

Williams L, Grigg SP, Xie M, Christensen S, Fletcher JC. 2005. Arabidopsis shoot apical meristem and lateral organ formation by microRNA miR166g and its AtHD-Zip target genes. *Development* **132,** 3657-3668.

Wu J, Wang F, Cheng L, Kong F, Peng Z, Liu S, Yu X, Lu G. 2011. Identification, isolation and expression analysis of auxin response factor (ARF) genes in Solanum lycopersicum. *Plant Cell Reports* **30,** 2059-2073.

Yanai O, Shani E, Dolezal K, Tarkowski P, Sablowski R, Sandberg G, Samach A, Ori N. 2005. Arabidopsis KNOXI proteins activate cytokinin biosynthesis. *Current Biology* **15,** 1566-1571.

Yao J, Dong Y, Morris BA. 2001. Parthenocarpic apple fruit production conferred by transposon insertion mutations in a MADS-box transcription factor. *Proceedings of the National Academy of Sciences* **98,** 1306-1311.

Yeung KY, Haynor DR, Ruzzo WL. 2001. Validating clustering for gene expression data. *Bioinformatics* **17,** 309-318.

Zhang J, Chen R, Xiao J, Qian C, Wang T, Li H, Ouyang B, Ye Z. 2007. A single-base deletion mutation in SlIAA9 gene causes tomato (Solanum lycopersicum) entire mutant. *Journal of Plant Research* **120,** 671-678.

Zhong R, Ye Z-H. 2001. Alteration of auxin polar transport in the Arabidopsis *ifl1* mutants. *Plant Physiology* **126,** 549-563.

Zhong R, Ye ZH. 2007. Regulation of HD-ZIP III Genes by MicroRNA 165. *Plant Signaling & Behavior* **2,** 351-353.

Zijlstra S. 1985. Parthenocarpie in tomaat; twee nieuwe lijnen uit soortkruising. Zaadbelangen **4,** 92–94.

Zimmermann P, Hirsch-hoffmann M, Hennig L, Gruissem W. 2004. GENEVESTIGATOR. Arabidopsis microarray database and analysis toolbox. *Plant Physiology* **136,** 2621-2632.

Websites

http://tgrc.ucdavis.edu/
http://elm.eu.org/
http://weblogo.berkeley.edu/
http://www.arabidopsis.org/
http://www.genemania.org/
http://www.csiro.au/
http://www.tm4.org/
http://www.blast2go.com/
https://www.genevestigator.com/
http://www.sgn.genomics.net/
http://sift.jcvi.org/
http://zhang.bioinformatics.ku.edu/ITASSER/
http://www.geneious.com/
http://tools.neb.com/NEBcutter2/
http://www.danafarber.org/
http://genevenn.sourceforge.net/
http://www.geneontology.org/

Acknowledgements

Firstly I wish to acknowledge Prof. Andrea Mazzucato…thanks for your time, guidance, support, encouragement and optimism not only during my PhD but throughout all my studies. I have learnt so much from you that I do not think I could ever thank you enough for all your help, patience and friendship! I wish to extend my sincere thanks to Prof. Gian Piero Soressi for invaluable discussions and suggestions during my studies. Deepest thanks to all past (Irene Olimpieri, Pietro Mosconi, Enrico Santangelo, Grazia Antonelli, Luigi Selleri, Venkata Rami Reddy Sanampudi, Leonello Bonifazi) and present lab members (Anna Pucci, Maurizio Enea Picarella, Svetlana Baldina, Marena Torelli) who have helped me directly and indirectly in accomplishing my studies giving me a learning and social environment to grow both professionally and in life.

I am grateful to the Australian Plant Industry Company CSIRO for supplying the pKANNIBAL and pART27 vectors for the RNAi experiment. Many thanks to Dr. Giorgio Morelli (INRAN, Italy) and Prof. José Luis Micol (University of Alicante, Spain) for providing seed of the Arabidopsis lines. Thanks to Prof. Lucia Colombo, Dr. Simona Masiero and people from their labs (University of Milan, Italy) for technical advices in performing experiments with Arabidopsis.

I would like to express many thanks to Dr. Shunsuke Imanishi (NARO, Japan) for his collaboration in performing the microarray experiment. I am grateful to Prof. Celestina Mariani and Dr. Ivo Rieu (Radboud University, The Netherlands) for seed of the *RNAi-ARF7* line, Dr. Filomena Carriero (Metapontum Agrobios, Italy) for seed of the *EMS-iaa9* line and to Joaquín Cañizares (University of Valencia, Spain) for RNA samples of the *pat-3/pat-4* line used in the transcriptomic analysis. I wish to extend my thanks to Prof. Rosario Muleo and Dr. Marco Cirilli (University of Tuscia, Italy) for advices regarding qRT-PCR experiments and to Dr. Antonio Di Matteo (University of Naples, Italy) for fruit biochemical analysis.

Thanks to all the friends from other labs (Linda, Francesco, Lina, Eleonora, Roberta, Gaetan, Silvia, Tiziana, Andrea, Paola, Liliana, Michela, Valentina, Ilaria, Silvio, Ravy, Marco, Christian…) for the enjoyable time we had together both in and out the university.

Finally, my heartiest thanks go to my family and to my love Samuela for their continued support during these years. Questa tesi è dedicata voi…non potrò mai ringraziarvi abbastanza per aver creduto così tanto in me e per l'amore e la comprensione che avete sempre mostrato!!!